An Assessment of Heavy Metal Concentrations in Surface Sediments from the Knysna Estuary

Michael Philip Anthony Armitage

Supervised by Professor Michael Edward Meadows

Submitted in fulfilment of the Dissertation component of a Master of Science in the field of Environmental and Geographical Science

Abstract

This research presents an analysis of surficial sediment samples in respect of total heavy metal concentrations, sediment grain size, and total organic carbon within 36 surface sediment samples from the Ashmead Channel in the Knysna Estuary. 15 surface sediment samples were also analysed from Chongming Island in the Yangtze Estuary of the People's Republic of China, and the results compared between the two systems, in addition to other South African and global estuaries with similar characteristics to Knysna. Metals analysed were Cr, Cd, Cu, Zn, Hg, As, and Al. Statistical analyses, including Pearson's Product–Moment correlation, enrichment factor analysis, and the assessment of heavy metal contamination were conducted between the variables to determine patterns of difference and similarity between the sites, as well as to determine the degree of contamination in the Knysna sediments. Results from Knysna were also compared to those from previous studies in the area. This study found that the Knysna sediments are not highly contaminated with heavy metals in relation to South African Revised National Action List levels, however, the degree of enrichment in the sediment has increased by a substantial margin over the past 20 years. Mean metal concentrations in Knysna are Cr: 7.37mg/kg, Cd: <1mg/kg, Cu: 6.43mg/kg, Pb: 7.43mg/kg, Zn: 57.4mg/kg, Hg: <1 mg/kg, As: <1mg/kg, and Al: 2138mg/kg. Mean enrichment factor classes of the concerning metals are Cr: 1.69, Zn: 3.89, Pb: 2.56, and Cu: 2.33. Upon comparison with sediments from Chongming Island, it was noted that the sediment in the Yangtze has much higher background heavy metal concentrations than Knysna. The study also found that the degree of enrichment in relation to background concentrations for the sediment sites in Knysna was surprisingly similar to that seen in the Yangtze estuary for select metals, despite the Yangtze being a highly polluted system. It must be noted that the results from the Ashmead Channel likely indicate greater contamination than what is present in the entire Knysna Estuary, due to the close proximity of a number of contaminant sources, as well as flow restrictions. The Yangtze also experiences much higher sediment accumulation rates, therefore reducing the degree of enrichment. This study, therefore, shows the value of frequent contaminant monitoring in the Knysna Estuary and recommends that additional work be conducted in the system to develop the picture of heavy metal contamination, in addition to other pollutant enrichment, in the system. Furthermore, this study demonstrates that the comparison of different estuarine environments can be a useful tool for understanding the severity of heavy metal contamination in these systems.

Acknowledgements

I am truly amazed that I have finally arrived at the end of this dissertation. This has unquestionably been the most trying period of my life, with major mental health struggles, the birth of my first child: Helena Mae Armitage, and the Covid 19 pandemic all playing their part. With that said, I have grown more in a personal and academic sense than I have in any other period of my life. There are, therefore, many people I wish to thank for helping me along and enabling me to reach this finishing line which felt so impossible for much of the past three years.

Firstly, I wish to thank my wife, Juliet, who has been with me every step of the way and has constantly helped me to achieve my goals despite a trying pregnancy and new motherhood. Without her constant love and support, I doubt I would have managed to get through this degree.

Next, I wish to thank my supervisor, Professor Michael Edward Meadows, for his academic guidance throughout this degree and for facilitating my trips to Shanghai. I also wish to thank my father, Professor Neil Armitage, for all the academic advice given to me and for connecting me with many important people in Knysna and the Civil Engineering department at UCT. Furthermore, I wish to thank Neil and my mother, Debbie, for financially supporting me through this marathon of a degree: you were the main reason I was able to work on my thesis while having a young child at home. Debbie also helped immensely by sacrificing much of her time to look after Helena and therefore gave me uninterrupted time to work on my dissertation. I also wish to thank my sisters, Lauren and Jessica for all their support over the past few years.

Next, I wish to thank the many academics and students at UCT and ECNU who helped me with various stages of my fieldwork and laboratory work, in addition to giving me general advice on how to complete this degree. Firstly, I wish to thank Calvin van der Merwe and Dr Nadia du Plessis, who both helped me considerably with my fieldwork excursions in Knysna. I thank all the people who helped me in Shanghai, with special mention to Dr Abdul Qadeer, who helped me while I was in the field and was such a kind, hospitable friend to me during my time at ECNU. I also wish to thank Dr Dhritiraj Sengupta, who is both a great friend and interpreter, who helped me communicate when barely anybody spoke English. Next, I wish to thank Dr Yongjie Wang, who facilitated much of my laboratory work at ENCU in 2019 and sacrificed a great deal of time and laboratory space to help me. I also wish to thank Dr Xinran Liu, who facilitated my laboratory work during my 2018 trip to Shanghai. I wish to thank Mr Wong Xi for his time and expertise in using the laboratory equipment while I was in Shanghai, and for sacrificing much of his time to assist me.

I also wish to thank all the organisations that helped fund and facilitate this dissertation, including the National Research Fund of South Africa, the National Natural Sciences Foundation of China,

the Knysna Municipality, The Knysna Basin Project, and South African National Parks. Without assistance from all these organizations, this project would have been impossible and I'm grateful for all who have contributed.

Finally, I wish to thank my many friends who have supported me along this journey. First, I wish to thank my fellow EGS students and Chinese jetsetters: Helen Antonopoulos, Yakhuluntu Dubazana, and Salwah Taylor, for keeping me sane while we were in China and for being such great company when conducting laboratory work at UCT. Finally, I want to thank my good friends: Jordan Schofield, K.C. Davel, Nicholas Hardwick, Martin Zaeske, and Cameron Davies for always being there when I needed a person to chat to or to reassure me that things would work out, I really would not have made it to this point without your constant friendship and I cannot thank you all enough.

I have learned that it takes a village for someone to complete a postgraduate degree and I, therefore, want to thank everyone who has helped me along the journey.

Plagiarism Declaration

1. I know that plagiarism is wrong. Plagiarism is to use another's work and pretend that it is one's own.

2. I have used the UCT Harvard convention for citation and referencing. Each contribution to, and quotation which is from the work(s) of other people, has been attributed and has been cited and referenced.

3. This dissertation is my work and is written in my own words.

4. I acknowledge that intentional or unintentional plagiarism of another's work is wrong, and I, therefore, declare that this dissertation is my own.

Signature: Signed by candidate

Table of Contents

List of Figures

List of Tables

List of Abbreviations

Metals

Al- Aluminium
As- Arsenic
Cd- Cadmium
Co- Cobalt
Cr- Chromium
Cu- Copper
Fe- Iron
Hg- Mercury
Pb- Lead

General

CSIR- Council for Scientific and Industrial Research
ECNU- East China Normal University
EGS- Environmental and Geographical Sciences
GMOM- geometric method of moments
GSA- grain size analysis
ICP-OES- inductively coupled plasma atomic emission spectrometry
LDC- London Dumping Convention and Protocol
MGS- mean grain size
NAL- National Action List
RNAL- Revised National Action List
SANParks- South African National Parks
SOP- standard operating procedure
SQGs- sediment quality guidelines
SuDS- sustainable drainage systems
TOC- total organic carbon
UCT- University of Cape Town

1. Introduction

Concern about heavy metal contamination in aquatic environments has been growing rapidly in recent decades in conjunction with a growth in the scientific awareness of the impact of humans on natural ecosystems, environmental change, and climate change (Niu *et al*., 2020). The rapid rate of urbanisation and large-scale human reliance on polluting industrial activities is putting sensitive aquatic environments at great risk of heavy metal contamination and threatening both the local ecology and the people who rely on these environments for their livelihoods.

Estuaries are coastal environments typically characterised by the presence of both salt and freshwater bodies with relatively low riverine and tidal shear forces, in addition to large quantities of fluvial sediment deposition (Levin *et al*., 2001). These depositional environments create large areas of valuable habitat for diverse species of fauna and flora (Kennish, 2018). Estuaries are considered to be critical transition zones, wherein monitoring and protection are of vital importance in order to prevent major losses in their functioning (Levin *et al*., 2001). There are many exchanges between the freshwater system and the ocean in these zones, as well as between the water column and the sediment. These fluxes include nutrients, organisms, and pollutants (Levin *et al*., 2001). A pressing issue for the conservation of these crucial environments is the fact that humans tend to choose areas of high ecological significance, such as estuaries, as sites of habitation, largely due to the abundant natural resources and ecosystem services that these areas provide (Zhao *et al*., 2004). This means that any approach to protect these environments needs to consider the protection of the health and livelihoods of its inhabitants. The continued monitoring of sensitive environments and critical transition zones for dangerous contaminants is therefore crucially important for understanding anthropogenic impacts in these zones and for assisting researchers and decision-makers in conserving these spaces and remediating contamination before it becomes a health risk.

This dissertation therefore primarily focuses on a local South African estuarine system, the Knysna Estuary, which has been identified as the most ecologically significant estuarine system in Southern Africa, in addition to supporting a growing town and tourist hotspot (Turpie *et al*., 2000). Furthermore, numerous studies have shown that this important system is under threat from anthropogenic pollution, including siltation, nutrient and bacterial pollution, in addition to some indicators of increased heavy metal contamination in recent years (Maree, 2000; Human *et al*., 2016; Harvey, 2019; and Armitage, 2018). However, no comprehensive sedimentary heavy metal studies have been conducted in the Knysna Estuary in the past 20 years and thus the state of heavy metal contamination in the system has remained relatively unknown up to this point. The central aim of this study is to determine the extent of recent heavy metal contamination in the Ashmead Channel region of the Knysna Estuary and to provide a contemporary snapshot of the threat of heavy metal contamination in the system.

The secondary component of this study is a comparative analysis between the Knysna Estuary and the Yangtze Estuary in the People's Republic of China. This form of comparative study between contrasting environments may be useful in developing a better understanding of the dynamics and states of such estuarine environments through the extrapolation of commonalities and differences (Gao *et al*., 2016).

The principal justification for the selection of these two systems was due to this research dissertation falling under a collaborative National Research Fund of South Africa (NRF) and National Natural Science Foundation of China (NSFC) research call for comparative study, and therefore estuaries from South Africa and the People's Republic of China were selected for heavy metal analysis and comparison. For this component of the overarching project, the sedimentary heavy metal concentrations, and their influencing variables, which include sediment particle size and organic matter composition, have been targeted. These variables are compared between the localities of the Knysna Estuary which lies along the South-East coast of South Africa, and Chongming Island, which has been selected to represent the Yangtze in this study. The Yangtze Estuary is situated along the east coast of the People's Republic of China (PR China), (**Figure 1.1**). These systems are differentiated by a substantial scale factor: the Yangtze River and estuary is the third-largest on Earth by surface area and the largest - and most important - river in Asia, while the catchment is home to a total population of 480 million people (WWF, 2020). Chongming Island itself is also a very important area, supporting a population of roughly 700000 people (Bao & Gao, 2021). Knysna, on the other hand, is a small, permanently open estuarine bay located along the southeast coast of South Africa, which supports a population of only about 75000 people (Allanson, 2000a; Western Cape Government, 2017). The scale difference present between these two systems is well described when considering that the total area of the Knysna Estuary is only 10km^2, while Chongming Island has a total area of 1200km^2, and the entire Yangtze River basin has a total area of 1808500km^2 (Maree, 2000; Ma *et al*., 2003, Parlovich Muranov, 2021).

Despite the difference in scale, both systems are of crucial importance for the local biodiversity and food security in their respective regions, as they act as nurseries for fish species and staging grounds for migratory birds, in addition to being major aquatic food resources for their respective human populations (Turpie *et al*., 2000; Zhao *et al*., 2004). Unfortunately, both systems are under threat from human development, which is resulting in land encroachment, solid waste pollution, chemical pollution and large-scale habitat loss on the inter-tidal mudflats which characterize much of the habitat in these estuarine environments (Turpie *et al*., 2000; Zhao *et al*., 2004). The plight of these estuaries is well described by Zhao *et al* (2004: 140) who states: "Despite the critical ecological functions that they provide, inter-tidal mudflats are often valued more for their development potential than the ecosystem services that they provide". The protection of these estuaries is therefore vitally important for maintaining estuarine biodiversity and food security in the two regions and protecting the ecosystem services that they provide (Turpie *et al*., 2002; Zhao

et al., 2004). Given similarities between these systems, it seems appropriate to compare their relative environmental status using total heavy metal concentrations as an indicator (Bryan & Langston, 1992).

For the purposes of this study, Lead (Pb), Mercury (Hg), Zinc (Zn), Aluminium (Al), Chromium (Cr), Arsenic (As), Cadmium (Cd) and Copper (Cu) have been selected for analysis, primarily for their potential health hazards for all except Al. Al, on the other hand, occurs naturally in high concentrations in sediment, and its concentration is, therefore, a useful benchmark for grain size and the presence of clay minerals and can be used as a tool to normalise the total concentrations of the other metals (Ma *et al*., 2015).

Figure 1.1: World map highlighting the locations of the Yangtze and Knynsa estuaries (Google Maps, 2019)

1.2 Aims and Objectives

1.2.1 Aim

In light of the social and ecological significance of the Knysna Estuary, there is a need to frequently monitor the system for chemical contaminants and, therefore, the aim of this study is to determine the extent of recent heavy metal contamination in the Ashmead Channel region of the Knysna Estuary and to conduct a comparative analysis between the Knysna and Yangtze estuaries, with respect to heavy metal concentrations and other sediment characteristics.

1.2.2 Objectives

Given this aim, the objectives of this study are as follows:

a) To sample surface sediments from representative localities within the Ashmead Channel and surrounding rivers and canals in Knysna.

b) To sample surface sediments on Chongming Island in two distinct, representative localities.

c) To conduct geochemical analysis on the sediment samples, including analysis for heavy metals, grain size and total organic carbon.

d) To conduct statistical analysis on the results, in order to determine the relationships between the variables and to facilitate comparative analysis.

e) To map contaminant concentrations across the study areas, with the goal of determining the extent of heavy metal pollution.

f) To compare the results from Knysna with those from past studies in the estuary, in addition to those from other similar estuarine environments in Southern Africa in order to determine the extent of recent heavy metal contamination.

g) To compare the contexts of the Knysna Estuary and Chongming Island, with respect to geochemical composition and extent of contamination.

2. Study Area

2.1 The Knysna Estuary

2.1.1 Background

The Knysna Estuary is located along the southeast coast of South Africa, in the scenic Garden Route, which is characterized by a spectacular coastline and picturesque tourist hotspots, which attract people from around the world (**Figure 2.1**). The estuary is an important locality along the South African coastline as it is both the largest permanently open estuarine bay in Southern Africa and is also considered to be the most ecologically significant estuarine system in the region, harbouring 42.8% of its total estuarine biodiversity (Largier, 2000; Day, 1952). Many of the species living in the estuary are endemic, like the Knysna Seahorse, which depends entirely on the survival of the local eelgrass: *Zostera capensis*, a species that is highly threatened by the large amount of siltation occurring in the estuary (Maree, 2000; Claassens *et al*., 2020). The estuary is a crucial staging area for migratory birds who utilize the abundant food resources in the estuary prior to migration. Additionally, some bird species use specific areas of Knysna, such as Thesen Island, as breeding sites (Turpie et al., 2002). Knysna is a breeding ground for many of the major southern African coastal fish species, therefore indicating that the preservation of this environment is important for the maintenance of the livelihoods of local fishermen in the region, as well as major fisheries along the Southern coast of South Africa. This is in addition to the simple ecological concern and priority of maintaining the stability of these fish populations (Turpie et al., 2002). As a consequence of the intersection between biodiversity, ecological significance and economic stability, Knysna is considered to have the highest conservation status of any of South Africa's estuaries (Allanson, 2000a; Claassens *et al*., 2020).

Knysna's permanent residents are also highly dependent on the health of the estuary for a variety of reasons. Firstly, the economy of Knysna is based largely on tourist activity coming into the region. These tourists are attracted by features such as the natural beauty of the estuary, the picturesque views from the Knysna Heads, the fishing town atmosphere, as well as the variety of water sports and activities which can be enjoyed in the estuary. Additionally, many people living within the town depend upon estuarine fish stocks for their livelihoods in local markets (Turpie, 2002). Furthermore, many of the recreational activities which take place in the region directly expose people to the water and/ or sediment of the estuary, such as sailing, diving and swimming, which therefore implies that the overall environmental quality of the estuary is important, both with regards to solid waste (plastics and other waste), and dissolved and suspended pollutants, such as Escherichia coli (E. coli), pharmaceuticals and heavy metals (Harvey 2019; Claassens *et al.*, 2020). Pollution in Knysna, therefore, poses a threat to both the local biodiversity, the local tourist and fishing economies, and the health of the local population, who could be exposed to

these contaminants while utilizing the estuary for a variety of purposes. Consequently, the continued health of the Knysna Estuary is crucial for ensuring the maintenance of the local biodiversity and the wellbeing of the many individuals who base their livelihoods and personal health on the preservation of the estuary (Allanson, 2000a; Claassens *et al.*, 2020). In addition, the issue of visible vs dissolved/ suspended pollutants is apparent in Knysna (Allanson, 2000a). For instance, visible pollution such as floating garbage, faecal matter, and oil slicks are typically more commonly acknowledged, while the inconspicuous but more dangerous pollutants go unnoticed (Allanson, 2000a). Although it is not inherently problematic or illogical to take issue only with visible pollutants, the fact that invisible pollutants often go unnoticed by residents and local governance, therefore, leads to less serious remediation efforts, whereas visible pollution may prompt public outcry and therefore pressure to enact change (Allanson, 2000a). This therefore means that there can be a mismatch in the remediation approaches taken in relation to the actual threat posed by a contaminant type.

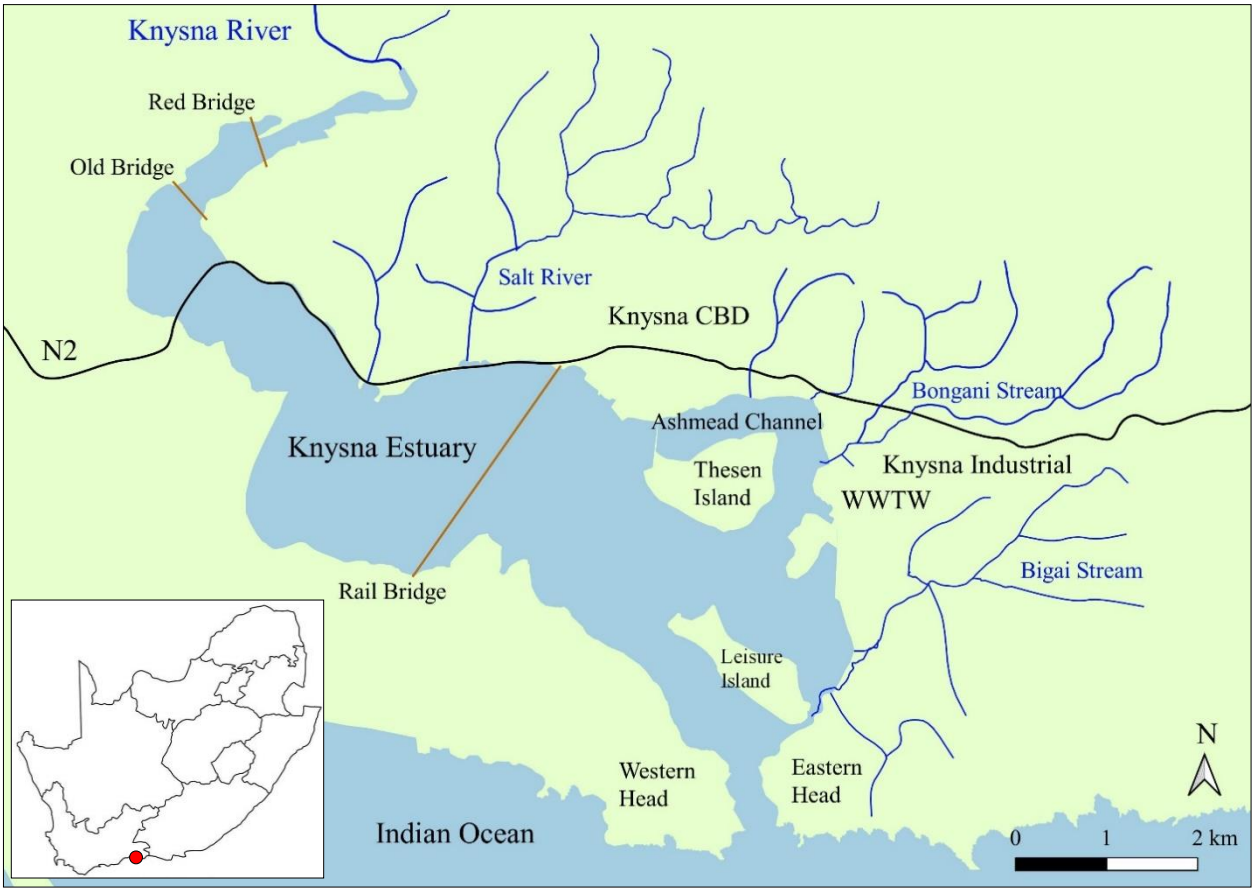

Figure 2.1: Site map of the Knysna Estuary. Map of South Africa from: Blankworldmap.net (2021), River GIS from SSI (2012), Estuary Outline from Sanparks (n.d). Map design inspired by Harvey (2019).

2.1.2 The Ashmead Channel

The eastern area of the estuary, known as the Ashmead Channel, and the surrounding rivers and canal systems, have been selected as the study area within Knysna, as this is seen as a hotspot of contamination within the estuary (**Figure 2.2**), (Watling & Watling, 1977; Watling & Watling, 1982; Monteiro *et al*., 2000; Human *et al*., 2016, Harvey 2019; Claasens *et al*., 2020). This is due to the Ashmead Channel receiving effluent from the industrial and residential areas of the town of Knysna, as well as the improperly treated effluent from the Knysna municipal water treatment works, in addition to sewage originating from public defecation due to inadequate access to sanitation services within the semi-formal settlements of Hornlee and Concordia. The channel also surrounds Thesen Island, which was developed into an upmarket residential area, with construction beginning in 2000, thus introducing new stressors and potential contaminants to the system (as a product of human habitation in the middle of the estuary). Moreover, as is typical of South African municipalities, much of Knysna's sewerage infrastructure is old and decaying, or simply does not have sufficient capacity for the needs of the local population (Bateman, 2009). As a result, there are many sewage pipes which are leaking into the local stormwater drains or rivers, causing localised pollution of these channels and thereafter the estuary where this water discharges. Furthermore, the primary drainage paths in Knysna are composed of canals and large stormwater drains, with their primary purpose being to force floodwaters from storm events rapidly through the system and into the estuary (Harvey, 2019). The Ashmead Channel is also an area in Knysna which has been historically sampled by both Watling & Watling (1977) and Moneteiro *et al.* (2000) and is considered by these authors to be a problematic zone for the accumulation of sediment and heavy metals due to its proximity to many effluent sources.

Due to the existence of the controversial causeway connecting the town of Knysna to Thesen Island, the natural tidal flushing of the channel has been greatly reduced, therefore, potentially reducing the dissipation and dilution of heavy metals and other pollutants throughout the estuary (Monteiro, Scott & Taljaard, 2000). The Ashmead Channel is found in the lower lagoon region of the estuary, as characterised by Largier (2000), and is characterised by lower tidal flow and flushing when compared to the rest of the estuary. This reduction in circulation, coupled with the continued development of the town of Knysna and the formation of the informal settlements on the slopes of the hills has dramatically increased the rate of siltation (the deposition of fine-grained sediment) and nutrient accumulation in this area of the estuary. This has created an ideal environment for algal blooms and associated dissolved oxygen depletion to occur, which is a fairly consistent issue in the channel and is causing degradation of the local habitat (Maree, 2000; Human et al., 2016, Harvey, 2019).

A remediation project was conducted as part of the initial construction of Thesen Island, between 2000 and 2003, wherein a section of the causeway was replaced with a bridge in an attempt to restore natural tidal flushing to the Ashmead channel. The bridge consists of approximately a fifth

of the total width of the northern edge of the channel, in addition to being closed on its lower edge. This bridge, although improving tidal flushing in the Ashmead, does not adequately restore tidal flushing to this region to the extent required to offset influents entering the channel (Harvey, 2019). Finally, the Ashmead Channel is the region where much of the fish-bait pumping takes place in Knysna and is, therefore, a region where inhabitants are directly exposed to estuarine water and sediment, which possibly places them at risk of harm from the pollutants entering the area (Simon *et al.*, 2019; Claassens *et al.*, 2020). This also raises an important social justice issue, as the majority of fishermen pumping for bait in the Ashmead channel come from the vulnerable, poorer socio-economic communities within Knysna and therefore should not be put further at risk of poisoning from e-coli, nutrients, and heavy metals.

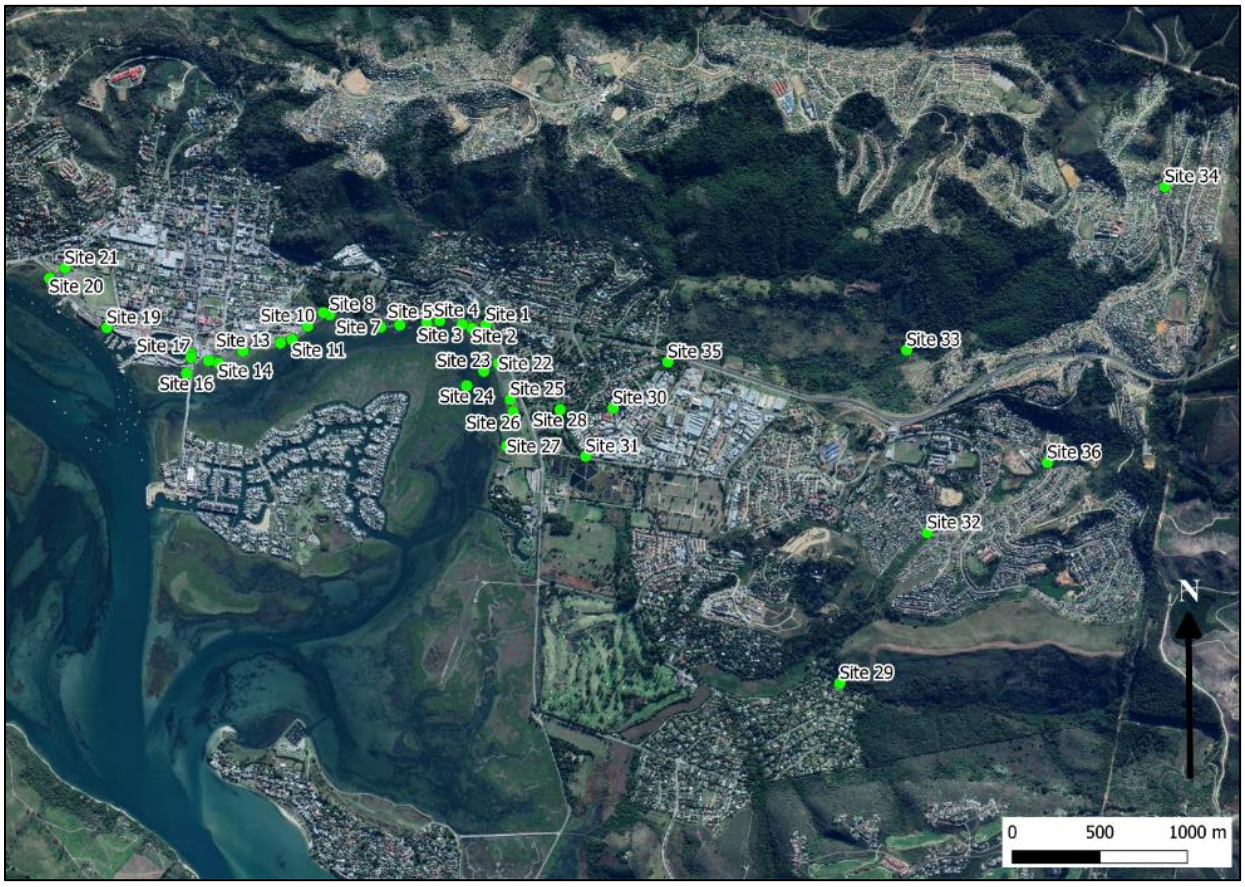

Figure 2.2: Map of the sampling sites in the Knysna Estuary (Google Earth Pro, 2019a)

As a result of these concerns and the long (18-years) time interval since the last heavy metal study on surface sediments in Knysna, the Ashmead Channel was selected as the site of a recent preliminary study on surface heavy metal concentrations by Armitage (2018), whose personal observations suggested that the heavy metal concentrations within the sediments in the channel could be increasing, although they were still well within safe guidelines. This pilot study included only nine surface sediment samples and therefore lacked the resolution required to adequately

capture the state of heavy metal contamination in the channel. This, presently unpublished data are integrated into this dissertation, as the recent nature of these results add to the richness of the current study and are likely be integrated into subsequent publications. The Ashmead Channel and surrounding rivers have therefore been selected as the primary study area for the Knysna estuarine component of this dissertation.

2.2 Chongming Island

Chongming Island is the world's largest alluvial island and is located within the Yangtze Estuary (**Figure 2.3**). The island is subject to a variety of land uses, including farming, forestry and the development of what local authorities have termed an 'ecological island' (Zhao *et al*., 2004; Wu *et al*., 2019). Chongming Island is also a crucial staging area for migratory birds and acts as a resting zone for birds travelling throughout Asia (Zhao *et al*., 2004). As previously mentioned, there is a huge scale difference present between the Knysna and Yangtze estuaries, and therefore, sampling localities chosen within the Yangtze needed to be small enough to replicate the methodology used in Knysna, yet also broadly represent the state of heavy metal contamination in the Yangtze. Due to the low resolution of study in the Yangtze, the present literature within the estuary is used to gain an indication of the sources of heavy metal contamination in Chongming. An additional problem occurring in Chongming is the rapid increase in anthropogenic land reclamation, which is resulting in the dramatic loss of wetland ecosystems, which support migratory bird species, in addition to important fisheries in the area (Zhao *et al*., 2004; Zheng *et al*., 2016). Furthermore, the size of the island is also increasing at a rapid rate due to the suitable conditions for natural sediment deposition and the ample sediment supply sourced from the Yangtze River (Chen & Wang, 2008; Wu *et al*., 2019). The sediment and flow characteristics within the estuary have also been changing in recent decades, due to large scale engineering projects within the Yangtze River, such as the construction of the Three Gorges Dam and the more than 50000 other dams throughout the catchment, in addition to increased erosion rates due to land use change including intensive urban development (Ying *et al*., 2005; Wu *et al*., 2019).

Sampling on Chongming Island took place on two distinct study areas, namely Gangyang and Xisha, which are of comparable sizes to Knysna, which should allow for adequate comparative analysis (**Figures 2.4**). Additionally, since Xisha is located to the west of the island, and Gangyang to the east, it should be possible to get a limited representative snapshot of the total heavy metal contamination on the island and should therefore offset some of the spatial differences in heavy metal contamination within the Yangtze. Chongming Island has also been selected to represent the Yangtze due to the beneficial access granted by the East China Normal University's ecological research station found on the island. Finally, Chongming Island represents a good comparative locality due the fact that it is mostly composed of agricultural land, a protected nature reserve and residential areas, therefore, suggesting that the sediment should not be contaminated with large quantities of heavy metals from industrial areas on the island itself. This further implies that the

majority of the heavy metal contamination in the sediments is likely sourced from the Yangtze River as a whole (Zheng *et al*., 2016).

Figure 2.3: Map of Chongming Island highlighting the two sites, Xisha and Gangyang (Google Earth Pro 2019b)

Figure 2.4: Site maps of Xisha (top) and Gangyang (bottom) highlighting the sediment sampling locations at the sites (Google Earth Pro, 2019b)

3. Literature review

3.1 Heavy metals

3.1.1 Background

Heavy metals, often referred to as trace metals, are metallic elements with high atomic masses, which typically occur in low concentrations in the environment (Bryan & Langston, 1992). These metals, while sometimes being necessary for life in small concentrations, can be toxic for plant and animal life when they exist in high concentrations in either sediment or water bodies (Bryan & Langston, 1992). Heavy metals can accumulate in sedimentary environments from both natural and anthropogenic sources, which are discussed in more depth in the following paragraphs. As a brief pre-emptive summary, it should be noted that, in the majority of cases, heavy metals reach dangerous concentrations and are harmful to people and aquatic life when their origins are linked to anthropogenic inputs (Bryan & Langston, 1992; Bradl, 2005).

Heavy metal concentrations in sediment are influenced by several factors primarily relating to grain size, with the finer-grained sediment (<60μm), also known as the cohesive fraction of the sediment, having significantly higher heavy metal concentrations than larger sediment grain sizes due to the associated increase in surface area, total organic carbon content and clay minerals, in addition to the higher electrical charge found within fine sediment (Thorne & Nickles, 1981; Yu et al., 2012; Monteiro, Scott & Taljaard, 2000). These fine sediments, therefore, provide the ideal environment for heavy metal accumulation (Thorne & Nickless, 1981; Yu et al., 2012; Soon & Bates, 1982; Gao *et al*., 2016). As a result, the movement and deposition of this fine-grained sediment plays a crucial role in the mobilization of heavy metals. Additionally, the pH of the surrounding water, the cation exchange capacity and the redox potential of the sediment influences the total concentrations of heavy metals found in sediment (Yu et al., 2012; Soon & Bates, 1982). The heavy metal concentrations in sediment can therefore increase from either the movement of the cohesive fraction of the sediment or from the absorption of these metals from the water column onto the surfaces of sediment if the conditions are ideal. Heavy metal-laden sediment will therefore travel downstream and eventually deposit in areas of low turbulence and energy (Gao *et al*., 2016). When catchments are modified to remove natural drainage channels and are replaced with artificial waterways, such as canals, the rate of stream flow is dramatically increased, therefore leading to sudden, large-scale transfer of water and sediments downstream. This is due to canals being designed to allow water to flow rapidly during rainfall events, with the design incentive of removing water from the inhabited area as fast as possible. As a results of this function, canals are built with the intention of preventing sediment build up, and therefore vegetation, which would lead to the slowing down of flow and hence deposition of sediment in natural systems. This is

problematic as it ultimately leads to most of this heavy metal laden sediment rapidly depositing in estuaries, lakes etc. without any time for these metals to be sequestered by biota higher upstream (Thorne & Nickles, 1981). Furthermore, artificial surfaces, such as roads and buildings, may accumulate metals on their surfaces, which are then mobilized during a rainfall event (Mahbub *et al*., 2010). During such events, a great deal of heavy metal-laden sediment and water are mobilized and flushed into the estuarine environment in a short period and, as a result, the natural environmental removal processes for sequestering these metals are totally overwhelmed and the concentrations in sediments and water bodies increase, which can therefore threaten estuarine health and functioning.

3.1.2 The importance of studying surface sediments

The term surface sediment in the context of this study refers to the top 5 cm of sediment for both subaqeous sites and sites found above the water line at the time of sampling. Surface sediments are important as they represent the exchange surface between the sediment and the water column, which therefore allows them to act as both a sync for heavy metals in the form of suspended particles as well as a reaction surface for the absorption of dissolved metals (Thorne & Nickles, 1981). Surface sediments are, conversely, also able to act as sources of heavy metals based on the changing chemistry of the water column, which can cause dissolution of the absorbed heavy metals from the surfaces of the sediment particles, in addition to remobilization of the sediment particles and organic matter through shear stresses and bioturbation (churning) from organisms (Bellucci, 2002; Watling & Watling, 1977; Monteiro, Scott and Taljaard, 2000). Organisms which feed on benthic microorganisms/ plant life are also able to interact with the surface sediments and can either disturb the sediments or consume contaminated biota, therefore resulting in the mobilization of these metals into the surrounding aquatic environment.

Studying heavy metal concentrations in surface sediments, rather than directly sampling water, is advantageous for several reasons. Firstly, even though surface sediments represent a dynamic environment, they are much more stable on a temporal basis, whereas many factors can drastically alter the composition of water on a short-term basis, especially in a system governed by strong tidal factors, such as Knysna (Monteiro, Scott & Taljaard, 2000; Largier, 2000). Additionally, due to their close relationship with the surrounding water, sediments can give an indication of the state of heavy metal contamination in an area that represents the longer-term impact of the chemistry of the overlying water and suspended particle load, without the impact of micro-scale short term anomalies in water circulation which can lead to dramatically different results. As such, surface sediments represent a good proxy for understanding the state of heavy metal contamination both in the sediment and the surrounding water itself. Heavy metals in sediments also typically exist in concentrations orders of magnitude higher than they would exist in water and are therefore more reliably measured by machines with limited sensitivity (Bryan & Langston, 1992; Newman & Watling, 2007).

Studying surface sediments can, therefore, be a useful means of determining the extent of estuarine pollution from anthropogenic sources as they capture the impact of repeated pollution events, whereas a single water sample may miss a pollution event that happened either before or after the time of sampling, as the contaminated water would have already been dissipated into the estuarine system and the signature would have been lost.

3.1.3 Natural sources of heavy metals in aquatic environments

All sediments typically have certain specific natural background concentrations of trace metals as a direct result of the provenance of the sediment, in addition to the geology of the surrounding catchments (Watling & Watling, 1977). Provenance refers to all the processes leading to the formation and the eventual deposition of sediment in its current form, from the formation of the parent rock to weathering and erosional processes of this rock, and finally to its mobilization into the water column and eventual deposition in a river/ estuary, etc. (Weltjie & von Eynatten, 2004).

Trace metals exist in a variety of forms in sediments, which includes being found within the lattices of the parent rock or absorbed onto the surfaces of the rock (Thornton *et al.*, 1975; Watling & Watling, 1977). These metals are mobilized into aquatic environments through several processes, including the weathering and erosion of the parent rock, which can lead to the formation of pores. Metals and sediment thereafter accumulate in pore-water, which then enters water bodies as groundwater and later flows downstream and accumulates within the sediment.

The background concentrations of trace metals in sediments act as a useful signature to indicate their origin which is of great use to geochemists (Watling & Watling, 1977; Newman & Watling, 2007). These natural background concentrations are typically non-harmful as large percentages of these metals are found within the non-bioavailable category within the sediment, meaning they are located within the lattices of the sediment itself, rather than absorbed onto the surface of the sediment (Watling & Watling, 1977). Trace metals which are absorbed directly onto the surface of the sediment are more likely to be absorbed by biota or dissolved into the water column, whereas metals found within the lattices of the sediment remain sequestered unless further erosion or weathering processes occur on the sediment (Vinodhini & Narayanan, 2008). It is therefore crucial, when attempting to assess the threat posed by total heavy metal concentrations in sediment, to take measures to account for the component of these concentrations which do not occur in the bioavailable state, rather than using total concentration as the only metric for gauging contamination. This is because certain sediments, particularly those rich in elements such as aluminium or iron, typically have higher total concentrations of trace metals which occur in the non-bioavailable state and are not harmful (Sinex & Wright, 1988).

3.1.4 The anthropogenic influence on heavy metal concentrations

Humans influence the heavy metal concentrations in aquatic environments in many ways, including contaminating processes, such as discharging heavy metal-laden water and sediment into these environments, and physically altering the catchments themselves, which causes intensification of heavy metal contamination in certain areas. Physical alterations include the construction of concrete canals, which lead to high water flow rates and result in the accumulation of sediments downstream. The vertical walls of canals also prevent the development of riparian ecosystems, which have sequestering effects for contaminated sediment and water when functioning properly (Verhoeven and Meuleman, 1998). Additionally, humans often destroy natural sequestration sites, such as wetlands, for purposes of development (Gopal, 1999). The net result of these alterations is that the majority of the heavy metal-laden sediment and water will enter depositional environments, such as lakes and estuaries, and lead to local contamination.

Actual anthropogenic sources of heavy metals include industrial activities wherein metals are used in chemical processes, the running and residues of motor vehicles and boats, the weathering of structures, and the disposal of waste products containing dangerous chemicals (Alloway, 2013). More specifically, heavy metals are often introduced into aquatic environments from artificial surfaces and objects, with some culprits including runoff from corrugated metal roofs, just checking these are different? roads, the breakdown of car tyres and the improper disposal of mechanical and industrial chemicals, in addition to the weathering of metal-containing paints (Watling & Watling, 1977; He *et al*., 2001; Dierkes *et al*., 2006). Sometimes metals are introduced into aquatic environments due to the desirable chemical properties they possess, with Zn sacrificial anodes being a good example, wherein the corrosion-prevention benefit of using submerged Zn blocks to protect other metal surfaces of boats can result in localised Zn enrichment in the surrounding water and sediment (Mathiessen *et al*., 1999).

The central concern posed by anthropogenic inputs of heavy metals into aquatic environments is that heavy metals are introduced into these environments at a rate that markedly exceeds the natural removal rates through organic uptake and dilution (Bryan & Langston, 1992; Alloway, 2013). As a result of this rapid influx of metals, high concentrations of heavy metals can accumulate in the sediment at the bottom of lakes and estuaries and can then be consumed by benthic (bottom-dwelling) organisms and potentially bioaccumulate, which is described in 3.1.5.

3.1.5 Heavy metal bioaccumulation

Heavy metals present in the water column can bind to the surfaces of both sediment as well as microorganisms. These metals can enter the cells of these organisms and form more toxic and easily absorbed compounds (Vinodhini & Narayanan, 2008). The issue is that these metals can accumulate faster in/ on these organisms faster than they can be removed, therefore leading to a

net accumulation over time, which is known as bioaccumulation (Vinodhini & Narayanan, 2008; Bradl, 2005). These microorganisms are then consumed by larger animals and, in turn, have these metals accumulated within their tissues. This process, therefore, continues up the food chain and can lead to the phenomenon of biomagnification, wherein the total concentrations of heavy metals are the highest within higher-order organisms, such as fish and other animals. This presents both a health risk for these animals, as well as the people who consume many of these higher trophic level species and can hence experience heavy metal poisoning (Vinodhini & Narayanan, 2008; Bonanno, & Giudice, 2010). The effects of such biomagnification are therefore more pronounced in predatory species higher up the trophic chain. The threat of heavy metal biomagnification further emphasizes the importance of preserving aquatic environments, which is a dominant theme within this dissertation.

3.1.6 The role of organic matter as a site of deposition

One of the key mechanisms for heavy metal accumulation within sediment is their precipitation and absorption by organic matter. Sediments with a larger organic matter contingent, therefore, provide a more suitable environment for the accumulation of dangerous heavy metals, and once assimilated into the tissues of these plant or animal species, they can move up the food chain threatening other species (Vinodhini & Narayanan, 2008; Monteiro *et al.*, 2000). Certain species of bacteria are, conversely, known to consume heavy metals, therefore making them an important sink for heavy metals within the water column and in the sediments (Monachese *et al*., 2012). This is possibly due to the bacteria creating nucleation sites on the outsides of their cell walls, which can bind to metals of opposite charge and hence lead to the accumulation of these toxic metals externally, rather than being absorbed into the cell itself (Monachese *et al*., 2012). These metals then form insoluble oxides and therefore are unable to be absorbed into the tissues of these bacteria (Monachese *et al*., 2012). As a result of this strategy, these bacteria are able to survive in much more heavy metal contaminated environments than other species. Water treatment via these forms of bacteria is known as bioremediation and hence form an important natural methodology for treating contaminated water or sediment. It should also be noted that environmental pH is an important factor in the ability of these bacteria to bind heavy metals as the pH change alters the charge of the surface of the bacterial cell, with pH neutral (+/- 7) water bodies being optimal for maximal binding of these metals (Monachese, Burton & Reid, 2012).

3.1.7 Limitations of using total heavy metals for determining toxicity

A primary limitation within the study of total heavy metal analysis is that, although it provides a basic indication of the state of heavy metal contamination within a system, it does not directly quantify the mobility and bioavailability of these metals, which are determined by analyzing the chemical speciation of these metals (Zheng *et al*., 2016; Impellitteri *et al*., 2003). Furthermore, the assessment of total heavy metal concentrations does not account for the metals which may be

bound within chemical structures within the sediment and, as a result, may be sequestered within this sediment for long periods and hence completely inaccessible for biota. This may lead to large overestimations of the health risks posed by certain sediments (Impellitteri *et al*., 2003; Newman & Watling, 2007; Yoon et al., 2015). Multiple environmental factors affect the fraction of the heavy metals within sediment which are bioavailable, including pH, organic matter content, and dissolved organic carbon (Kim & Owens, 2007). The pH of the sediment acts to reduce the bioavailable fraction in more alkaline sediments and to increase this fraction in more acidic sediments. Despite these limitations, due to the large cost of heavy metal testing in sediment, the assessment of total heavy metal concentrations in sediment represents a popular opportunity-cost methodology for assessing heavy metal contamination, when coupled with the inexpensive methodologies of GSA and TOC (Impellitteri *et al*., 2003). This is particularly important in regions where funding for toxicological research is limited. Furthermore, normalising methodologies, such as Enrichment Factor Analysis, discussed below, can be used as proxies to determine the bioavailability and contamination state of sediments without doing more intensive chemical analysis (Sinex & Wright, 1988).

Sediment quality standards in South Africa

A further issue faced when assessing total heavy metal concentrations in South Africa is the lack of sediment quality guidelines (SQGs) (DEA, 2019). As stated previously, the background heavy metal concentrations in sediments can vary by large amounts, even orders of magnitude, as a result of local geology and environmental characteristics (Newman & Watling, 2007; Vinodhini & Narayanan, 2008). It is therefore important that different regions have SQGs and standards for total heavy metal concentrations. A current problem in South Africa is that the only available SQGs and concentration ranges were initially selected from ranges present within the London Dumping Convention and Protocol (LDC), of which South Africa is a signatory (DEA, 2019). This protocol sets guidelines for the concentrations of heavy metals when screening sediments for dredging in coastal environments and was implemented in South Africa in the National Action List (NAL) (DEA, 2019). The primary constraint is that these SQGs were based on sediments from Hong Kong, Ireland, Iceland, Germany, Norway and Canada and do not account for the local sediment composition present in South Africa and, as such, are somewhat arbitrary guidelines for determining if estuarine sediment is contaminated or non-contaminated (DEA, 2019). Additionally, these concentration guidelines give little input as to the impact of heavy metals at concentrations below where dredging should be considered. This is a major shortcoming as it is better to identify the problem of contamination and remediate it before dredging is necessary, as dredging is an environmentally destructive process and should be reserved for only the most extreme cases (DEA, 2019). It appears, however, that there is some research currently underway to establish suitable SQGs for SA, with an amended version of the NAL guidelines being created, known as the Revised National Action List (RNAL) (**Table 3.1**), which slightly alters the guideline concentrations and is more refined than the original NAL guidelines (DEA, 2019). The RNAL has concentration guidelines termed as action levels and prohibition levels, with action levels implying

that further biological testing is required to determine if dredging is necessary and if it is possible to dump this dredged material at sea. If the metals exceed the prohibition levels it means that the sediment should be dredged, however, these sediments are considered too contaminated to be dumped at sea and another means of disposal needs to be found. Despite being an imperfect set of SQGs, the Revised National Action List has been used in conjunction with enrichment factor analysis to determine the extent of heavy metal contamination in the Knysna sediments.

Table 3.1: Revised National Action List concentrations for South African Sediments (Dea, 2019: 89)

Range(mg/kg)	**Action level**	**Prohibition level**
Cd	1.5-10.0	>10.0
Hg	0.5-5.0	>5.0
or for a combined level of these two:	1.0-5.0	>5.0
As	30-150	>150 (1000)
Cr	50-500	>500
Cu	50-500	>500 (1000)
Pb	100-500	>500 (500)
Ni	50-500	>500
Zn	150-750	>750 (1000
or a combined level of these substances:	50-500	>500 (1000)

3.1.8 Enrichment factor analysis

A useful proxy when attempting to determine whether heavy metal concentrations present within a sediment sample are indicative of natural background concentrations or anthropogenic enrichment, is enrichment factor (EF) analysis (Sinex & Wright, 1988). EF relies on the principle that the ratio of the concentration of a given metal to the concentration of a normalizing element, typically Al or Fe, is approximately consistent in uncontaminated sediment samples from a region. This is due to Al and Fe concentrations being indicators of the presence of fine-grained clay minerals, with the greater component of these minerals typically indicating higher concentrations of other naturally occurring trace metals (Sinex & Wright, 1988). Moreover, Fe and Al naturally exist in very high concentrations in sediments and thus anthropogenic enrichment of these two metals would have a negligible effect on their total concentration in any given sediment sample (Zhang et al., 2009). Additionally, higher, naturally occurring concentrations of heavy metals associated with high Al concentrations typically lie within the non-bioavailable fraction of the soil, with the metals predominantly being bound within the lattices of the sediment and therefore posing no biological threat (Vinodhini & Narayanan, 2008). Al has been selected as the normalizer for this study due to Al being preferentially quantified in samples from both the Knysna Estuary and

Chongming Island sediments in the current, and past, studies from the region. EF is consequently conducted by comparing the ratio between the trace metal and normalizing metal (Al) concentrations in the sample against the ratio between the trace metal concentrations in an uncontaminated sample representing background concentrations, according to the formula: $EF=(M/Al)_S /(M/Al)_B$ (Sinex & Wright, 1988; Gao et al., 2015). This ratio gives an indication of the degree of enrichment in a given sediment sample, with a ratio between 0.5 and 1.5 typically being indicative of purely background concentrations occurring from the crustal or weathering conditions in the area (Gao et al., 2015; Zhang & Liu, 2002). To accommodate for the extremes of natural variation, An EF ratio of >2 is typically used as an indicator of heavy metal enrichment, with an increase in the EF ratio being indicative of greater degrees of contamination, see **Table 3.1** (Yongming et al., 2006; Gao et al., 2015; Barbieri, 2016).

Table 3.2: Enrichment factor classes for sediments (Barbieri, 2016)

Value	Soil Dust Quality
EF<2	Deficiency to Minimal Enrichment
2<EF<5	Moderate Enrichment
5<EF<20	Significant Enrichment
20<EF<40	Very High Enrichment
EF>40	Extremely High Enrichment

EF analysis is valuable as it gives an indication as to the degree of anthropogenic heavy metal enrichment in a sediment sample. Additionally, since a high EF value indicates that many of the heavy metals present within a sample do not occur naturally in the sediment, it can be inferred that these metals are likely bioavailable or easily mobilised in the system. This is due to the metals being absorbed onto the surfaces of sediment particles, or assimilated into the tissues of benthic micro-organisms, rather than being bound within the lattices of the sediment itself (Impellitteri *et al*., 2003). As a result, EF analysis provides a useful proxy for determining the bioavailability of heavy metals without conducting the highly complex and expensive process of heavy metal speciation (separating the metals into their bioavailable and non-bioavailable forms).

The selection of the background ratio for the EF analysis is highly important as this determines the accuracy EF calculations and classes. For the determination of this ratio, authors have taken several approaches. Firstly, some researchers choose to use the average ratio of the trace metal to Al in the Earth's crust to give an indication of the degree of contamination (Newman & Watling, 2007). Whilst this can be viable in extreme cases of contamination or for study areas where there are no baseline concentrations available, this can be misleading as the natural sediment composition, and hence the ratio, can vary greatly between regions (Newman & Watling, 2007). Many authors preferentially use the baseline ratio of what they deem to be uncontaminated sediments from the

region of their study area, to further increase the accuracy of the baseline ratio. This can be determined, either by analysing surface sediments or, more ideally, by analysing old, preferably pre-industrial, layers in core samples to reduce the impact of potential recent anthropogenic contamination (Newman & Watling, 2007). It is, however, usually not possible to determine the true background concentrations in soil due to the widespread impact that humans have had on the environment, and atmosphere, since the start of the industrial revolution and our subsequent altering of many natural systems (Newman & Watling, 2007). As such, these concentrations are typically referred to as baselines, rather than background concentrations.

The final method for determining the baseline ratio, which is used for the Knysna concentrations, is the use of baseline models to give the ratio on a per-sample basis. Fortuitously, a 2007 benchmark study by Newman and Watling analysed the results from many thousands of heavy metal samples collected in the 20th century for the south-east coast of South Africa, and in the process generated baseline models for the EF ratios of the metals concerned in this study (Newman & Watling, 2007). This is very useful as the baseline EF ratio changes based on the concentration of Al, and thus the baseline models allow for a highly accurate baseline EF ratio to be used for every sediment sample. Furthermore, the authors modelled the 99% prediction limits for these ratios, therefore providing a useful tool for determining what EF results can be considered to be anthropogenically enriched and outside of the range of natural variability. The authors also separated their study into sub-regions for the generation of these models, with the westernmost sub-region situated approximately 100km to the east of Knysna at the Kromme River estuary and extending westwards to the Sundays River estuary (Newman & Watling, 2007). The baseline results would have been more applicable in this dissertation had the Knysna Estuary been included in the study, however, due to the level of precision used to determine the models and the geographical proximity of the study area to Knysna, the results are the most accurate baseline EF ratios available. For Chongming Island, the baseline results from Chen (2008) and He *et al.* (2019) are used to conduct EF analysis for the comparative portion of this study.

3.2 Past heavy metal studies in the Knysna Estuary

3.2.1 Watling & Watling, 1977

The earliest in-depth studies on heavy metals within the Knysna Estuary are the reports conducted by Watling & Watling (1977, 1982) (**Figure 3.1**). The 1977 report for the CSIR focused on studying heavy metal concentrations within the surface sediments across the Knysna Estuary, including from drains and river inlets. These samples were collected using a steel trowel and heavy metal analysis was conducted using acid-digestion for sample preparation, and atomic absorption spectrometry for the heavy metal quantification. In total, the researchers collected 158 surface sediment samples and analysed them for Zn, Cd, Cu, Pb, Fe, Mn, Ni, Co, Cr, Al, Ag, Bi, Ti and Mo. This is the most comprehensive study on surface sediments in the Knysna estuary to date. The researchers concluded that the Knysna estuary was relatively unpolluted with heavy metals and that the concentrations of these metals were, on average, very low, with the exception of a few isolated sites of elevated concentration which they attributed to urban contamination. They noted that there were a few areas of relative enrichment, specifically the region to the south of Leisure Island), the area known as Point, located to the west of the main town of Knysna, and the Ashmead Channel region, located between Leisure Island and the Thesen Island Causeway.

The area of relative enrichment found near the Knysna Heads, with elevated concentrations of Cd, Pb, Ni, Co, Cr, Ag, Bi, Mo and V, was attributed to the breakdown of the parent rock by the intense tidal and wave forces present, rather than from anthropogenic contamination, and therefore represents a secondary anomaly. The authors identified that the elevated Cu and Zn concentrations present within some regions of the estuary primarily occur in spatial proximity to urban development and therefore propose that these are of anthropogenic origin. Nevertheless, none of these concentrations were dangerously high. In general, Pb concentrations were low throughout the system, except for the Heads region, and in the vicinity of the town of Knysna, in proximity to the drains from the town. The authors further identified that the most serious issue facing the Knysna system was siltation, which occurred as a result of the introduction of silt to the system during the rapid development of the town as well as the limitations on natural tidal flushing present due to the existence of the Thesen Island Causeway. This siltation was considered a concern as it was leading to alterations in the circulatory patterns within the estuary and potentially altering the habitat present.

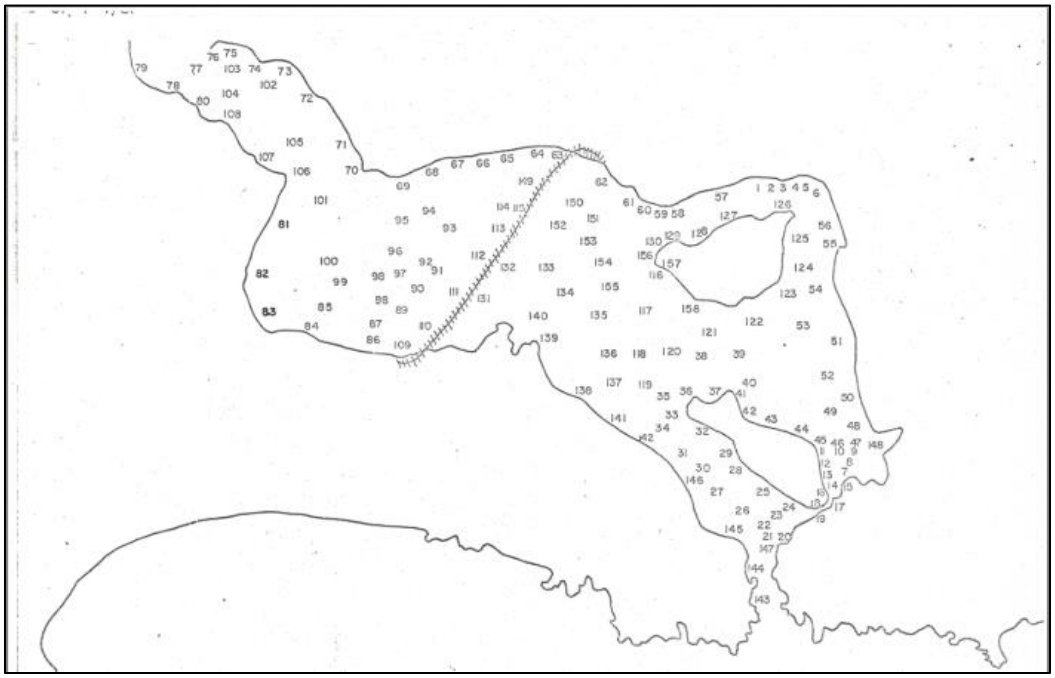

Figure 3.1: Site map of the surface sediment sampling locations sourced from Watling & Watling (1977)

3.2.2 Watling & Watling, 1982

The conclusions drawn from the 1977 study influenced the trajectory of the 1982 study also by the same authors who conducted a full survey of heavy metals throughout the Knysna Estuary, including sampling estuarine water, surface sediment, sediment cores and oysters. Of particular interest to the present study is the fact that the authors studied sediments from the inlets of drains and seepage sediments, to gain an understanding of the potential sources of metals into the system (**Figure 3.2**). The surface sediment samples were collected with a steel trowel and heavy metals quantified via atomic absorption spectroscopy. The authors came to the same conclusion as the 1977 study which was that in general, heavy metal concentrations in Knysna were low, however, certain elements were elevated above background concentrations for the region and there were specific anomalous sites that represent small-scale contamination. In particular, they noted that the saltmarsh located to the north of Leisure Island and enclosed by the Leisure Island causeway was acting as a metal trap, with anomalously high concentrations of heavy metals when compared to the rest of the estuary. Additionally, the authors identified increased Zn concentrations in proximity to urban and industrial development, with the most contaminated sites being located to the north of the Ashmead Channel. Finally, the authors identified high Hg concentrations present in the surface sediments to the west of Town, in the area known as point, which was also the area of the estuary most heavily utilized for the mooring of boats. They suggested that this Hg anomaly occurred as a result of the leaching of Hg-containing antifouling paints but did not consider this to represent a pollution threat.

The drain and seepage sediment samples were tested for Zn, Cd, Cu, Pb, Ni, Co and Hg concentrations. From these sediments, elevated Zn, Cu, Pb and Ni concentrations were identified at two sites to the south of Leisure Island, with one of these sites also having very high Hg concentrations. The authors tentatively attributed these elevated concentrations to seepage from drains located further east, which were fed by the Hunters Home and industrial areas. They identified the greatest levels of heavy metal enrichment in the Heads region to the south of Leisure Island, which is consistent with the 1977 study. Sites of high local concentrations of Zn, Cu, Pb, Hg and Ni were identified at the inlets of stormwater drains in the north of the Ashmead Channel, which is consistent with the findings of the surface sediment study. The easternmost of these sites, D13 (**Figure 3.2**), had the highest overall heavy metal concentration. This site lies downstream of what was then the Waterways Caravan Park, and therefore received runoff from the park, in addition to an amount of runoff from the eastern edge of the town of Knysna, located a short distance to the west, which are probable sources for these elevated metal concentrations. Drain sites D14-18, which directly received runoff from the town of Knysna, had elevated concentrations of these metals which is indicative of anthropogenic pollution. Site D14 had very high concentrations of Pb (254mg/kg), which the authors attributed to old car batteries which were discarded/stored outside the motor repair yard located just upstream. These North-Ashmead drain results form the basis of the comparison in heavy metal concentrations in drain samples with the current dissertation as they closely mirror a number of the contemporary sample sites, which are addressed later. The authors also found that their sample located at the outflow of the Thesen's factory, D19, on Thesen Island, had similar heavy metal concentrations to the surrounding area, except for Hg, which was elevated. From these drain results, the authors concluded that heavy metal concentrations in these drain sediments were considerably higher than those present in other sediment samples from the area, indicating that these elevated concentrations are a local phenomenon and were not leading to significant contamination of the estuary as a whole.

The authors also found anomalously high Co and Hg concentrations in surface water samples from downstream of the national road bridge, with the highest concentrations present near Leisure Island. They also identified several samples with elevated Cd concentrations. They, however, concluded that besides Co and Hg and several isolated samples containing other metals, the surface waters in the estuary did not exceed background concentrations for the region. The authors also studied bottom water from throughout the estuary and, importantly, found elevated metal concentrations in the vicinity of the heads, which they attributed to geological activity and inflows from low-level French drains and soak-aways. Furthermore, they also found a Cu anomaly in the bottom and surface waters located in the vicinity of the yacht club.

From this study, the researchers concluded that the overall impact of the heavy metal contamination in Knysna was small, due to the relatively minor impact that the contaminated

stormwater and sediment had on the heavy metal concentrations in the estuary as a whole, and consequently concluded that the Knysna Estuary was, at that time, relatively unpolluted.

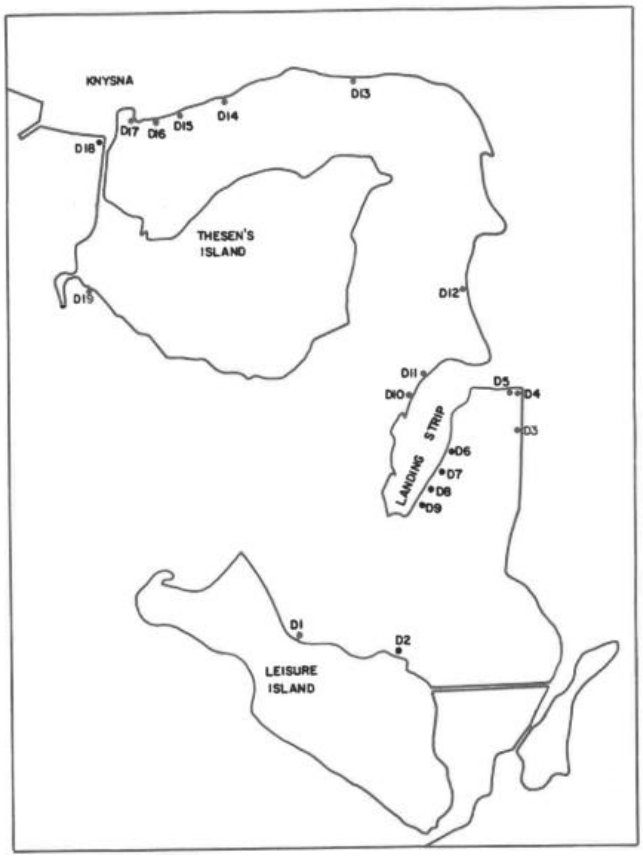

Figure 3.2: Site map of the drain and seepage sampling sites from Watling & Watling, 1982

3.2.3 Monteiro *et al*., 2000

The most recent benchmark study on the state of heavy metal contamination was conducted by the CSIR in 2000 as part of the "Knysna Lagoon - Thesen Island Development Water Quality Baseline Study". The study aimed to assess the state of water and sediment quality in the estuary and indicate the environmental impact of the Thesen Island conversion project, in which it was changed from an old wood processing facility into an upmarket residential area **(Figure 3.3)**. Total heavy metal quantification, heavy metal speciation analysis, Polycyclic Aromatic Hydrocarbon (PAH) analysis, total organic carbon quantification (TOC) and grain size quantification were conducted on the surface sediment samples. Sediment samples were collected using diver-operated corers, enabling researchers to access the lagoon bed and regions of the estuary inaccessible on foot. They also collected effluent samples from ten residential and industrial sites to test for both dissolved and particulate heavy metal concentrations. Particle size analysis was conducted by sieving the sediment samples and separating the sample into its gravel, sand and mud constituents then weighing these components to determine the distribution. The sediments were pre-treated with

acid and digested in a microwave to bring the metals into solution before Flame Atomic Absorption Spectrophotometry was used to quantify total heavy metal concentrations.

The authors focussed extensively on the fine cohesive fraction of the sediment and suggested that this acts as a good proxy for predicting where sediment contamination could occur, as the cohesive fraction is typically the most conducive for creating suitable environments for the deposition and absorption of heavy metals, and it is also typically transports metals within a system. They identified that metals closely associated with clay minerals, Al and Fe would, in turn, be indicators of a high cohesive fraction component and used a form of EF analysis to find the ratio between the concentration of a given metal in a sample to its the % of the sample mass that is made up of Al. This is expressed as: (E(mg/kg)/Al%)s/(E(mg/kgc/Al%)c), where the numerator (s) represents the ratio of the concentration of the sample element to the sample Al%, and the denominator (c) represents the typical baseline ratio of the same element in crustal sediment to the baseline crustal Aluminium %

The researchers concluded that the Knysna Estuary was not significantly contaminated with heavy metals as most of the surface sediment samples either had trace metal concentrations below the analytical detection limits for Pb, Cd, Ni and Sn or below the London Dumping Convention and Protocols trace metal concentrations for Cr, Cu, Zn, As and Hg. This is consistent with the conclusions drawn by Watling & Watling (1977). Several suggestions were made as to potential sources of these metals and the environmental factors that govern their distribution.

The size of the cohesive fraction was found to be dependent on the degree of bed shear stress, with regions of low shear stresses having the highest cohesive fraction. The authors linked this to several construction projects, such as the Thesen Island causeway, local marinas, and harbours, which caused significant reductions in bed shear stress and an associated increase in the cohesive fraction. The Ashmead Channel was found to have a comparatively high cohesive fraction, which the authors suggest was due to the restrictions on natural tidal flow from the Thesen Island causeway, high volumes of sediment from the town, and the high particulate organic carbon content found in the sediment from the influx of Nitrogen and organic matter through the sewerage system. The natural flocculation zone found in the upper lagoon also contributed to this high cohesive fraction. From their normalized Al ratios, the authors identified enrichment of Zinc, Cr, As and Cu concentrations in the Ashmead Channel, which indicated that these concentrations were dependent on anthropogenic inputs from both urban and industrial activities, even though the concentrations of these metals are still low on an absolute scale. Since a previous study had shown that Cu, Cr and As are the primary contaminants produced by leachates from waste dumps on Thesen Island, the authors suggested these were the primary source of the enriched metal concentrations in the Channel and were therefore hopeful that the termination of wood treatment on the island would cease this contamination (CSIR, 1991). They also identified urban and industrial runoff from the town of Knysna to be a major source of Zn and Cu enrichment in the area, with drain sediments

located downstream of the town's main industrial area (to the east of the Ashmead Channel), having a Zn/Al ratio substantially greater than any of the other sediment sites from this study, which represented a likely source of Zn. The authors recommended the construction of a sediment trap upstream of this inflow, which was indeed subsequently constructed. From the sedimentary Polycyclic Aromatic Hydrocarbon Results (PAH) results, the authors identified that the primary hydrocarbon pollutants in the sediments originated from wood treatment and the burning of light motor fuels used in cars due to the high levels of vehicle traffic through the area.

From the water samples collected in the study, the authors identified dissolved concentrations of Zn and Cu to be above detection limits, with Cu existing within the recommended water quality guideline concentrations, except for one site, whereas Zn exceeded the guidelines in 4 out of 10 samples, causing concern. Furthermore, it was concluded that most of the trace metal flux within Knysna occurred due to the movement of solid particles, rather than the movement of water-dissolved metals, which was particularly evident for Cr and Pb.

It should be noted that, unlike the previous study conducted by Watling & Watling (1982), the researchers did not analyse sediments within the tributaries of the estuary (Monteiro, Scott & Taljaard, 2000).

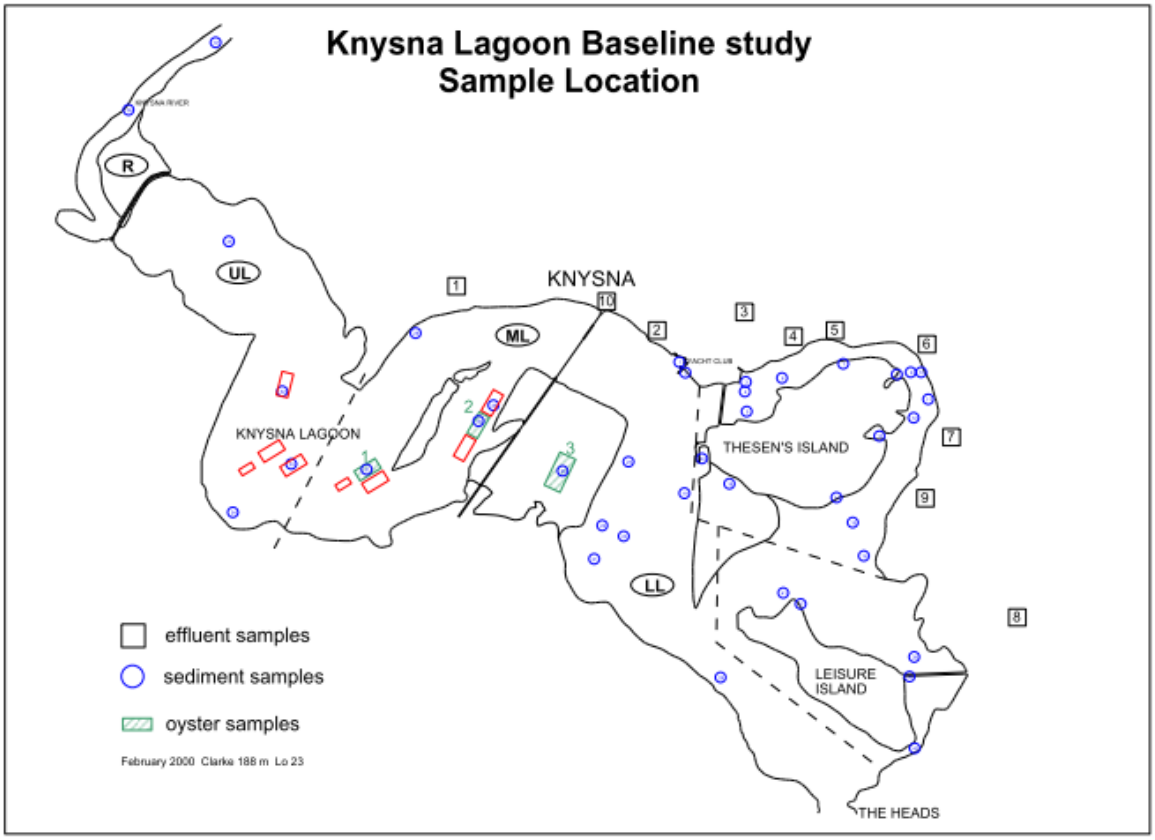

Figure 3.3: Map of the Knysna Estuary highlighting the sampling sites from the 2000 study by Monteiro *et al.*

3.2.4 Human *et al*., 2016

In a recent study by Human *et al*. (2016), a species of macroalgae (*Ulva lactuca* Linnaeus) present within an algal bloom in the Ashmead Channel was sampled and analysed for Nitrogen, Phosphorous and the metals: Cd, Cu, Pb and Zn. The authors found that the algal blooms and associated eutrophication were resulting in a reduction in the natural *Zostera capensis* (eelgrass) bed in the Ashmead Channel, due to light disruption caused by algae. They also found that the *Ulva* had low metal concentrations in their tissues, with Cu and Pb having no significant difference in tissue concentrations between sites. Zn and Cd showed contrasting trends, with two sites to the east of the Channel, near the outflow of the industrial area, having significantly higher tissue concentrations of Zn than the other sites, and Cd, conversely, being found in lower concentrations on the eastern edge of the channel. The authors did note that it was not possible to fully ascribe these concentrations in the channel to specific inflows or sources due to the likely movement of the algae throughout the channel but did suggest that these metals could originate from the industrial area located to the north-east of the channel. The authors concluded that the influx of nutrients into the channel was primarily originating from improperly treated wastewater entering the channel from the WWTW, in addition to the lack of tidal flushing, thus resulting in a nutrient-abundant situation where, under natural conditions, the water would be oligotrophic (nutrient-poor). This study is important as heavy metal concentrations in the algae were low enough for the authors to recommend its use in fertilizers, suggesting that the conditions in the channel are currently not contaminating local flora (and hence fauna) to a concerning level.

3.2.5 Armitage, 2018

The most recent study on heavy metals in Knysna is an honours dissertation conducted by Armitage (2018). In the study, nine surficial sediment samples from the Ashmead Channel were analysed for total heavy metal concentrations, including Pb, Cd, Cr, Zn, Al & Mn **(Figure 3.4)**. The author compared the concentrations and findings from the CSIR (2000) report to the results of their study and hence suggested that average heavy metal concentrations in the channel could be increasing (Monteiroe *et al*., 2000). The analysis also showed that the concentrations were still well below the trace concentration limits present within NAL (Armitage, 2018). Total heavy metal concentrations were also found to be strongly correlated with sediment grain size and TOC, which is consistent with the literature, indicating that the heavy metals adhere to the cohesive fraction of the sediment (Yu et al., 2012; Soon & Bates, 1982). In particular, the author found that the north and east sides of the channel were most contaminated with heavy metals, with the sediments surrounding the discharge point of the Bongani River, the WWTW, and the Long Street canal all having the highest concentrations. These inlets therefore represent likely sources of the pollution. The area to the south of Thesen Island was found to be unpolluted with heavy metals. Furthermore, Zn was found to have relatively high concentrations, approaching the dredging action level concentrations proposed by the NAL. The sample from the Long Street Canal was found to have

relatively high concentrations of heavy metals, even though it was composed of large particles. The author infers that these sediments would likely have higher concentrations if the sediment was composed of finer-grained particles.

It should be noted that this study only utilized nine sediment samples and the statistical analyses conducted on these results are less accurate than they would be if the study were conducted with a larger sample size. The results from this dissertation are included in the current thesis as the results are currently unpublished and sufficiently recent that they add depth to the research presently being conducted. The methodology for determining heavy metal concentrations, grain size and total organic carbon concentration were also consistent between this study and the current dissertation.

Figure 3.4: Map of the Armitage (2018) sediment sampling sites in the Ashmead Channel

3.3 Studies from the Yangtze Estuary

The Yangtze Estuary is a vast system and consequently extensive literature exists regarding heavy metal contamination within the system, although much of this is only available in Chinese. As a result, this analysis of literature focuses on selected papers pertaining to heavy metal contamination specifically within the Chongming Island region of the Yangtze.

Chen *et al* (2004) conducted heavy metal analysis on core samples taken from localities around Chongming Island and unexpectedly concluded that, despite the large quantity of polluted wastewater and sediment which was being produced by the city of Shanghai and discharged into the estuary, heavy metal concentrations were lower in the sediments surrounding Chongming Island than in other sediments along the nearby Chinese coastline (Chen *et al*., 2004). They attributed this to an intense dilution effect caused by the vast quantities of unpolluted sediment and water which travel through the Yangtze system (Chen *et al*., 2004). The researchers also attributed the higher heavy metal concentrations found within several of the cores to the silty clay which comprised the majority of these cores, which, therefore, acted as a depositional sink for these metals. Another study addressing this phenomenon was conducted by Chen *et al.* (2001) in which they took short cores on Chongming Island and tested them for total heavy metal concentrations and attempted to ascertain a Pb dating chronology for the cores. The researchers made the striking discovery that, due to the rapid sedimentation rates within the catchment, several of their approximately 1-metre-long cores may comprise sediments accumulated only within the last two years due to the approximately 40cm/year vertical accretion rate on the north-east end of the island (Chen *et al*., 2001). This is particularly interesting as the area of most rapid deposition happens to also be very close to the second site within this thesis (Gangyang) and therefore need to be accounted for when analysing the results from the region (Chen *et al*., 2001). The dilution effect demonstrated by these two studies should be considered when conducting the comparative aspect of this study, as they indicate that the concentrations of heavy metals within the Chongming Island sediments may not truly represent the large quantities of polluted sediment and wastewater entering the system. Additionally, these papers stress the importance of having multiple study areas in Chongming, since there is clearly a large degree of spatial variation and many factors influencing the heavy metal concentrations around the island.

4. Methodology

4.1 Fieldwork in Knysna

4.1.1 Formation of the fieldwork plan

Several planning sessions were conducted prior to entering the field in order to determine the best possible sediment sampling sites in Knysna. These sites were ascertained from a combination of the consideration of past studies about heavy metals in the Knysna Estuary and through extrapolation of what areas were likely to most at risk of heavy metal contamination (Watling & Watling, 1977; Watling & Watling, 1982 Monteiro *et al*., 2000). More recent studies on other contaminants were also used to gain insight into where likely problem areas could be found, based on the assumption that areas with an abundance of nutrients, such as *E.coli*, nutrients etc., may also have higher heavy metal concentrations (Human *et al*., 2016; Harvey, 2019). Finally, information was also gained from a workshop hosted in Knysna in February 2019 by the Knysna Municipality, which included researchers from UCT, members of the Municipality, the Knysna town council, South African National Parks and community stakeholders. In this workshop, contaminants were discussed, and input was gained as to the location of some of the likely problem areas. The decision was then made to primarily focus on the eastern area of Knysna including the Ashmead Channel and the systems which feed into it, which would be a manageable scale for a master's dissertation and would complement the parallel research being conducted on other pollutants in the same area. These cumulative factors allowed for the drafting of a base map using Google Earth with possible sampling sites, all of which were either located within the Knysna Estuary itself or within the tributaries and canals that feed into the system.

4.1.2 Fieldwork methodology

Fieldwork in Knysna took place between the 26th and 29th of March 2019 (**Figure 2.1**). Samples were collected from the surface 2-5cm of sediment with a trowel cleaned thrice with water to prevent contamination and placed within plastic zip-seal bags and clearly labelled. The details of the site were logged into a notebook with the GPS coordinates, a temporary site name and any other useful observational data from the site. An attempt was made to take photographs at every site; however, this was not always possible. Duplicate samples were collected at each of the sites. One sample per site was given to the Knysna municipality, who would later send them to the AL. Abbott laboratory for heavy metal quantification. The other sample was brought back to Cape Town for further analysis at UCT.

The samples were stored in a freezer before analysis, as this preserves the sediment characteristics and allows for later analysis. It is important to note that, since sites were selected adjacent to strormwater outlets and streams, it is likely that major sediment turbation (with sediment from greater than 10cm in depth being drawn to the surface) such as from prawn pumping, is not a major factor determining sample quality. This is due to the majority of the prawn pumping occurring further out on the mudflats. A degree of bioturbation and man-made mixing from foot traffic in the top sediment is expected and should not compromise the integrity of the samples representing the contemporary heavy metal concentrations in Knysna.

4.1.3 Sampling limitations

Sampling was affected by both logistics and access, with some areas, particularly in the Bigai system, being inaccessible due to private property laws and overgrowth of vegetation. Additionally, funding constraints dictated a short sampling period. As a result, it was not possible to acquire samples from the Bigai wetland, as originally planned. Furthermore, the expensive nature of sediment analysis, in particular high-accuracy heavy metal analysis, restricted the number of sediment samples which could be tested. A further limitation of this sampling strategy was the lack of samples acquired from further south in the Ashmead Channel, towards Leisure Island and, as a result, the samples do not fully represent the entire deposition zone of the Bongani stream and WWTW. The tributary found to the north of the Bongani stream was not sampled due to a lack of knowledge of the system and resources, hence there are no data indicating whether this sub-catchment is contributing to the heavy metal concentrations in the lower Bongani. Beyond these limitations, a suitable distribution of samples was achieved to gain a good understanding of the heavy metal concentrations in and around the Ashmead Channel.

4.2 Laboratory work on Knysna samples

The following section contains a highly abbreviated version of the laboratory methods used in this dissertation as they predominantly follow standard operating procedures. For a detailed version of the laboratory methods, consult **Appendix A**, where the methods are listed using the title numbering system below.

4.2.1 Initial sample preparation for loss on ignition and grain size analysis

The samples were removed from the storage freezer, thawed and heated in a drying oven to remove moisture while retaining organic matter (**Figure 4.1**). They were lightly ground with a pestle and mortar to disaggregate the particles and placed in plastic zip-seal bags for storage (**Appendix A**)

Figure 4.1: Left: A photograph of the wet sediment in oven trays prior to drying. Right: A photograph of the trays in the drying oven prior to drying

4.2.2 Loss on ignition

The loss on ignition (LOI) process took place in the Biological Sciences Department at UCT (**Figure 4.2**). The process involved heating the sediment in a muffle furnace to cause combustion, and hence removal, of the total organic carbon (TOC) within the sample, according to standard methodologies (Heiri *et al*., 2001; Schumacher 2002).

4.2.3 Preparation for grain size analysis

The post-LOI samples were sieved to remove large particles and then sub-sampled through coning and quartering to attain the correct amount of sediment for Malvern Mastersizer 2000 analysis (**Figure 4.3**) and placed into 50 ml test tubes according to SOP (Switzer and Pile, 2015).

Figure 4.2: Top left: Photograph of the crucibles in their furnace trays, prior to entering the furnace. Top right: Photograph of the two muffle furnaces used for LOI. Bottom left: Crucibles with TOC removed after the LOI process. Note the colour change from the top left image. Bottom right: The system used to weigh and record the mass of the sediment samples

Figure 4.3: Laboratory photographs of: Top left: The sediment quartering process. Top right: The sediment samples diluted in test tubes prior to Malvern analysis. Bottom left: the Malvern Mastersizer 2000, composed of the dispersion unit in the foreground and the Malvern in the background. Bottom right: The operating computer for the Malvern with the small centrifuge on the left

4.2.4 Malvern Mastersizer 2000 grain size analysis

The quantification of the grain size distribution was conducted using a Malvern Mastersizer 2000 instrument (**Figure 4.3**) and consisted of running the previously subsampled sediment several times in order to ascertain a representative result. This procedure was conducted using standard methodologies (Ryżak & Bieganowski, 2011)

4.2.5 Heavy metal quantification

Overview of the ICP-OES method for heavy metal quantification

Inductively Coupled Plasma Optical Emission Spectrometry analysis (ICP-OES) has been selected as the heavy metal quantification technique for this study as it is an effective technique for the quantification of the total concentrations of heavy metals (Olesik, 1991). A simplified description of the process, which occurs in the ICP-OES machine, involves forcing superheated plasma into contact with the vaporized sample, which causes the molecules within the sample to break up into individual elements. This process generates a light spectrum that is measured by the machine and can be used to calculate the concentration of the elements in the sample (Olesik, 1991). A limitation of ICP-OES analysis exists due to the relatively large background noise present, which reduces the accuracy of the generated results when the sample has low concentrations of a specific element, therefore making the quantification less accurate at lower concentrations. ICP-OES has been selected as the quantification method for this study due to it being both affordable and sufficiently accurate for quantifying total heavy metal concentrations, when compared to other methodologies (Olesik, 1991).

ICP-OES procedure

Heavy metals were analyzed within the laboratories of A.l. Abbott using standard SANS 11885: 2008 methodologies during March of 2019 (SABS, 2008; APHA, 1998; A.L Abbott. 2016). It should be noted that the author was not present during the following processing of the samples and therefore the following methodology represents a summary of the standard methodology stated by Al. Abbott and Associates. The detail present in the following section subsequently lower than is present in the rest of the methodology (A.L. Abbott, 2016). No photographs of the digestion and quantification process were made available to the author.

Acid digestion

The process involved digesting the samples in an acid solution and heating with a hot plate to reduce the sediment into its constituent elements (Hseu *et al*., 2002). The remaining residue was diluted in 50ml flasks with Milli-Q water in preparation for ICP-OES analysis.

Total heavy metal quantification via ICP-OES

Total heavy metal concentrations were quantified using a Prodigy ICP-OES (Inductively Coupled Plasma Atomic Emission Spectrometry) machine with standardised methodologies. Blank samples and standard solutions were used to calibrate the concentrations and to calculate the percentage recovery, however, the actual recovery percentages are not available.

4.3 Fieldwork in Chongming Island

4.3.1 Fieldwork strategy and procedure

The fieldwork strategy at Chongming Island was similar to that used at Knysna, as seen in **5.1.2**, with a few key exceptions. Firstly, the formation of the sampling plan and site selection not planned in as much detail as at Knysna, due to the incredible size of the island, lack of local knowledge and access constraints imposed by the national park status of a large portion of the island. The two sampling sites, Gangyang and Xisha, were selected by academics at UCT and East China Normal University, as they appeared to be suitable sites for the longer-term analysis which was being conducted by other members of the research team (**Figure 2.3; Figure 4.4**). The two locations were found in contrasting conditions, on opposite ends of the island, which is suitable for the snapshot of heavy metal concentrations in the Yangtze estuary necessary for this dissertation.

The actual sampling methodology was similar to that at Knysna, with the key exception that the samples were collected in a composite manner, which entailed collecting several samples from a 2 by 2-metre square and combining, then mixing, them into a single sample to remove the effect of small point anomalies. This methodology was employed here and not at Knysna, as further information about sampling strategy was gained from researchers at ECNU after having already completed sampling in Knysna several months prior. In Total, 7 samples were collected at Xisha and 9 at Gangyang, which were collected on the 6th and 7th of May 2019 respectively. It should be noted that Sample M04 was collected from an unsuitable site in a sand harvesting pond at Xisha and therefore the results are not used in the thesis.

Figure 4.4: Top: Site photograph of the Xisha site. Bottom: Site photograph of the Ganyang site, located alongside a river which cuts through the wetland

4.4 Chongming laboratory work

The following section contains an abbreviated version of the laboratory methods used for the Chongming samples as they predominantly follow standard operating procedures. For a detailed version of the laboratory methods, consult **Appendix A**, where the methods are listed with the same title numbering system as below.

4.4.1 Initial sample preparation

The sample preparation for the Yangtze samples involved freezing the samples and then using a freeze-dryer to remove moisture (**Figure 4.5**). The sediment was then lightly ground with a pestle and mortar to disaggregate the particles and sieved to remove large particles (**Figure 4.6**).

Figure 4.5: Laboratory photographs of: Left: The high-power freezer. Right: the freeze dryer

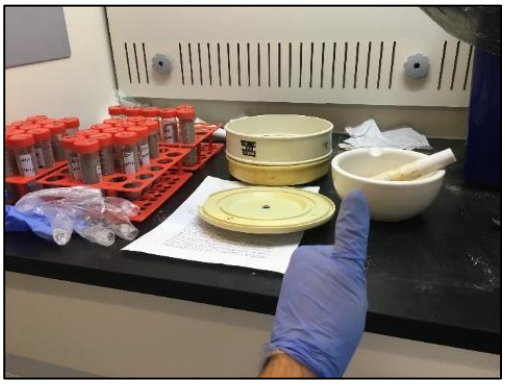

Figure 4.6: Laboratory photograph of the pestle and mortar (right) and sieve (background)

4.4.2 Loss on ignition

The Loss on Ignition process followed the methodology detailed in section 4.2.2. **Figure 4.7** shows the furnace used.

Figure 4.7: Photograph showing the interior of the muffle furnace used for loss on ignition analysis

4.4.3 Sample preparation for grain size analysis

Sample preparation for grain size analysis was different to that used for the Knysna samples in several ways. Firstly, the organic carbon content and calcium carbonate content were removed by digesting the sediment samples in acid and heating them on a hot plate for a short time, according to SOP (**Figure 4.8**) (Harris *et al.*, 2001; Mikutta *et al.*, 2005; Vaasma, 2008). Once the organic matter was removed the residue was diluted and suspended in a dispersion agent and then vibrated in a water bath to disaggregate the particles and suspend them for grain size analysis.

4.4.4 Grain size analysis by Malvern Mastersizer 2000

The methodology to quantify grain size is described in section 4.2.4. **Figure 4.9** shows the specific apparatus setup used.

Figure 4.8: Laboratory photographs of: Left: beakers partially filled with sample and HCL undergoing the evaporative process to remove organic matter with heating from a hot plate. Right: The vibration machine used to suspend the sediment particles

Figure 4.9: Photographs of the Malvern Mastersizer 2000: Left: the Malvern can be seen in the background with the small dispersion unit and circulation speed dial in the foreground. Right: The operating computer for the Malvern can be seen

4.4.5 Heavy metal analysis

Acid digestion

The process of sample preparation and acid digestion is as detailed in section 4.2.5. **Figure 4.10** showing the instruments used.

Heavy metal analysis via ICP-OES

Total heavy metal concentrations were quantified via ICP-OES according to a similar methodology as described in section 4.2.5. **Figure 4.11** shows the specific machine that was used. Each sample was run a single time in the machine, and 3 blank and standard solution runs were done for the purpose of calibration.

Figure 4.10: Laboratory photographs from the acid digestion process: Top left: the standard sample used for calibration for the experiment. Top right: the high accuracy scale and system used for measuring the sediment mass. Bottom left: the Teflon bottles can be seen arranged with their lids off during the process of adding the acids. Bottom right: the Teflon bottles can be seen sealed and placed on a hot plate at a temperature of 150°c

Figure 4.11: Photograph of the Agilient Varien 710 ES ICP-OES machine used for heavy metal quantification

Mercury analysis

Mercury quantification was conducted using a LECO AMA254 Mercury Analyzer (**Figure 4.12**). The process involved placing a defined amount of sediment sample within a nickel boat and allowing the machine to generate a result for the Hg concentration

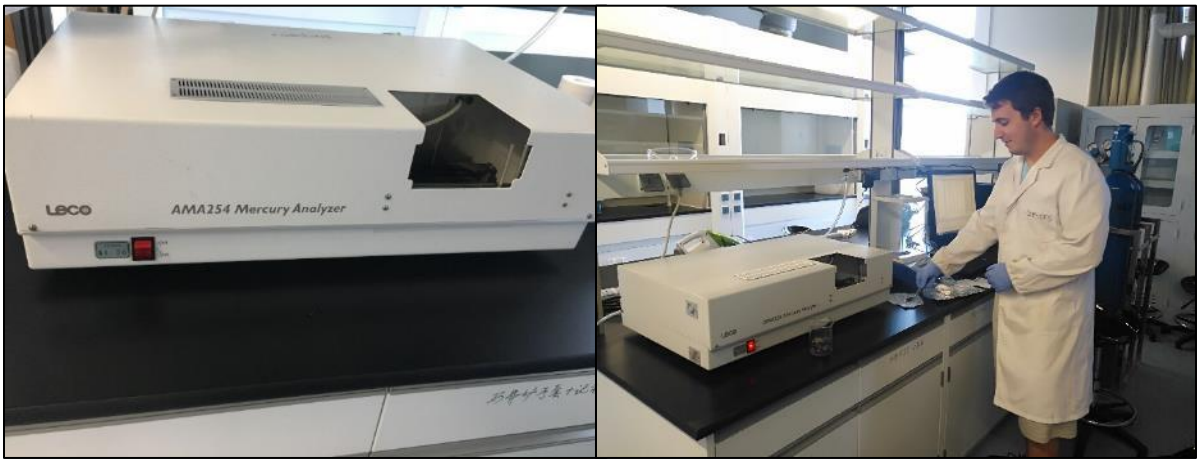

Figure 4.12: Left: Photograph of the AMA254 Mercury Analyzer machine. Right: Photograph showing the process of weighing sediment for mercury analysis

4.5 Statistical analysis and calculations

Pearson's Product-Moment correlations (linear correlations), Descriptive statistics, grain size analysis with Gradistat and EF analysis were conducted. Additionally, Excel and SPSS were utilized to run the necessary calculations and graph the data, as detailed below.

4.5.1 Initial organizing of results

After receiving the unprocessed results from the laboratory procedures mentioned above, the data needed to be converted into a usable, standardized form, which varied by process.

ICP-OES calculations

For the ICP-OES data, the results required conversion from concentrations in parts per billion into milligrams per kilogram and multiplication by the various dilution factors necessary during analysis, to ascertain the accurate concentration of the heavy metals within a given sample. Additionally, the mean of the 3 blank ICP-OES runs was calculated, and this value was subtracted from the sample results in order to remove machine error. Percentage heavy metal recovery was, however, not used to calibrate the Chongming Island results.

Grain size calculations

For the grain size analysis, the Gradistat software package was used to organize and graph the grain size results received from the Malvern Mastersizer 2000 (Blott and Pyre, 2001). The Microsoft Excel-based software takes an input of the aperture and class weight results from the Malvern software and outputs summary statistics and graphs of the data, including several different results for the mean grain size, based on standard methodologies, it also calculates compositional percentages of the different types of sediment, which were used in statistical analysis (Blott and Pyre, 2001). For this study, the geometric method of moments mean (GMOM) was used when describing the mean grain size (MGS) at any given site and for statistical analysis. A further useful statistic acquired from Gradistat was the percentage of the sample composed of mud (<63μm), which is important for gauging the suitability of a sediment sample for heavy metal accumulation.

Determination of TOC

To acquire the results for TOC percentage, the following formula was used: 100-[(Wf /Wi) * 100], where Wi is the initial weight of the sample (with the weight of the crucible removed) and Wf is the final weight of the sample after the loss on ignition process (also with the crucible weight removed).

4.5.2 Statistical analysis

General analyses

Statistical analysis took place using two statistical packages. First the data were organized into a usable format using Microsoft Excel. Once the data had been organized into a series of spreadsheets, they were transferred into the SPSS software package for most of the calculations and statistical analyses, due to the more powerful and easy-to-use nature of the software package.

A number of statistical analyses took place using SPSS. Initially descriptive statistics of the metal concentrations, grain size data and TOC data were calculated. The descriptive statistics include the mean, minimum and maximum values, the range, and the standard deviation of the data. These summary statistics are useful for understanding the overall values of these parameters in the study. These descriptive statistics were also found for sub-regions in Knysna as it is useful for understanding the difference in metal concentrations and sediment composition across the sub-regions. When inputing heavy metal concentrations into SPSS which have concentrations of <1mg/kg (for Knysna) or have readings that appear to be negative from the ICP work done in Shanghai, the values have been replaced with 0.5mg/kg. This is due to the software not functioning with inequalities. 0.5 was chosen as it is the midpoint of 0 and 1, therefore representing the best approximation of the concentrations when conducting calculations.

The next form of analysis that took place was the Pearson product-moment linear correlation which was calculated for all the variables. This correlation tests for linear correlations between the variables and indicates the strength of the correlation and whether a given correlation is significant at the 5% or 1% levels. A correlation that is significant at the 5% level indicates that there is a less than 5% chance of the relationship existing purely as a result of natural variability or the variables being linked in some manner (Puth *et al*., 2014). This analysis allowed for the formation of a correlation matrix which gave correlations and significance ratings for all the variables in the study and hence an understanding of the relationships between these variables in the systems of Knysna and Chongming. These correlations were also conducted for sub-regions in Knysna, to allow for comparative analysis between these regions.

4.5.3 Enrichment factor (EF) analysis

Enrichment factor analysis was conducted using the formula: EF = (Metal/Al)Sample/(Metal/Al)baseline, on the results from Knysna and Chongming Island. See **Section 3.1.8** for further details.

The models generated by Newman & Watling (2007) were used to calculate the baseline EF ratios for the Knysna samples at each given Al concentration. The baseline results presented by Chen *et*

al. (2008) and He *et al.* (2019) were used to determine the baseline EF ratios for the Chongming Island samples.

The EF results were mapped using red scale intensity maps with QGIS to represent the distributions of heavy metal enrichment at the different sites.

5. Results: Knysna

The following chapter describes the results from the 2018 and 2019 sampling in Knysna. The correlation results are considered extensively within the discussion.

5.1 Descriptive tables and graphs for heavy metals

The following section contains the graphs and tables for the Knysna results. **Tables 5.1, 5.3-5.9** are in **Appendix B**.

Table 5.2: Heavy metal concentrations in the 2019 Knysna sediment samples								
	Element (mg/kg)							
Sample number	**Cr**	**Cd**	**Cu**	**Pb**	**Zn**	**Hg**	**As**	**Al**
	Northern Ashmead							
1	<1	<1	<1	<1	21.9	<1	<1	1332
2	17.2	<1	<1	<1	17	<1	<1	924
3	2.1	<1	<1	<1	16	<1	<1	3297
4	3.3	<1	<1	<1	11.2	<1	<1	1121
5	3.2	<1	2.6	2.3	15.2	<1	<1	1180
6	4.4	<1	2.2	2.6	18.5	<1	<1	1861
7	3.6	<1	2.1	2.6	17.4	<1	<1	905
	East CBD							
8	4.1	<1	4.9	9.8	32.6	<1	<1	1255
9	3.7	<1	4.2	14.7	30.3	<1	<1	1883
10	4.9	<1	9.4	17.9	67.2	<1	<1	1680
11	2.9	<1	2.7	5.3	20.7	<1	1.9	1558
12	6.2	<1	6.4	7.6	49.5	<1	<1	1683
13	15.2	<1	29	22.3	345	<1	<1	2700
14	5.5	<1	1.2	2.9	27	<1	<1	580
15	2.6	<1	2.4	12.1	27.8	<1	<1	3582
	West CBD							
16	7.9	<1	11.1	17.5	92.7	<1	<1	2670
17	1.1	<1	3.7	3.6	55.9	<1	<1	494
18	10.6	<1	21.6	16.4	172	<1	<1	1280
19	14.7	<1	18.4	20.2	162	<1	<1	2063
20	6.1	<1	7.9	9.8	78	<1	<1	1891
21	5.6	<1	4.6	7.6	58.5	<1	<1	1718
	East Ashmead							
22	5.9	<1	1.6	3.2	16.4	<1	<1	2549
23	4.1	<1	<1	7.1	11.4	<1	<1	1100
24	6	<1	<1	3.1	15.1	<1	1.1	1659
25	5.7	<1	3.5	5.6	27	<1	<1	1144
26	6.5	<1	1.7	3.3	14.3	<1	<1	975
27	7.4	<1	7.4	4.4	37.7	<1	<1	1480
28	14.2	<1	11.5	10.8	121	<1	<1	6035
	Bongani Catchment							
30	5.4	<1	7.4	4.9	65.1	<1	<1	2222
31	22.8	<1	30.4	12.2	182	<1	<1	1535
33	9	<1	4.5	6.7	41.4	<1	<1	3699
34	18	<1	12.6	12.6	93.6	<1	<1	4617
35	15.9	<1	8	6.4	63.6	<1	<1	7600
	Bigai Catchment							
29	<1	<1	<1	<1	1.3	<1	<1	512
32	1.8	<1	<1	<1	8.9	<1	<1	1006
36	16.6	<1	4.5	8.9	30.3	<1	<1	5180
Mean	7.37	<1	6.43	7.43	57.4	<1	<1	2138
RNAL Action level	50-500	1.5-10	50-500	100-500	150-700	0.5-5	30-150	N.A

5.2 Brief overview of absolute heavy metal concentrations

Of the eight metals analysed in this study, As and Cd concentrations were negligible throughout the system. This is a very good result from an environmental health perspective as these elements can be very harmful in high concentrations (**Table 5.2**). Hg was also found to either be below the detection range of the ICP-OES machine or to be in negligible concentrations, which is again a good result. The statistical analyses in this study therefore only closely consider Cr, Cu, Pb, Zn concentrations, with Al being used as a proxy for clay minerals and a reference element for other analyses.

From the above tables, it is evident that the total heavy metal concentrations in Knysna fall below the RNAL action levels, which is also a desirable result. A few notable exceptions include Zn concentrations at **Sites 13, 18, 19 and 31**, with the first three sites all being located to the south of the main Knysna CBD and site 31 being adjacent to the industrial area. The highest total concentrations for the metals in question can be found in the sediments surrounding the Knysna CBD, the industrial area and the Bongani catchment. Conversely, the areas with the lowest heavy metal concentrations include the Bigai catchment, the sites south of Thesen Island, and the Costa Sarda area.

On average, Zn concentrations are found closest to the RNAL action levels, with Cu, Cr and Pb all being found well below the RNAL guidelines in most samples. From total heavy metal concentrations alone, it can be concluded that heavy metal concentrations within Knysna are predominantly safely below the guideline levels, however, Zn contamination is concerning. More exhaustive analyses are provided in the discussion section.

5.3 Correlations from the Knysna sampling

Table 5.10, found in **Appendix B**, shows the correlation results for Knysna. Note that: Cd, As and Hg have been included in the correlation matrix but have near negligible concentrations within the system at almost all sites and, as such, the correlations do not provide useful data and are discussed further. Details on the correlations are provided in the following paragraphs.

Firstly, all metals in the analysis (Pb, Cu, Zn and Cr), have strong positive correlations with each other, which are significant at the 1% level. This indicates that, where one of these metals has higher concentrations, the others will also likely be high. Additionally, these metals have weak positive correlations with TOC. These correlations are significant at the 5% level for Cu and Pb, and at the 1% level for Zn, whereas Cr is not significantly correlated with TOC. Al has significant (1%) positive correlations with TOC and Cr, yet no other significant correlations with other variables, whereas Cr and TOC correlate to a variety of variables. The correlations between the

metals and TOC likely occur as a result of sediment composition, absorption sites provided by the organic matter, as well as heavy metal pollution occurring in the same areas as nutrient pollution, such as the opportunistic algal growths in the Ashmead Channel (Vinodhini & Narayanan, 2008; Human *et al*., 2016).

A negative correlation between heavy metal concentrations and MGS was expected, due to the more favourable accumulation settings found within fine-grained sediment (Thorne & Nickles, 1981), yet despite a negative correlation observed, it proves not significant at the 5% level. The lack of significant correlations between MGS and heavy metal concentration is thus not due to the effect of grain size on heavy metal accumulation and is, therefore, due to other factors at the 36 study sites having a greater influence on heavy metal concentrations. One such influence may be the wide range of sediment types sampled in this study, with riverine, estuarine, and canal sediments all presenting differing environments for heavy metal accumulation. Furthermore, the intentional site selection near to suspected contaminant sources likely means that variance in heavy metal inputs has a greater influence on total heavy metal concentrations than grain size. Conversely, it can be assumed that MGS would be significantly correlated with heavy metal concentrations if the sites were randomly sampled from more uniform estuarine sediment (Thorne & Nickles, 1981; Yu *et al.*, 2012). The sites in the study with the lowest MGS are in estuarine environments and the relatively low heavy metal concentrations at these sites may indicate that the dilution of the heavy metal inputs into the Ashmead Channel is sufficient in preventing a high degree of contamination. Grain size has a moderate negative correlation (-0.69) with TOC, significant at the 1% level, which is consistent with the literature. This is due to fine-grained soils typically having more biological activity than sandier soils (Zhang *et al*., 2009). The fact that TOC but not MGS is significantly correlated with heavy metal concentrations may be indicative of sample quality, with heavy metal inputs occurring together with nutrient (Nitrogen and Potassium) contamination, therefore leading to organic matter thriving in areas with large heavy metal inputs. The most important finding evident from the correlation results is that the metals have strong positive correlation with each other, suggesting that they also share the same sources within the system or that an array of different contamination is occurring in particular areas that then feed into the same drainage channels.

5.4 Grain size and TOC results

The following section contains the graphs and tables for the TOC and Grain size results. **Table 5.11** is in **Appendix B**.

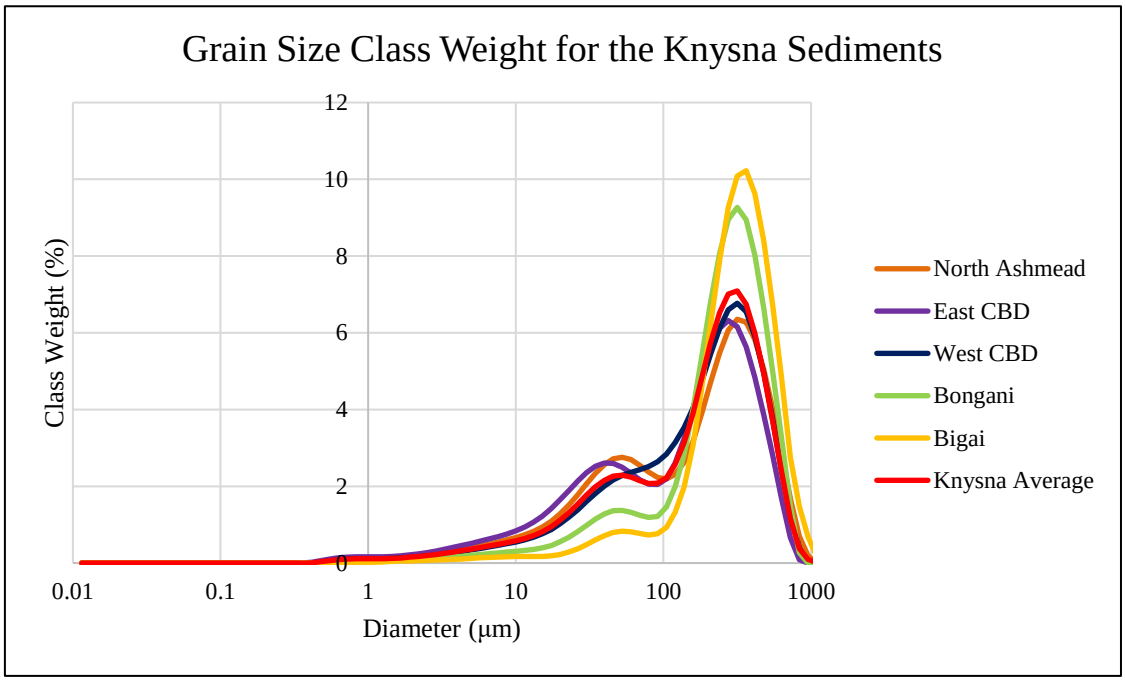

Figure 5.1: Grain size class weight line graphs for the Knysna sediment samples

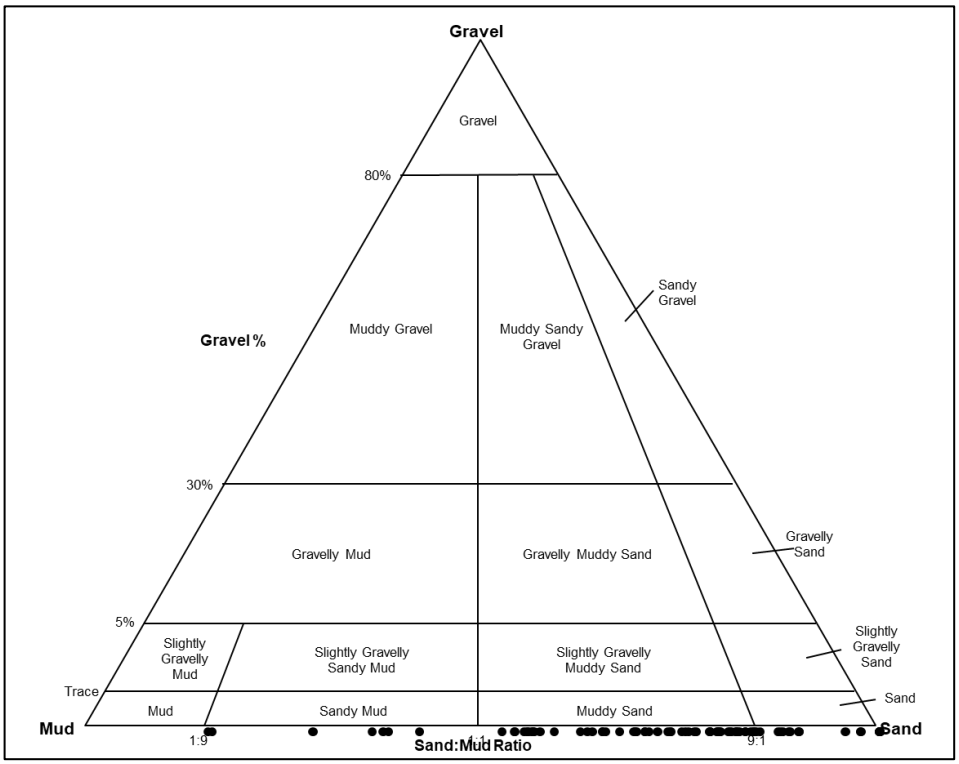

Figure 5.2: Gravel-Sand-Mud diagram for the Knysna sediments (Blott and Pyre, 2001)

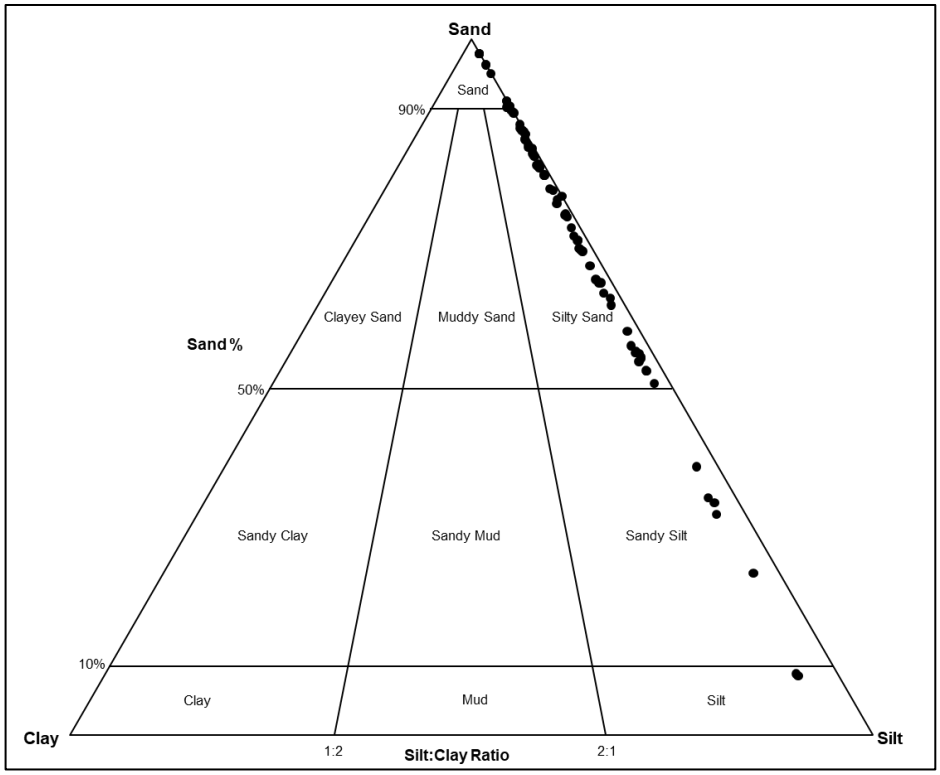

Figure 5.3: Sand-Silt-Clay diagram for the Knysna sediment samples (Blott and Pyre, 2001)

5.4.1 Overview of grain size results.

Table 5.11 and **Figures 5.1-5.3** highlight the grain size characteristics of the Knysna sediments. From these results, it is possible to make several observations: firstly, from **Figure 5.1**, it appears that the sediments are slightly bimodal, with a distinctive sand and silt component, with the largest class weights falling within the sand range. The grain-size profiles for the sub-regions appear to be very similar, however, the Bongani and Bigai catchments both have a larger sand component than the estuarine sites, likely due to the greater flow rates and poorer sedimentary conditions present in the riverine environments. The Knysna sediments would therefore be classified as "Very Coarse Silty Medium Sand" or more simplistically as Muddy Sand (Blott and Pyre, 2001). On average, the Knysna sediments have a Mud component (<63μm) of 11.1% and a Geometric Method of Moments (GMOM) mean of 173.0μm.

5.4.2 Overview of TOC results

There is a great deal of variability within the TOC results from the Knysna sediments, with a minimum result of 0.5% and a maximum of 19.5% (**Table 5.11**). The average TOC for the entire sample is 5.26%, with each subregion having very similar mean TOC values of approximately 5%, except for the Bigai samples which have very low TOC results, with a mean of 1.82%. This is

likely a result of their only being three samples collected from the Bigai catchment and therefore poor representation of the catchment as a whole.

5.5 Enrichment factor results

5.5.1 Enrichment factor tables

The enrichment factor tables for Cu, Cr, Pb, Zn (**Tables 5.12-5.15**) are found within **Appendix B**. These tables show the EF values and classes for Watling & Watling (1982), Monteiro *et al.* (2000), Armitage (2018), and the present study. A description of these results is presented in **5.5.3** and **5.5.4.**

5.5.2 Categorized enrichment factor maps for Knysna

The following pages include red-scale intensity maps which display the enrichment factor results for Knysna. Note that the 2018 honours results are denoted with **H-1**, for example.

2018-2019 EF results for the entire study area

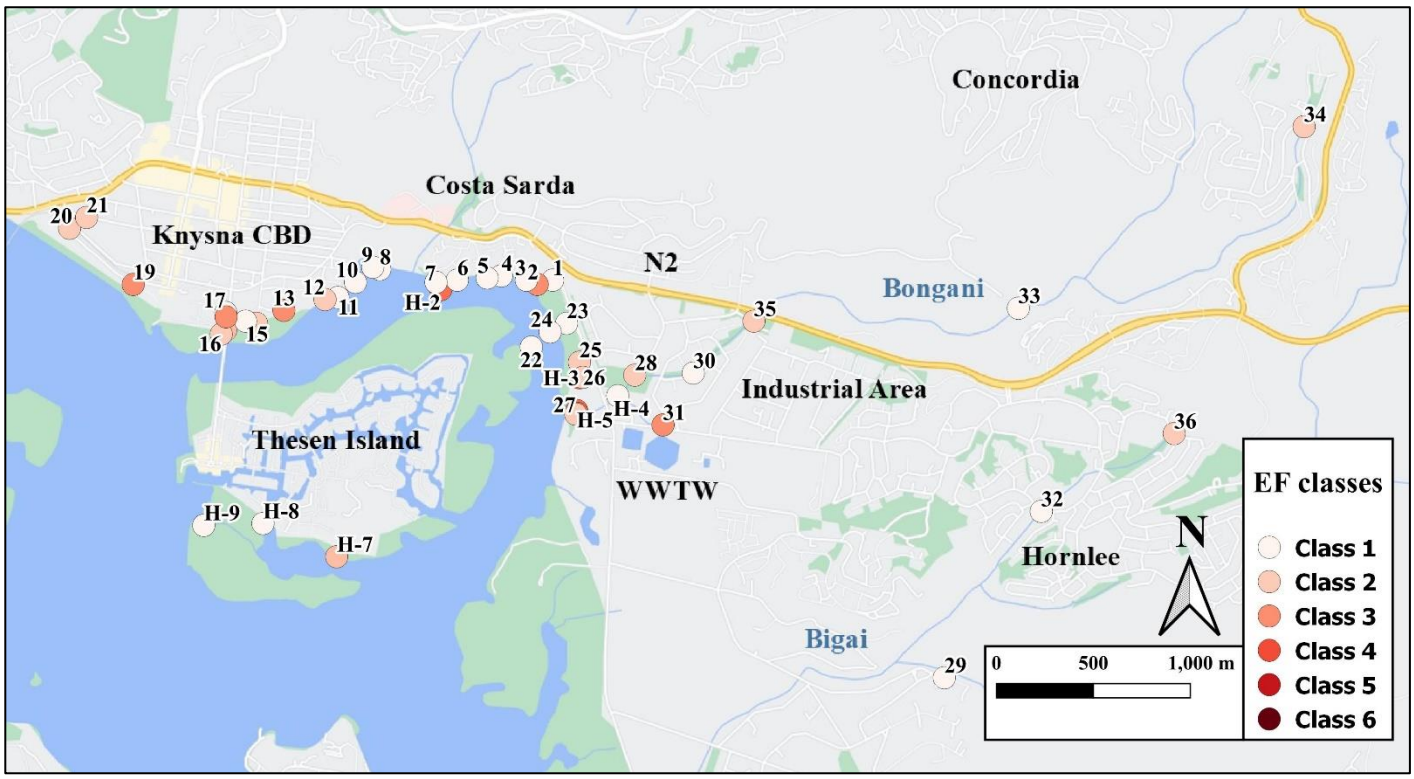

Figure 5.4: Map representing the EF categories of Cr from the 2018 and 2019 sampling in Knysna (Google Maps, 2021)

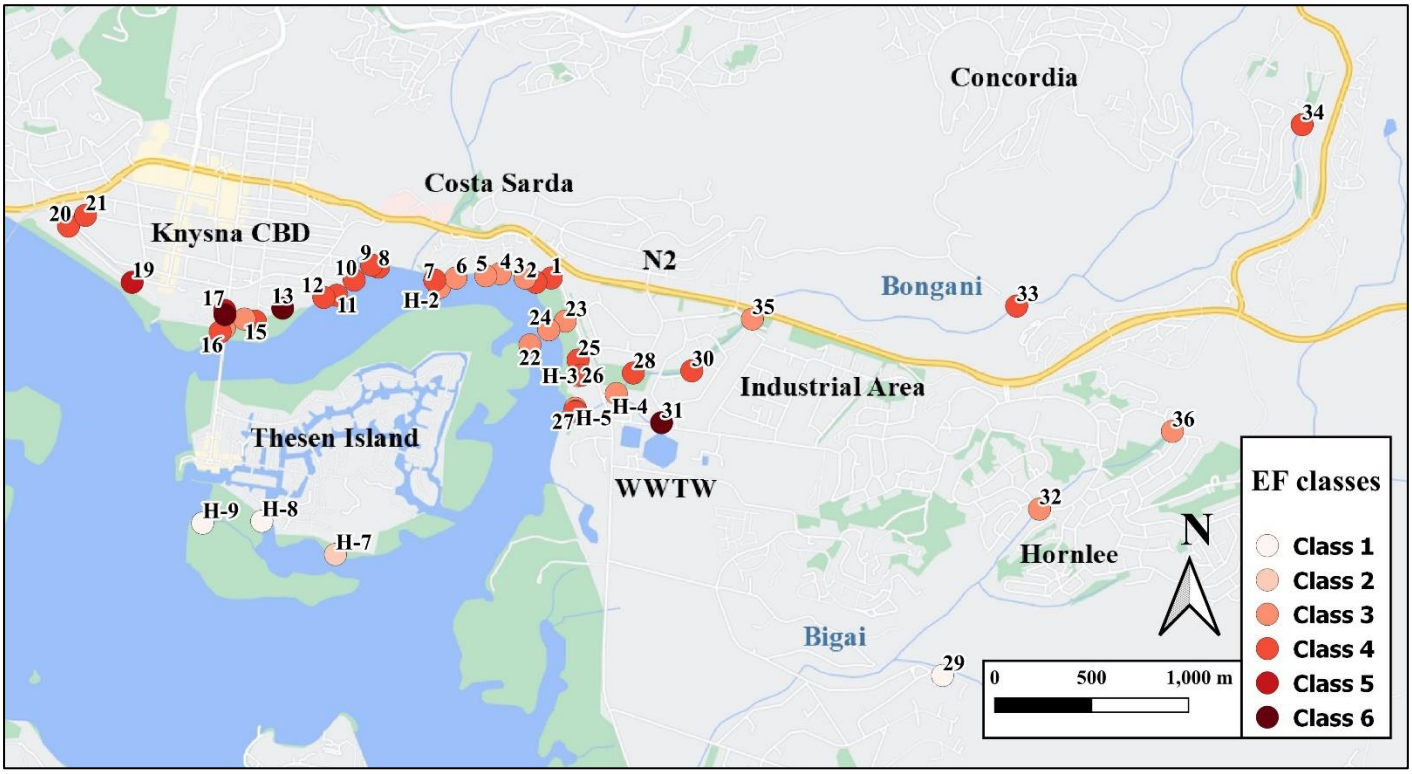

Figure 5.5: Map representing the EF categories of Zn from the 2018 and 2019 sampling in Knysna (Google Maps, 2021)

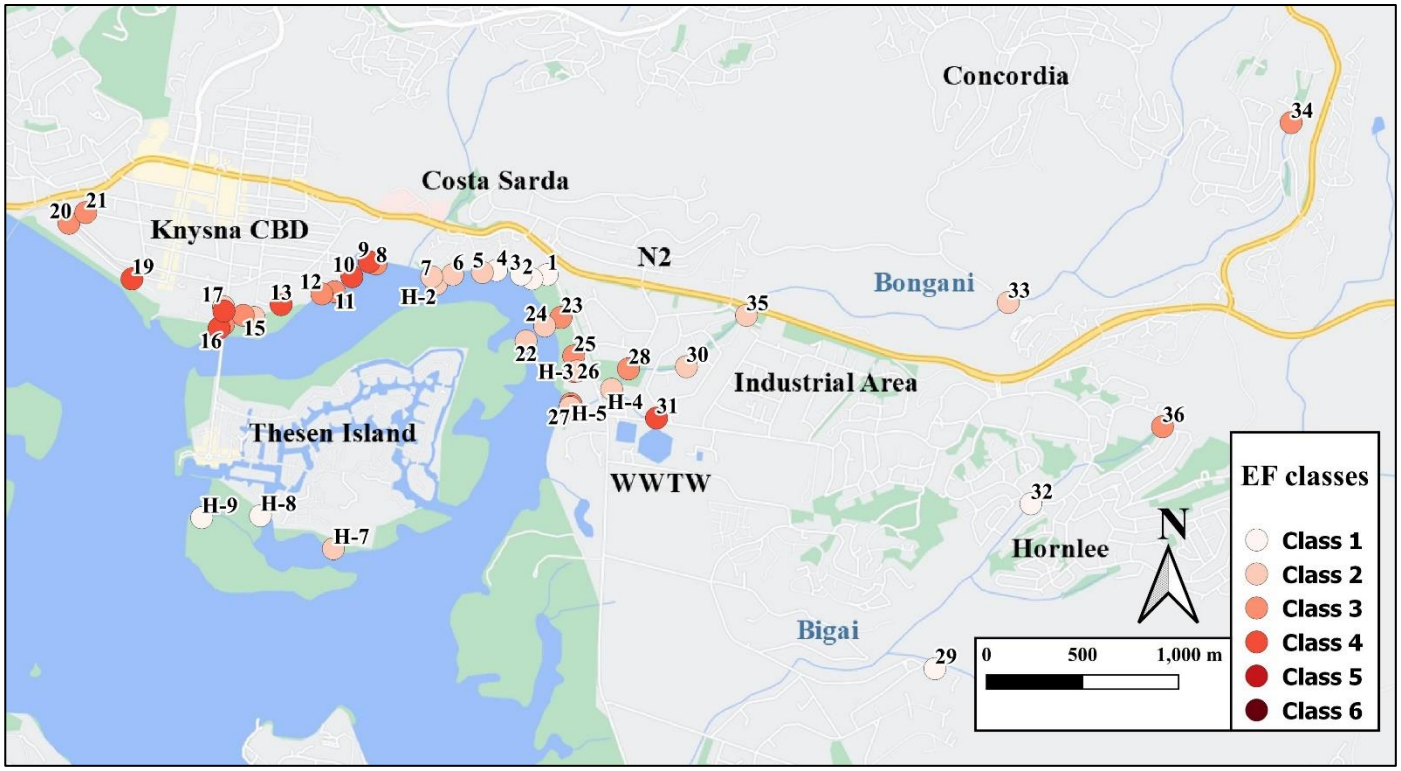

Figure 5.6: Map representing the EF categories of Pb from the 2018 and 2019 sampling in Knysna (Google Maps, 2021)

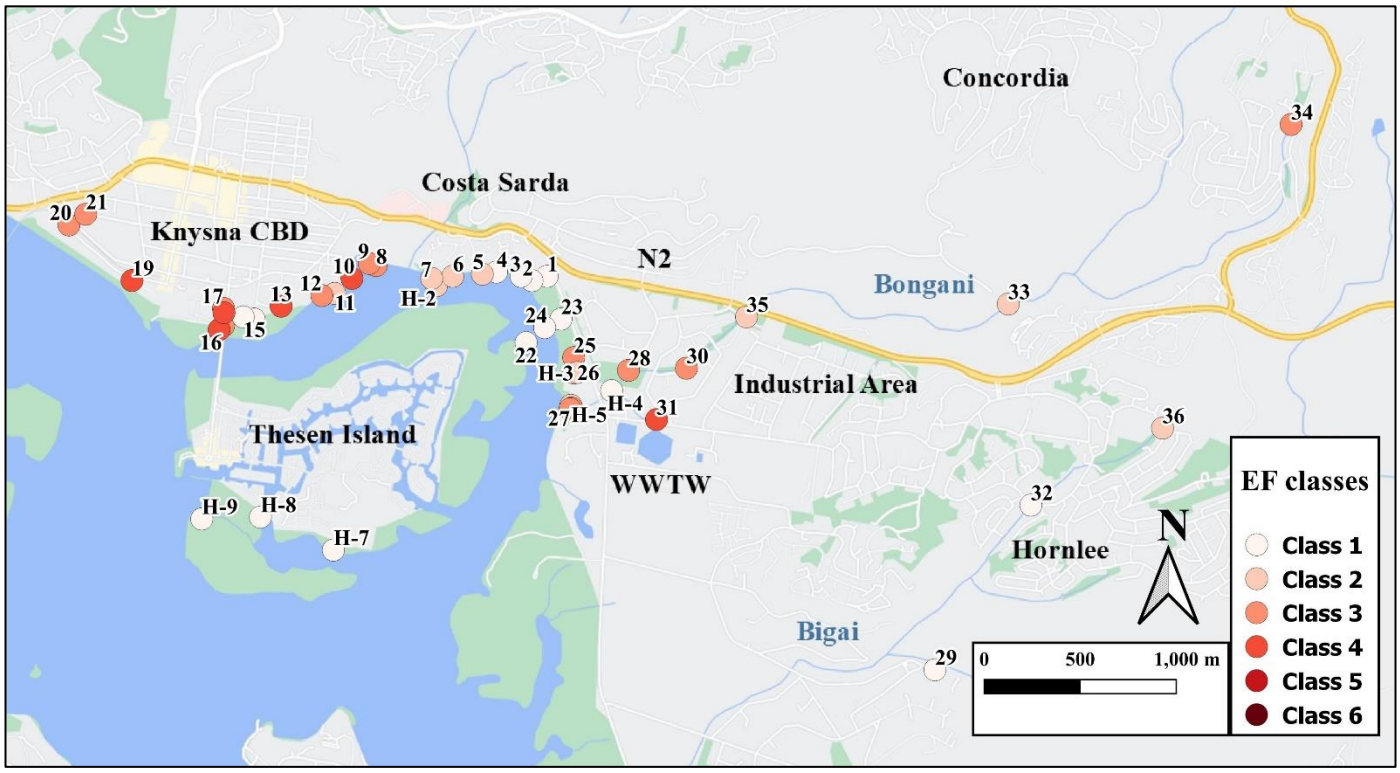

Figure 5.7: Map representing the EF categories of Cu from the 2018 and 2019 sampling in Knysna (Google Maps, 2021)

EF results for the Ashmead Channel area from 1977 to present

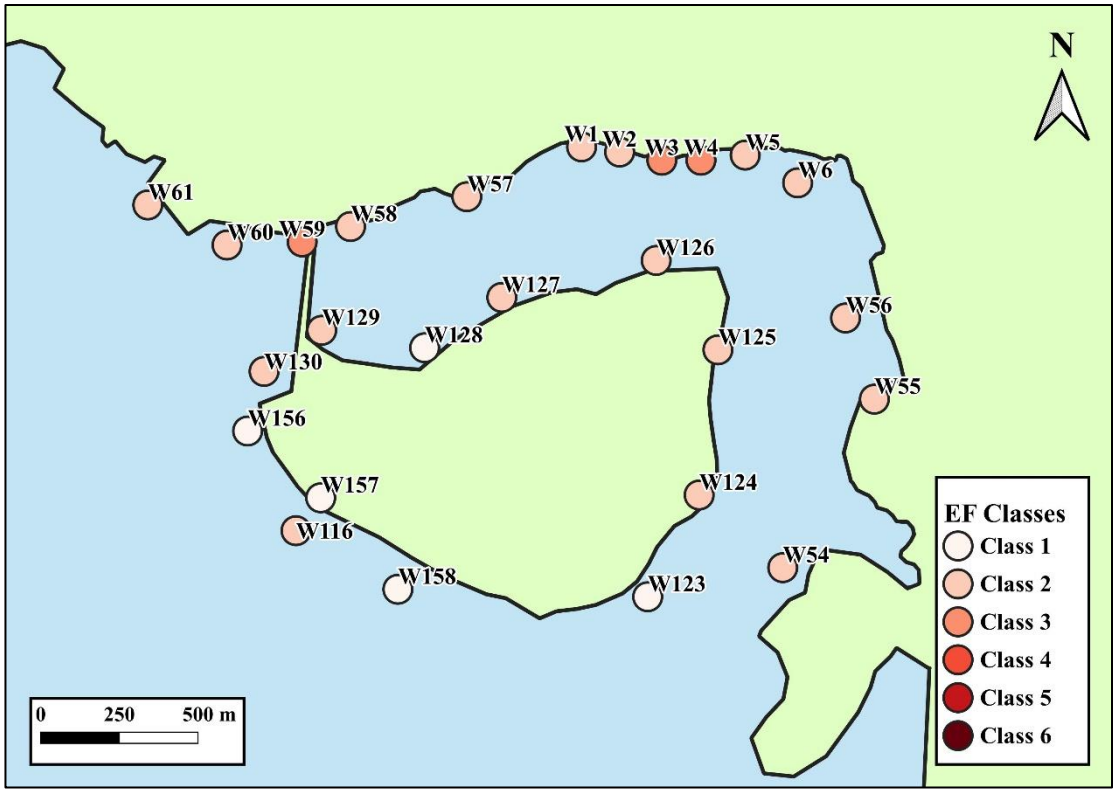

Figure 5.8: Cr EF map for Watling (1977), (SANParks, 2020)

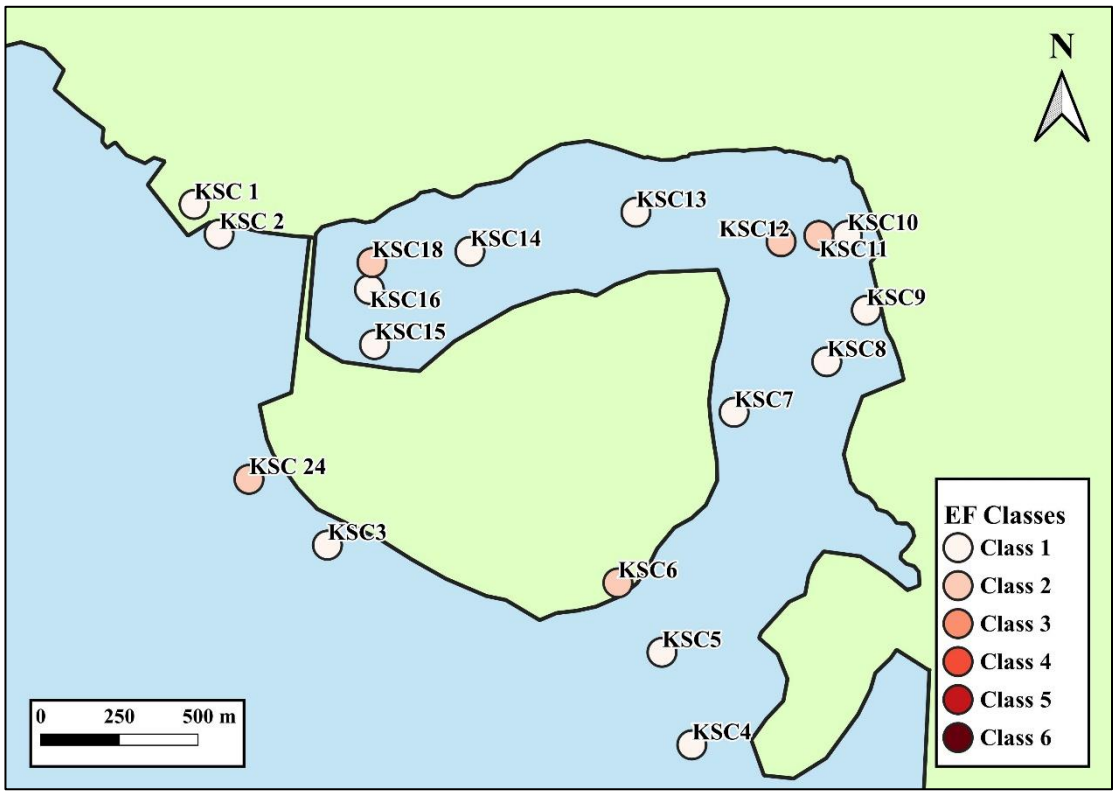

Figure 5.9: Cr EF map for CSIR (2000) (SANParks, 2020)

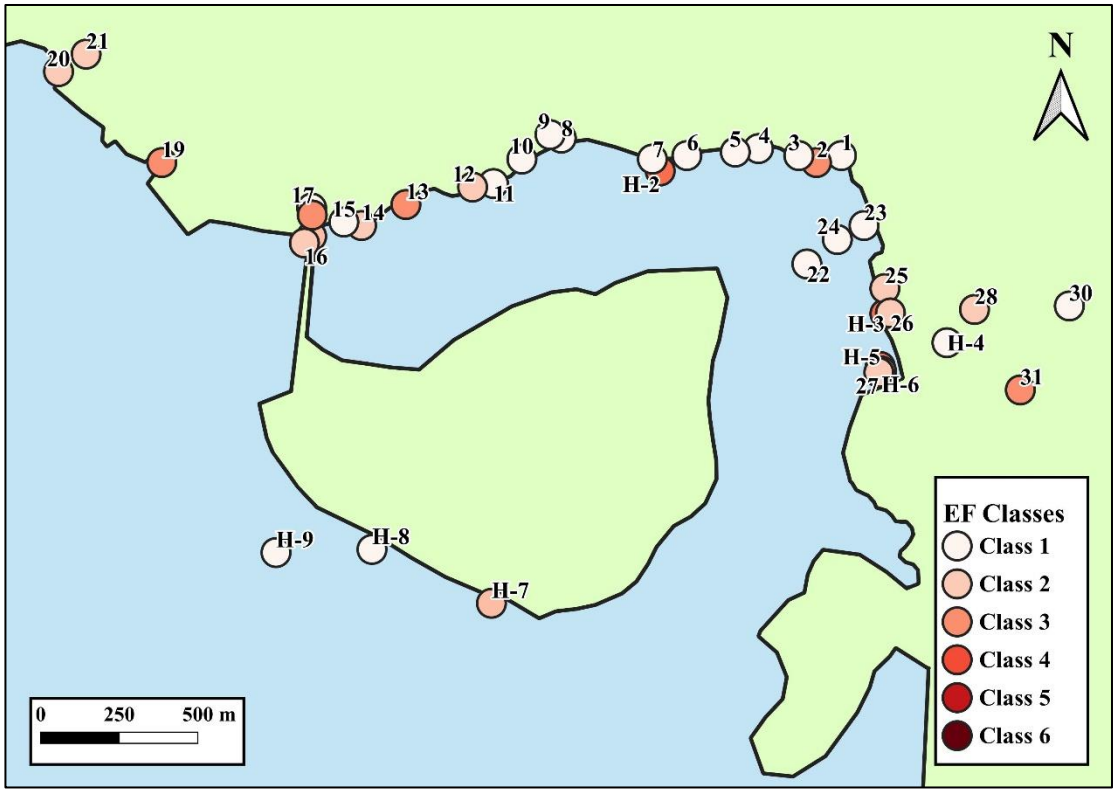

Figure 5.10: Cr EF map of 2018-2019 results (SANParks, 2020)

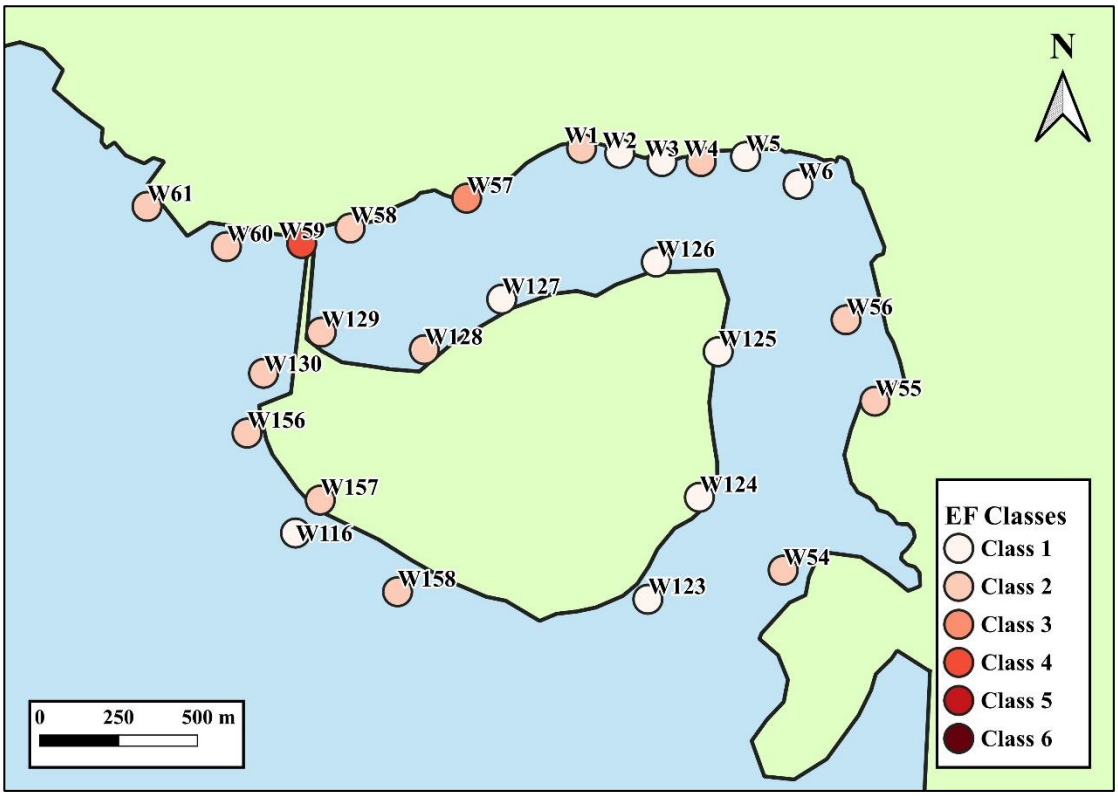

Figure 5.11: Zn EF map for Watling (1977) (SANParks, 2020)

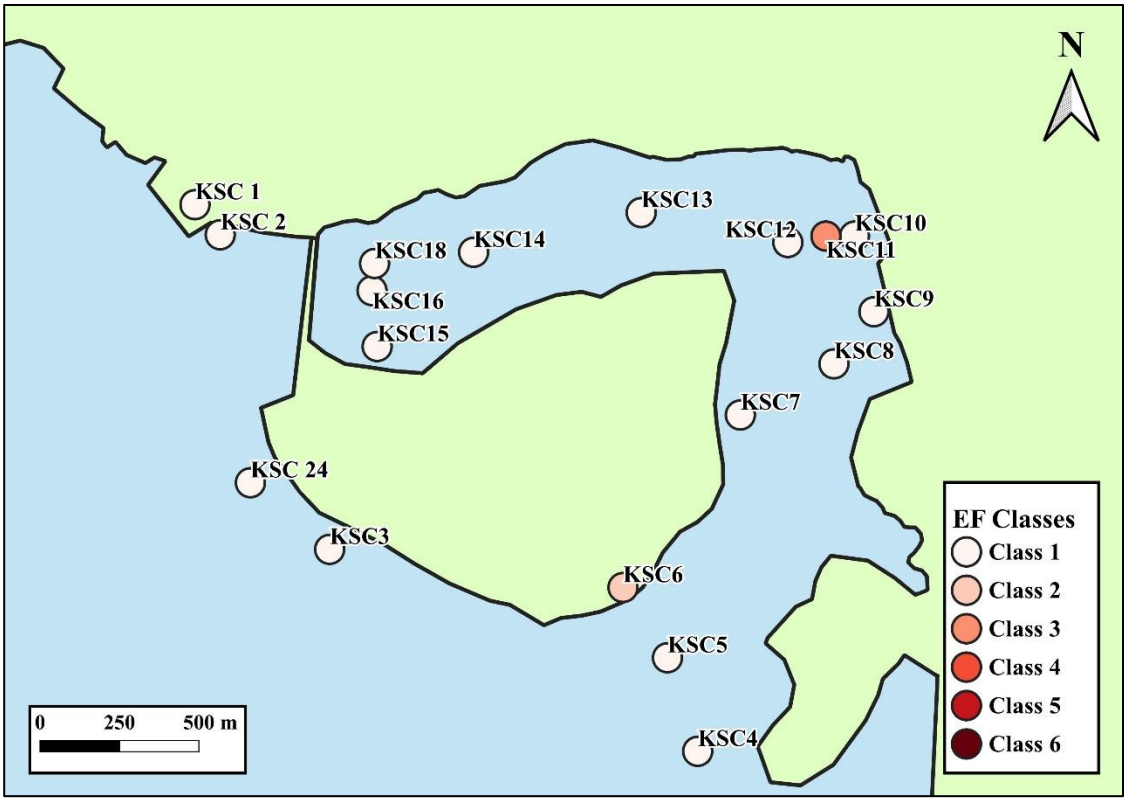

Figure 5.12: Zn EF map for CSIR (2000) (SANParks, 2020)

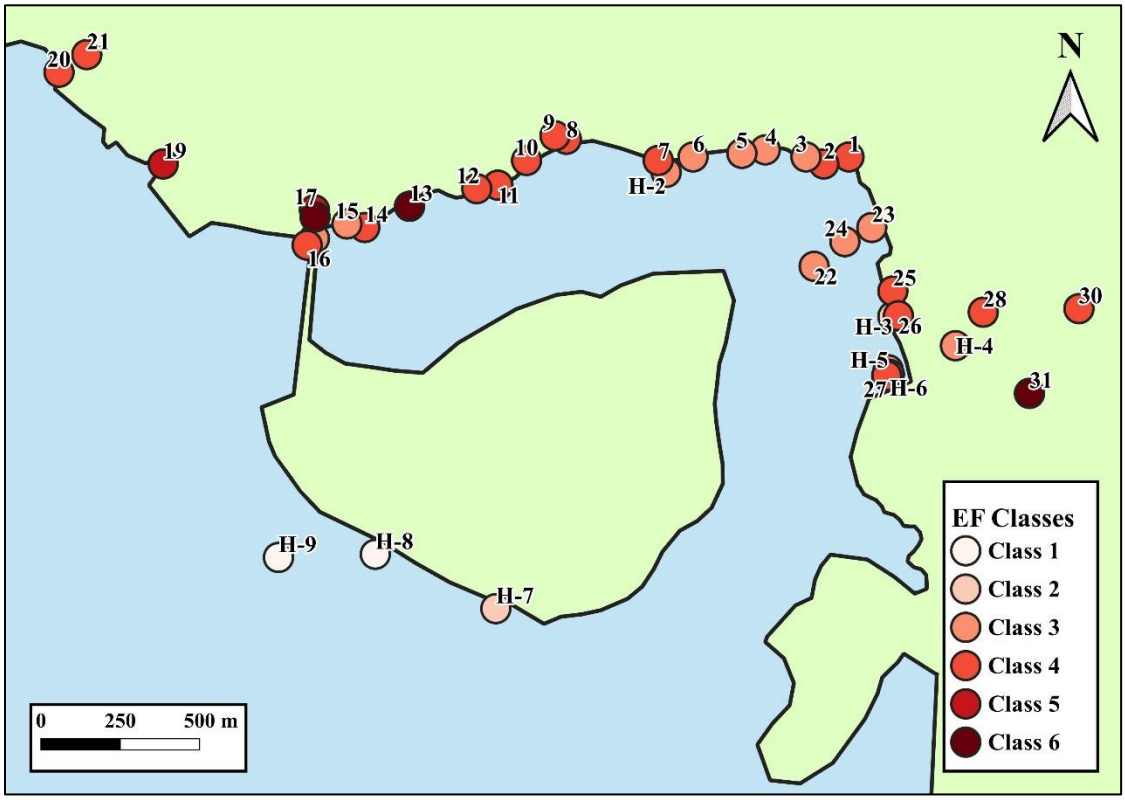

Figure 5.13: Zn EF map for the 2018-2019 sampling period (SANParks, 2020)

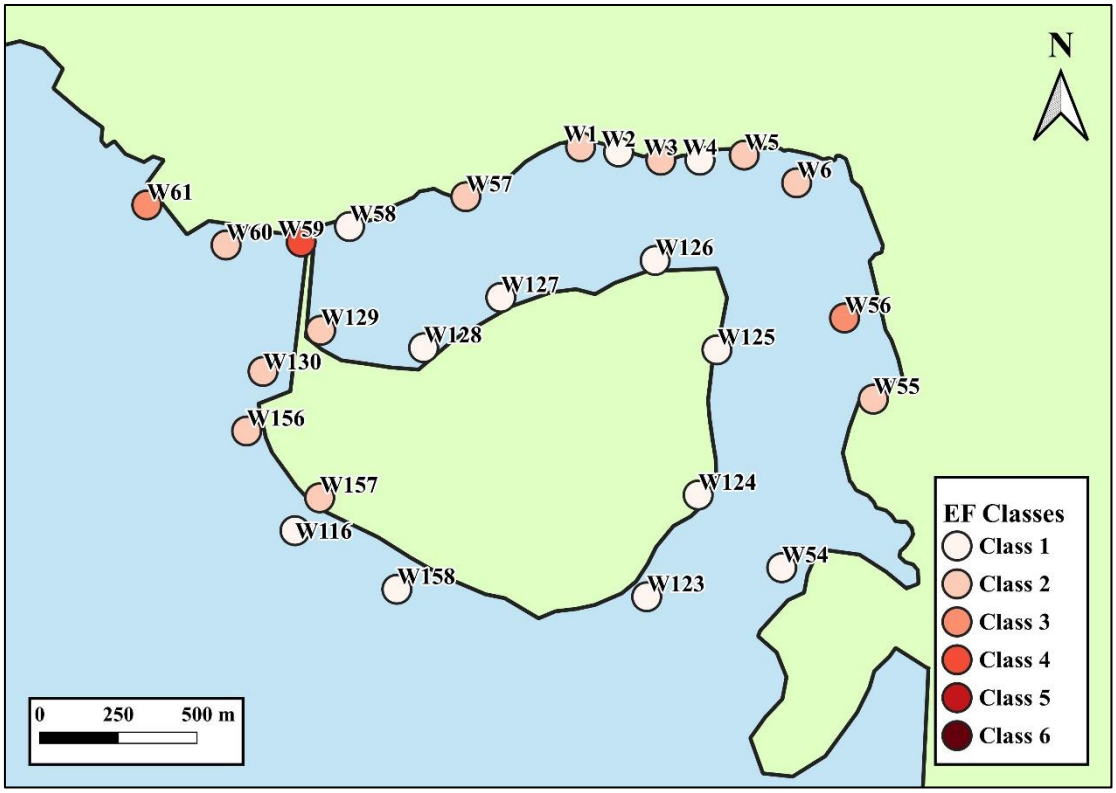

Figure 5.14: Cu EF values for Watling (1977) (SANParks, 2020)

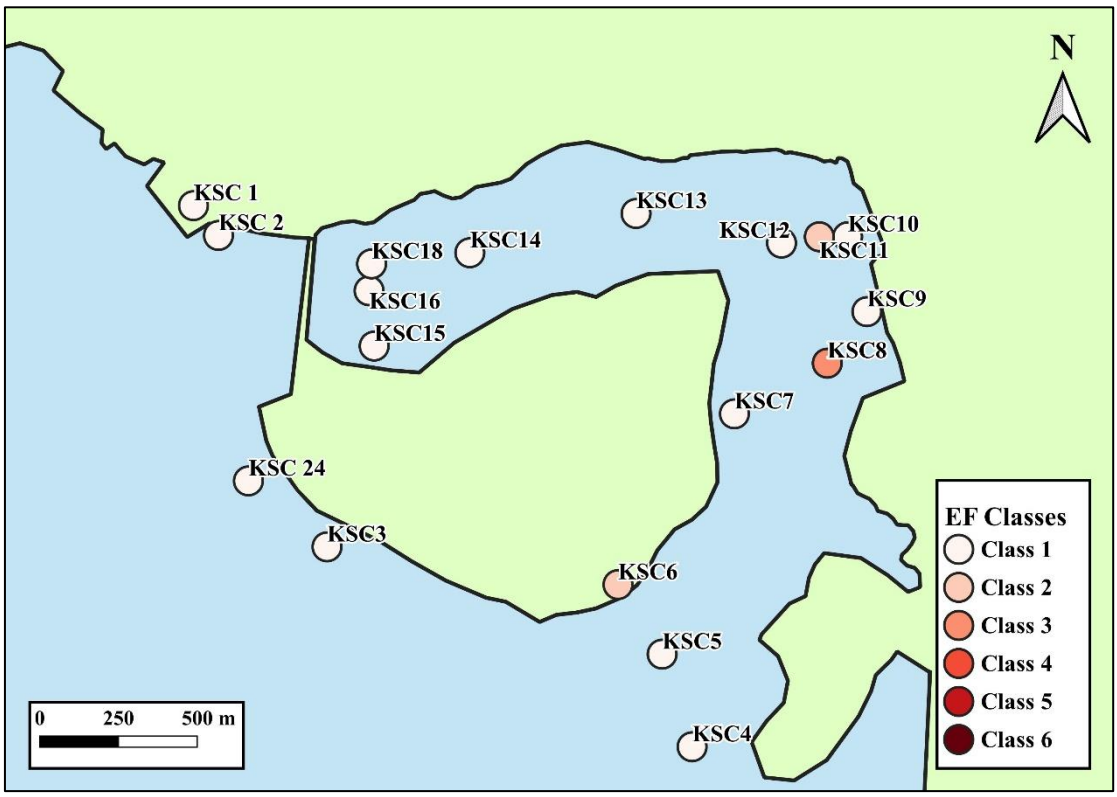

Figure 5.15: Cu EF values for CSIR (2000) (SANParks, 2020)

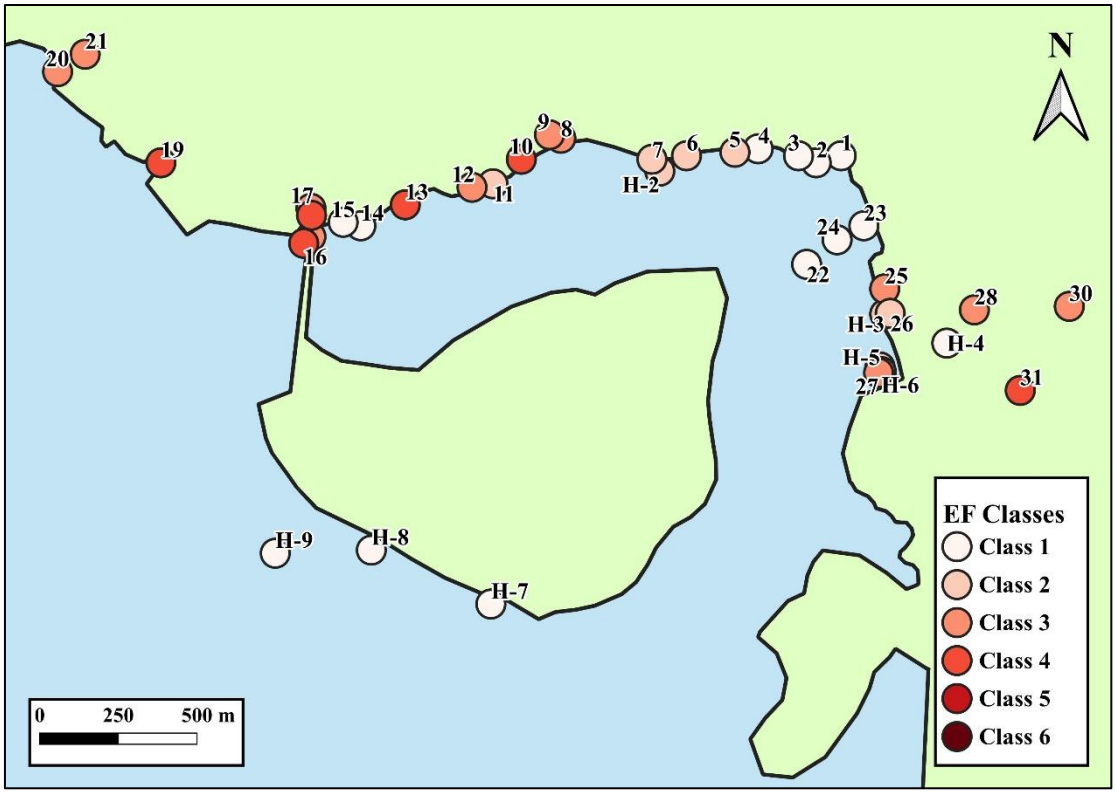

Figure 5.16: Cu EF values for the 2018-2019 sampling period (SANParks, 2020)

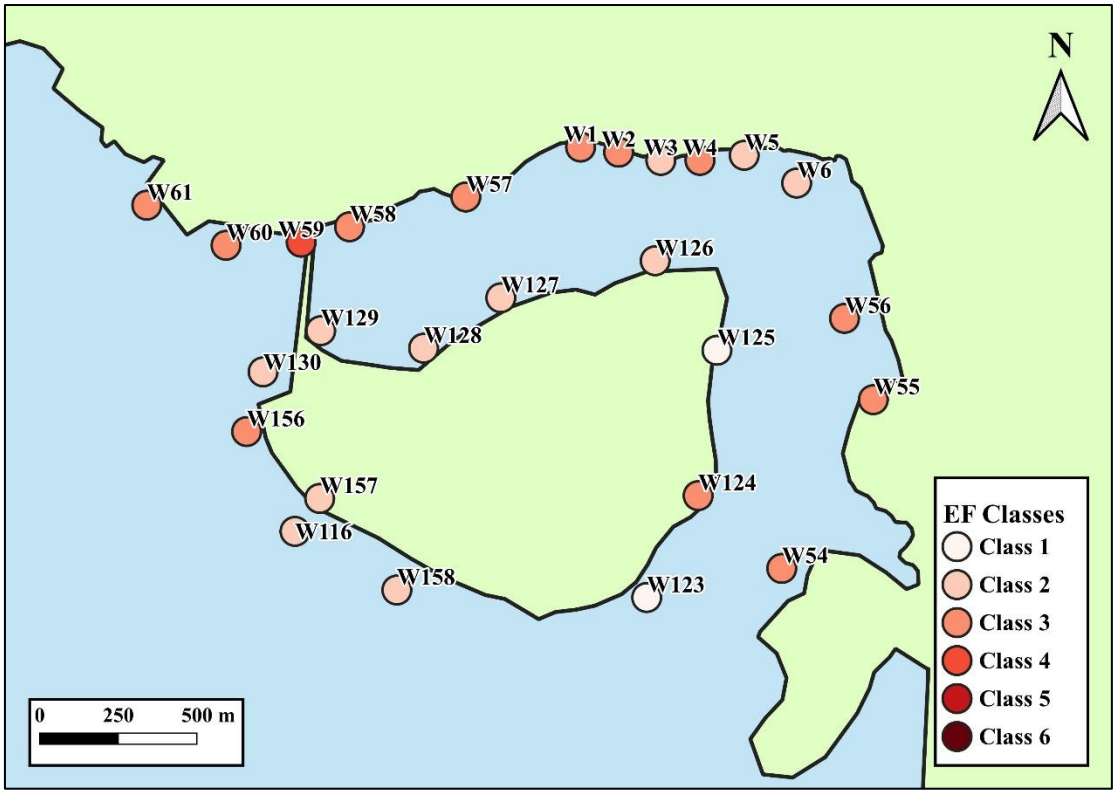

Figure 5.17: 1977 Pb EF values for the Ashmead channel (SANParks, 2020)

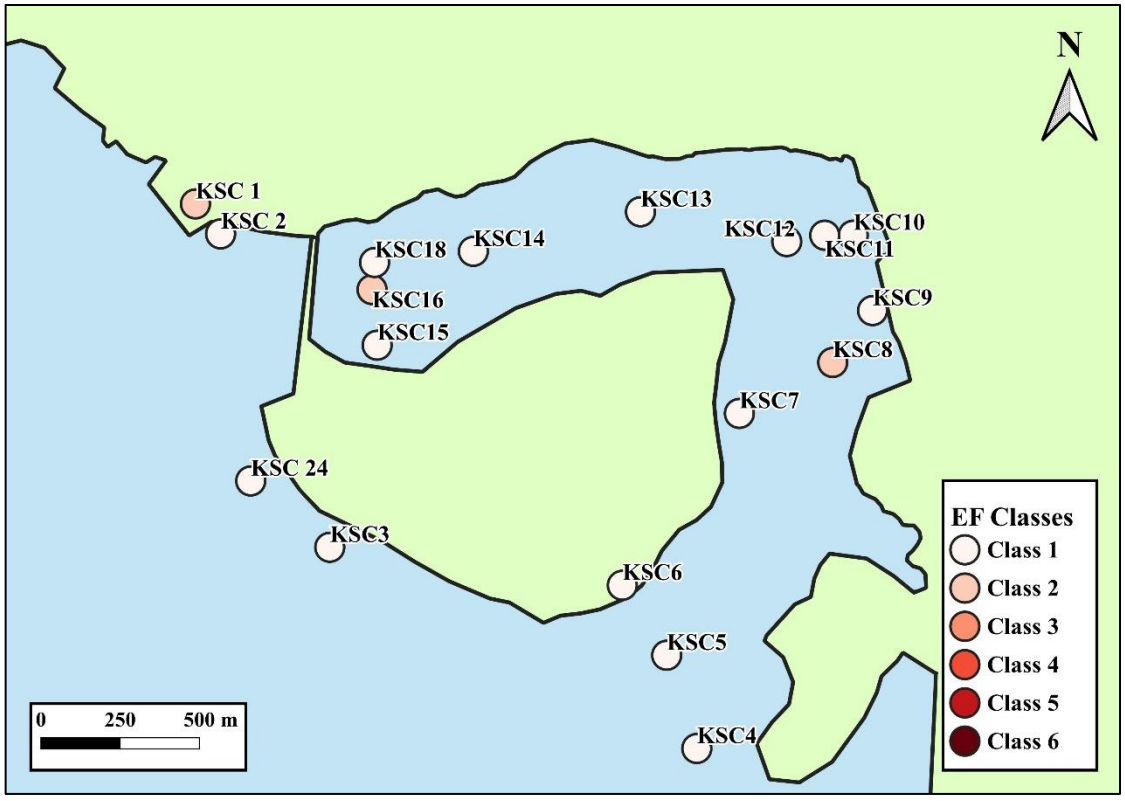

Figure 5.18: Pb EF values for the CSIR 2000 (SANParks, 2020)

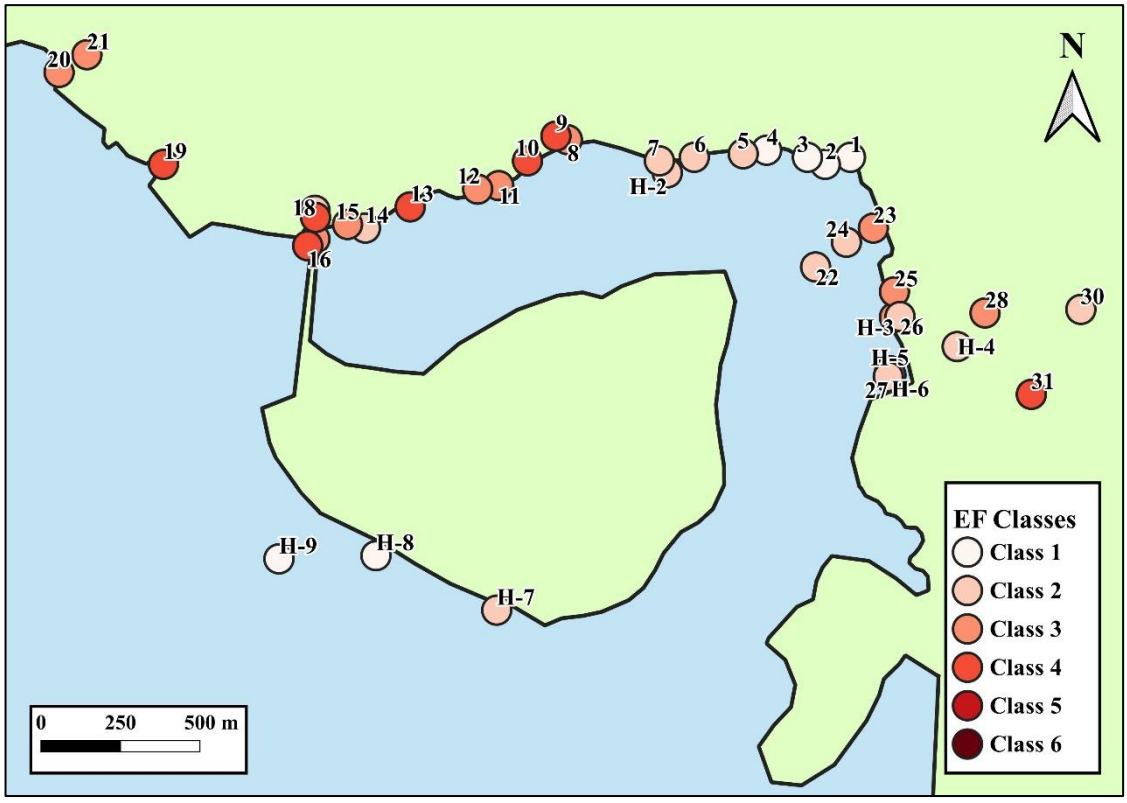

Figure 5.19: Pb EF values for 2018-2019 sampling period (SANParks, 2020)

5.5.3 Overview of 2018-2019 results

The 2018-2019 enrichment factor results are presented in **Tables 5.12** and **5.13 (Appendix B),** in addition to **Figures 5.4-5.7,** and show several interesting trends. From these normalized results, it is clear that, of the metals analyzed, Cr exists in concentrations closest to the background concentrations for the region. Zn contamination in the Ashmead is the highest, with EF classes of 3-5 being prevalent throughout the system. The results show that Cu and Pb are also significantly enriched in the system, albeit to a lesser degree than Zn.

The distribution of contamination within Knysna seems to be consistent between the metals, with the most significantly contaminated regions being found on the eastern side of the channel near the outflow of the industrial area, the Bongani Stream and WWTW, in addition to the sites adjacent to the Knysna CBD in the north-west of the Ashmead Channel.

The Costa Sarda area to the east of the main town of Knysna shows relatively little heavy metal contamination, which is consistent for all the metals besides Zn, which is still marginally enriched The area to the South of Thesen Island has no heavy metal enrichment. The samples from the Bongani Stream appear to be mostly non-enriched, except for Zn. There appears to be a small heavy metal hotspot at Site 34 in the upper Bongani which does not appear to continue downstream. The Bigai Stream System appears to be relatively unpolluted from the small number of samples taken, with slight Zn enrichment present in the upper Bigai at Sites 32 and 36, and Pb enrichment at Site 36. The Bigai Mountain Stream Tributary (Site 29) appears to have no heavy metal enrichment.

5.5.4 Trends in EF values from 1977 to present

The following section describes the trends in the EF values of each element between the three sampling periods, first the 1977 results from Watling & Watling, then the CSIR study from 2000 and finally the results from the 2018-2019 sampling within this study. It must be noted that the sampling points are not symmetrical for each study, with the 2000 CSIR study being most notable as it has a distinct lack of sampling sites from the north Ashmead close to the Knysna CBD.

Chromium

Cr enrichment appears to be consistent throughout the time series, with minimal-to-no enrichment present over the past 40 years. There may even have been a reduction in Cr enrichment from the 1977 paper, particularly for the Costa Sarda area of the channel (**Figures 5.8-5.10, Tables 5.12-5.15**). Cr, therefore, does not seem to pose a threat in the Knysna estuary.

Zinc

Zinc enrichment within the Ashmead Channel appears to show an opposite trend to that of Cr, with minimal enrichment present within the 1977 and 2000 studies, yet a very high degree of enrichment present in the 2018-2019 sampling (**Figures 5.11-5.13, Tables 5.12-5.15**). In the recent analysis, the entire Ashmead Channel and surrounds have some degree of contamination, except for the sites to the south of Thesen Island. The extreme increase in enrichment between **Figures 5.12** and **5.13** is likely exaggerated by the lack of sampling sites from the 2000 study in the North Ashmead. It is concerning that Zn enrichment has increased by such a large amount in the past 20 years, even though the absolute concentrations are still within acceptable ranges for most of the sites.

The most enriched sites are in the lower Long Street Canal, the outlet of the Grey Street Canal, the area south of the Taxi Rank, and the Knysna Industrial Area. This would therefore suggest that the areas that these canals drain are primary sources for Zn in Knysna. Furthermore, the very high EF values at outlets spanning the north and east strips of the Channel suggests that many of the drains are sources for Zn in the system. The Costa Sarda region appears to be the least contaminated, however, Sites 1 and 2, in the vicinity of the George Rex Drive Culvert, would suggest that the surrounding area is also introducing Zn into the system.

Lead

Pb enrichment in the Ashmead Channel shows an interesting trend with time (**Figures 5.17-5.19, Tables 5.12-5.15**). The 1977 study shows a low-to-moderate degree of enrichment with EF classes between 2 and 3 for much of the channel, and higher levels of enrichment at the outflow of the Long Street Canal. The concentrations appear to have lowered by the time of the 2000 study, with all but two of the sites being EF class 1 and two being EF class 2, indicating an uncontaminated system with respect to Pb. This changes in the current study, in which Pb has a high level of enrichment through much of the channel. The most contaminated regions are found adjacent to the Knysna CBD and at the outflow of the Bongani/WWTW/Industrial Area. The Costa Sarda area has much lower levels of Pb enrichment than the main town, with all the sites being either in EF class 1 or 2. The East Ashmead sites are more enriched than Costa Sarda but still significantly less than the CBD, with EF classes between 2 and 3. The Vigilance Drive Canal is a local hotspot for Pb, with an EF class of 4, suggesting that the Industrial Area is a likely source of Pb in the area. Since the Knysna CBD is the area with the highest degree of Pb enrichment, it would therefore, suggest that the most significant sources of Pb lie in the vicinity. This Pb is likely introduced into the system through the stormwater drains and canals draining the area.

Copper

Cu enrichment in the Ashmead Channel shows a similar trend to Pb (**Figures 5.14-5.16, Tables 5.12-5.15**), in that small, isolated cases of enrichment are present in 1977, with most of the sites from the perimeter of the channel being EF class 2 (background concentrations), a class 4 site at the Long Street Canal and two class 3 sites, at the Grey Street discharge and near to the outfall of

the Bongani Stream. The area surrounding Thesen Island was almost entirely uncontaminated with Cu at this time.

Cu enrichment seems to decrease by the time of the 2000 study, with most of the sites in the channel being EF class 1, with the exception of a class 2 and a class 3 site in the Eastern Ashmead. Cu enrichment increases drastically in the 2018-2019 results, with the highest levels of enrichment present in the Western Ashmead Channel adjacent to inflows from the main town of Knysna showing EF classes of mainly 3 and 4. Cu shares the same distribution as Pb, with higher enrichment also present in the east of the channel near to the outflow of the Bongani/WWTW/ Industrial Area, (EF classes of 2 and 3) with a class 4 hotspot at the Vigilance Drive Canal.

Cu differs from Pb in that Cu has even less enrichment in the northeast of the channel, with the George Rex Culvert area and cross-Ashmead transect having an EF class of 1 predominantly, whereas the same transect has an EF class of 2 and 3 for Pb. As with the other metals, the area to the South of Thesen Island is not enriched with Cu.

5.6 Per site analysis of heavy metal concentrations

5.6.1 Background

In this section, sites from Knysna are identified on the basis of their predetermined region (**Table 5.1**) and discussed based on their heavy metal signature and level of contamination, and explanations for these signatures suggested. It should be noted that the concentrations are discussed both in terms of absolute contamination (the concentrations compared to pre-determined guidelines for contaminated sediment), and in relative terms by comparing between the site and Knysna as a whole. Therefore, if a site has a high concentration of a specific metal relative to sites from the whole Knysna System or subsystem, this does not necessarily imply that the concentrations are high on an absolute scale. Furthermore, sites are described as either contaminated or uncontaminated. This refers to whether the concentrations are significantly below the guideline "action levels" stipulated within the RNAL guidelines. Furthermore, a site being uncontaminated does not imply that it is free from anthropogenic enrichment. This section also uses the normalised EF values to determine the extent of heavy metal enrichment in the sediments and to better compare the sites.

Finally, this analysis cannot be used to determine if the sediment is dangerously contaminated with heavy metals from a biological health perspective Additionally it is not only possible but very likely that some of these sites are contaminated with other pollutants (such as e-coli or excessive nutrients) that could be harmful, however, determining this is beyond the scope of this study (Harvey, 2019; Human *et al*., 2016). Therefore, an important objective of this section is to identify sites that represent anomalies within the entire Knysna System or sub-section and to discuss potential reasons.

Additionally, it is noteworthy that**,** due to the samples from this study being single point source samples rather than composite samples (which involves taking small samples from a 3-metre radius and combining them), the samples are possibly subject to a degree of sample bias, wherein a sample taken from a few metres away could influence the concentrations, so the trends seen have the potential to be influenced by confounding variables.

5.6.2 Analysis of the Bongani Catchment

The Bongani Catchment (**Figure 5.20**) includes Sites 34 (Upper Bongani), 33 (Bongani downstream of wooded area), 35 (Bongani just downstream of N2 highway), 30 (Bongani Industrial Area) and 28 (Bongani downstream of Industrial Area). The samples from the Bongani are presented due to the interlinked nature of the catchment. Additionally, the samples are

described as a transect from the upper catchment towards the estuary, imitating the flow of the river.

Figure 5.20: Google Earth map highlighting the sampling sites in the Bongani Stream (Google Earth, 2019)

Site 34 (Upper Bongani)

Heavy metal concentrations in the Upper Bongani (Site 34), located in one of the tributary streams of the Bongani, are relatively high, with Cr: 18.0, Cu: 12.6, Pb: 12.6 Zn: 93.6 and Al: 4617. TOC and mean grain size (MGS) are 6.0% and 259.1µm respectively. These concentrations are higher than one would expect so high up in the catchment, and it is proposed that this is a result of heavy metal enrichment due to the low total flow rate of water in this stream in conjunction with a local heavy metal source. EF results show minimal Cr enrichment, moderate Pb and Cu enrichment and significant Zn enrichment. Since this site is in the semi-formal settlement, Joodse Kamp, it is likely that some of these metals are sourced from vehicle repairs taking place there, and that Zn enrichment is contributed to by the runoff from corrugated metal roofs, (Dierkes *et al*., 2006). The TOC at this site is about average for Knysna. The MGS is significantly above the study-wide mean of 173.0µm , which is expected considering that grain size at riverine sites is typically larger than at estuarine sites. This makes the conditions are sub-optimal for heavy metal accumulation. The concentrations are relatively low when compared to RNAL guidelines and the site may be considered uncontaminated.

Site 33 (Bongani downstream of wooded area)

Site 33 is located about 2km downstream of Site 34 and immediately downstream of a thickly wooded area (**Figure 5.21**). The site was selected due to the hypothesis that the overgrown vegetation may have a SUDS effect and could play a role in sequestering heavy metals. It is therefore interesting that the heavy metal concentrations at this site are lower than those seen at Site 34, with Cr: 9.0, Cu: 4.5, Pb: 6.7 and Zn: 41.4 and Al: 3699. TOC is above average at 9.0% and MGS is significantly below average at 118.5μm. This is indicative of above-average conditions for heavy metal accumulation within the Knysna system. The EF values show baseline results for Cr, minimal enrichment for Cu and Pb and significant enrichment for Zn.

Figure 5.21: Site Photograph of Site 33, located downstream of the wooded area in the Bongani

It is apparent that this site has lower heavy metal concentrations and enrichment than the Upper Bongani despite having more ideal sediment characteristics for heavy metal accumulation. This trend could be explained by several factors, with a SUDS effect being a potential partial explanation and a contributing factor to the overall cleanliness of the sediment at Site 33 It is, however, more likely that there is a dilution effect occurring in the Upper Bongani, where several tributaries converge to form the Bongani River which dramatically increases the total volume of water flowing downstream, thus diluting the more heavy metal-laden waters of a single tributary such as the one seen at Site 33 (Chen *et al*., 2004). It is interesting to note that the extent of Zn

enrichment is similar to Site 34, indicating that the other tributaries may also be similarly contaminated with Zn. In summary, this site has very low heavy metal concentrations and is not considered contaminated.

Site 35 (Bongani Downstream of the N2 Highway)

As the Bongani flows downstream from Site 33, the river receives some effluent from the Organic Waste Dump Site located upslope to the north. The river then flows for about one kilometre before passing under the N2 highway where it receives direct runoff from this highly trafficked roadway (**Figure 5.22**). Site 35 is located in a pool about 30 metres downstream of the highway crossing point, a short distance upstream of a waterfall. This pool, in which the flow is temporarily slowed, is visually peculiar as the sediment is grey and is colonised by unidentified larvae. Downstream of the pool is a large amount of foam, which gathers below the waterfall. According to members of the Knysna municipality, a thick layer of this foam is always present in this pool, and may be indicative of large volumes of domestic cleaning products being suspended in the water.

Figure 5.22: Photographs showing Site 35, located downstream of the N2, Left: a demonstration of the sampling process. Right: a close-up view of the organic matter present in the sediment

Site 35 has slightly higher heavy metal concentrations than those seen at Site 33 with the exception of Pb which is essentially the same, with Cr: 15.9mg/kg, Cu: 8.0 mg/kg, Pb: 6.4 mg/kg, Zn: 63.6 mg/kg and Al: 7600 mg/kg. TOC is below average at 4.5% while MGS is approximately average at 186.3µm and. This indicates that the conditions for heavy metal accumulation at this site are approximately above average for Knysna as a whole and very good for riverine sediment. This is largely due to the very high Al concentrations present here, which is indicative of large quantities of clay.

The site has minimal EF enrichment for Cu, Pb and Cr. The moderate Zn enrichment is lower than the enrichment at Site 33, despite the higher HM concentrations. This is also predominantly due to the high Al concentrations at this site. The low flow in this pool likely allows for the deposition of finer-grained clay particles containing these metals. From the EF results, it is not possible to identify a direct increase in contamination from the N2. The absolute concentrations at this site are still very low for all metals, when compared to the RNAL guidelines and the sediment should therefore be considered non-contaminated.

Site 30 (Bongani upstream of the Industrial Area)

Site 30 is located under a small wooden pedestrian bridge alongside the Industrial Area, about 400 metres southwest of the N2 (**Figure 5.23**). This site is located upstream of the major effluent discharge points of the Industrial Area and was selected as a comparative site in order to assess the impact that the Industrial Area is having on the state of heavy metal contamination in the Bongani. Heavy metal concentrations at Site 30 are Cr: 5.4mg/kg, Cu: 7.4mg/kg, Pb: 4.9mg/kg, Zn: 65.1mg/kg and Al: 2222mg/kg. This is nearly the same as Site 35, with the exception of Cr, which is much lower here than upstream. TOC is 4.6%, which is the same as Site 35. MGS is 232.4μm which is higher than at Site 35. The vastly lower Al concentration here are indicative of less ideal conditions for H.M accumulations. The EF results show that Site 30 has no Cr enrichment, minimal Pb enrichment, moderate Cu enrichment and significant Zn enrichment. The concentrations of these metals are very low when compared to the RNAL action levels, and therefore this sediment is non-contaminated.

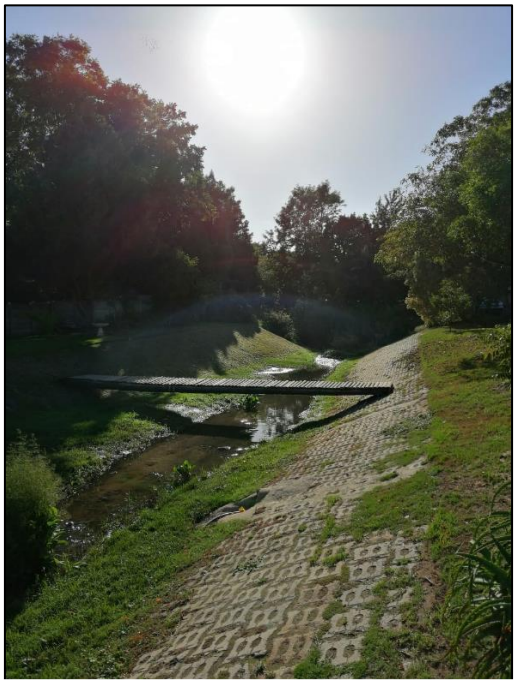

Figure 5.23: Photograph showing Site 30 located upstream of the Industrial Area

Site 28 (Bongani downstream of the Industrial Area)

Site 28 is located 250m downstream of Site 30 and receives effluent from the Industrial Area via stormwater channels and surface runoff. The concentrations at Site 28 are amongst the highest in the Knysna system, with Cr: 14.2mg/kg, Cu: 11.5mg/kg, Pb: 10.8mg/kg, Zn: 121mg/kg, and Al: 6035mg/kg. TOC and MGS are 19.2% and 33.3μm respectively. This is interesting as it shows that there is a large difference in metal concentrations over a short stretch of river, with roughly a doubling in total heavy metal concentrations between the two sites for almost all metals. This pattern may be partially indicative of the quality of the sampling site. Site 28 has more reeds and a slower overall flow, resulting in a vastly larger TOC and lower grain size, in addition to a higher Al concentration which provide a much more ideal site for heavy metal accumulation and higher background concentrations.

EF results show minimal Cr enrichment, Moderate Pb and Cu enrichment and Significant Zn enrichment. These results are interesting as they indicate that the higher concentrations do not solely exist as a result of sedimentary background levels because in addition to having relatively high HM concentrations and high Al concentrations, there is still enrichment. It is therefore likely that some of the enrichment at this site occurs as a result of contamination from the Industrial Area. This site is non-contaminated with respect to the RNAL guidelines.

Site 31 (Vigilance Drive)

Site 31 is located to the south-east of the Industrial Area in the Vigilance Drive Canal and drains much of the stormwater from the Industrial Area (**Figure 5.24)**. The Canal discharges first into the Bongani before finally discharging into the Ashmead Channel and is hence included in this section. Samples were collected downstream of a litter trap.

This site is one of the most contaminated sites in this study with Cr: 22.8mg/kg, Cu: 30.4mg/kg, Pb: 12.2mg/kg, Zn: 182mg/kg and Al: 1535mg/kg. This site has a TOC of 1.4% and a MGS of 308.7μm. With such a low TOC percentage, large mean grain size and low Al concentration, this sediment is not ideal for heavy metal accumulation, and it is therefore interesting that the concentrations are so high.

Site 31 also has a similar, although higher, heavy metal signature to the one seen at Site 28, even though the conditions at Site 28 are much more suitable for heavy metal accumulation. This is interesting as both of these sites receive effluent directly from the Industrial Area. EF values at Site 31 show moderate Cr enrichment, Significant Cu and Pb enrichment and extremely high Zn enrichment, which make it one of the most enriched sites in this study. Consequently, it is reasonable to assume that the sediment at these two sites is being enriched from the Industrial Area. Zn concentrations at this site are above the RNAL action level concentration of 150mg/kg. Other heavy metal concentrations at this site are still relatively low according to the same guidelines.

The concentrations seen at the Site 31 likely signify much more severe contamination. An obvious explanation for the difference in heavy metal concentrations between sites adjacent to the Industrial Area is that there are more contaminants released on its southern side. Another probable explanation is a dilution effect converse to the dilution of heavy metal-laden water in the upper Bongani as previously discussed. The relatively stagnant waters of the Vigilance Drive Canal are further slowed by the litter trap, and due to this low energy flow, the majority of the sediment carried by the water is deposited immediately upon entering the canal. This results in a relative intensification of heavy metal concentrations. It may be inferred that the contaminant load entering both the Bongani (at Site 35) and the Vigilance Drive Canal (at Site 31) may not necessarily differ.

Figure 5.24: Photographs showing the litter net on Vigilance Drive (left), and the sampling site (right), located about five metres downstream of the net

5.6.3 Bongani summary

Several sources of heavy metals are present along the course of the Bongani. In its upper courses, possible sources include the car mechanic workshops and roof runoff (Watling, 1978; Dierkes *et al*., 2006). The primary contaminant at this point is Zn. The river then runs through/along a small, wooded area before passing beneath the N2. No increase in enrichment is noticeable at this site. The Bongani then receives effluent from the northern side of the Industrial Area and the Vigilance Drive Canal prior to discharging into the Ashmead Channel. Despite concentrations being high at some of these sites, these findings are likely not representative of the whole system, but rather indicative of sources of contamination in the immediate vicinity.

5.6.4 Analysis of the Bigai system

Background

The Bigai Stream is a small stream located to the south-east of the Ashmead Channel, which has its headwaters in several mountain springs located near the informal and semi-formal settlement of Hornlee, approximately 3km East of the Ashmead Channel. It ultimately discharges into a large reeded wetland, known as the Bigai Wetland (**Figure 5.25**). The Bigai region within this study comprises only 3 Sites; 36, 32 and 29. The sparse sampling of the Bigai is due to several constraints and has resulted in gaps in the data. Constraints include limited access to various areas of the catchment due to vegetation overgrowth, private property laws and limited knowledge of the system. Additionally, sampling sites and analytical resources were focussed on the Bongani system which received priority due to the proximity of contaminant sources to the system.

Figure 5.25: Google Earth map of the sampling sites in the Bigai River system, with the river catchment included (Google Earth, 2020)

Sample 29 (Mountain Stream)

Site 29 is located in a small mountain tributary stream of the Bigai and seemed to be very visually clean when sampling. This sample had negligible concentrations for almost all heavy metals, with Cr: <1, Cu: <1, Pb:<1, Zn: 1.3 and Al: 512. The sample has very large MGS and low TOC, with TOC: 0.6% and MGS: 453.9μm, therefore the sample was not ideal for heavy metal accumulation and may contribute to why the concentrations were so low. EF values for this site show baseline

concentrations for all the metals. The concentrations at this site are all so low that this site can be considered clean and completely non-contaminated.

Site 36 (Upper Bigai)

Site 36 is located in a tributary of the Upper Bigai, near to its source at a mountain spring. This site has heavy metal concentrations of Cr: 16.6, Cu: 4.5, Pb: 8.9, Zn: 30.3, Al: 5180. These concentrations are higher than expected so high in the catchment. This is likely due to the sample being taken from a semi-informal settlement and was thus likely contaminated by local human activities, like those seen in the Bongani catchment. EF values from Site 36 show baseline Cr enrichment, minimal Cu enrichment and Moderate Pb and Zn enrichment. Moreover, due to the relatively low amount of flow in the river, there is likely a local intensification of enrichment in this sediment, making it probable that the concentrations dilute along the steams lower course. The concentrations are very low relative to the RNAL action levels and hence this site is non-contaminated.

Site 32 (Sunridge Street)

Site 32, located in the Upper Bigai alongside Sunridge Street, has metal concentrations that are close to negligible for all metals. Mean grain size and TOC values are similar to Site 36, with Cr: 1.8, Cu: <1, Pb: <1, Zn: 8.9, and Al: 1006. TOC and MGS were 2.8% and 212.3µm respectively. The EF values of Site 32 show baseline enrichment for Cr, Cu and Pb and moderate Zn enrichment. Interestingly, the concentrations are orders of magnitude lower than those seen at Site 36. This may be caused by a lack of HM inputs and through the dilution effect of other tributaries providing clean, uncontaminated water (and sediment) into the system. It does appear that there is a source of Zn enrichment in the area, which is possibly linked to corrugated metal roofs. The concentrations are low relative to the RNAL levels and the site is non-contaminated.

5.6.5 Overview of the Eastern Ashmead Region

Background

The eastern area of the Ashmead Channel (**Figure 5.26**) ranges from Sites 22 to 28, north to south, the region includes all the samples collected south of the George Rex Drive Culvert, in addition to the transect across the channel which was collected to mimic the transect sampled by Monteiro *et al.* (2000) and extends south to include the samples collected from the discharge point of the Bongani River and WWTW.

This region represents the intersection of a large number of factors and inputs, including the Bongani Stream, the WWTW, and the Vigilance Drive Canal, all of which have their associated issues and dynamics. The Bongani, as mentioned in the previous section, has varied heavy metal concentrations occurring as a result of contamination in the upper catchment, potential further

contamination from the N2 and effluent from the industrial zone, which occurs prior to depositing some sediment into a retention pond and then finally discharging into the Ashmead Channel.

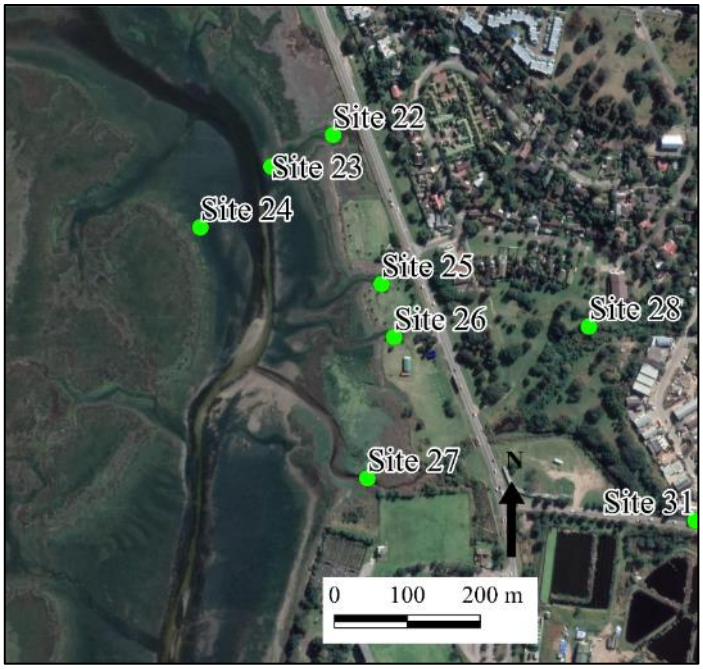

Figure 5.26: Google Earth site map of the Eastern Ashmead Region (Google Earth, 2020)

Figure 5.27: Photograph displaying the warning sign concerning health risks associated with the contaminated water of the Ashmead.

To date, there has been no definitive evidence showing that the WWTW is contaminating the system with heavy metals, however, multiple sources show that it has been a major source of e-coli and nutrients into the Ashmead, which has led to dangerous algal blooms and eutrophication in recent years (Human *et al*., 2016; Harvey 2018). This nutrient pollution is threatening local species, in addition to the e-coli which can pose a health risk to the humans utilizing the space as it acts as a vehicle for pathogens and water-borne diseases, which is especially concerning since the area is well utilized for bait pumping and recreational activities.

In recent years, the situation has become so dire that the municipality placed a signpost warning residents against utilizing the space due to the aforementioned health risks (**Figure 5.27**). Finally, the region also receives effluent from the Vigilance Drive Canal, which is the primary drainage channel for the Industrial Area and has some degree of heavy metal contamination. Corporately, the East Ashmead would be expected to be the area of the estuary with the greatest amount of input of potentially contaminated sediment and water.

Sites 22, 23 and 24 (Cross-Ashmead Transect)

The transect, including Sites 22, 23 and 24 (**Figure 5.28**), sampled across the central channel, shows near negligible concentrations for the key metals, with Cr <6mg/kg for all 3 sites. Cu is 1.6mg/kg at site 22 and <1mg/kg for Sites 23 and 24. Pb concentrations are also low, with concentrations of 3.7mg/kg, 7.1mg/kg and 3.1mg/kg respectively. Zn concentrations are also very low for the Knysna system, with respective concentrations of 16.4mg/kg, 11.4mg/kg and 15.1mg/kg. TOC values at these sites were 2.3%, 1.4% and 1.8%, which is very low for the system. MGS values were 173.5µm, 236.4µm and 170.4µm, which is average for this study, with Site 23 being marginally above average, likely due to its location in the centre of the channel and exposure to greater flow. The suitability for heavy metal accumulation of these three samples is roughly average for the system, with the low TOC values slightly reducing its suitability. EF values for the transect show baseline enrichment for Cr and Cu, with moderate enrichment for Zn for all three sites. Pb is more interesting, with moderate enrichment at site 22 and minimal enrichment for sites 23 and 24, with enrichment decreasing across the channel. In summary, these three samples have very low heavy metal concentrations and are considered non-contaminated.

Figure 5.28: Photographs showing the sample locations of the transect across the Ashmead Channel. Left: Site 22 Right; Site 23.

Sites 25 and 26 (East Ashmead Channel Rivulets)

Sites 25 and 26 are located in small rivulets and estuarine channels which weave into the area to the east of the Ashmead Channel. They drain stormwater from the east of Knysna and appear to have tidal backflows during specific times of the day. Interestingly, they are located near the main effluent discharge points mentioned earlier in this section. Site 25 has concentrations of Cr: 5.7, Cu: 3.5, Pb: 5.6 and Zn: 27, which are all low. Site 26 has Cr: 6,5, Cu: 1.7, Pb: 3.3 and Zn: 14.3, which are also very low concentrations. Finally, Site 27 has Cr: 7.4, Cu: 7.4, Pb: 4.4 and Zn: 37.7, slightly higher than the previous two samples, but still very low.

Site 25 has EF classes of 2 for Cr, 3 for Cu and Pb and 4 for Zn, whereas site 26 has EF classes of 2 for Cr, Cu and Pb and 3 for Zn. These two sites show that the East Ashmead is enriched with Zn, and it is noteworthy that enrichment is more severe in the channel at Site 25 than at Site 26. A theory for these low concentrations is given in the following section, which highlights the Bongani Outlet.

Site 27: The Bongani, Vigilance Drive and WWTW Outlet

Site 27 is adjacent to a channel draining runoff from the Bongani, the WWTW and the Vigilance Drive Canal, which converge immediately upstream. As a result, it may be expected that this site shows relatively elevated heavy metal concentrations, but surprisingly they are low. Heavy metal concentrations at this site are; Cr: 7.4, Cu: 7.4, Pb: 4.4 and Zn: 37.7. These concentrations are slightly higher than those seen at sites 25 and 26 yet still very low when compared to many of the other sediments from the catchment. TOC and MGS are 8.3% and 134.9μm respectively, which is an above average TOC value and below average value for MGS, rendering this sediment more suitable for heavy metal accumulation than the system as a whole, which is typical of the estuarine samples. Site 27 has EF classes of 2 for Cr, 3 for Cu, 2 for Pb and 4 for Zn, indicating a similar degree of enrichment to the previous two outlet samples, despite the low absolute heavy metal concentrations.

The absolute heavy metal concentrations are lower than expected when considering the concentrations upstream, which may be due to a dilution effect.

Samples 25, 26 and 27 were largely composed of dense, water-logged organic sludge to a depth of at least 50cm. Due to the substantial influx of nutrients into the area (Harvey, 2019, Human et al., 2016), organic matter is accumulating at a greater rate than the rate of sediment deposition, which leads to a dilution of the heavy metal concentrations and a short time of exposure to the flow of the channel.

The composition of the mud impacted the quality of the sediment sample collected at this site. Once the sample was dried, as described in section 4.2.1, the volume had been reduced to the extent that it was insufficient for optimal TOC and GS analyses and reduced the accuracy of these results in relation to the other samples. In future studies, a greater volume of sample should be collected from any similarly water-logged sites to ensure that enough sediment is present for analysis. The calculation of moisture content prior to loss of ignition might also prove valuable in testing this hypothesis. These factors suggest that while the results indicating absolute heavy metal concentrations in the sample are low, there may be greater heavy metal contamination in reality, which is corroborated by the EF results.

Overall, the heavy metal concentrations in the sediment at Site 27 all very low relative to the RNAL guidelines and not indicative of contamination.

5.6.6 Overview of the Northern Ashmead Region

Background

The Northern Ashmead Region, comprised of Sites 1-7 (**Figure 5.29**), is valuable as it is the most diverse region in the study in terms of riverine and low flow estuarine samples.

This region is near the null point of the channel, which is the area of the channel least circulated by the tide. (Largier, 2000). The flow in this region of the estuary is further slowed by the Thesen Island Causeway. For these reasons, the most suitable sites for the accumulation of sediments and heavy metals are in this region.

Figure 5.29: Google Earth map showing the sites comprising the Northern Ashmead Region (Google Earth, 2020)

Site 1: The George Rex Culvert

Site 1, located in the stream which passes under the Culvert on the corner of the Ashmead Channel and George Rex Drive (**Figure 5.30**), is a riverine sample and has negligible concentrations of all metals except Zn, with Cr: <1 Cu: <1, Pb: <1 and Zn: 21.9mg/kg. Al, MGS and TOC were 1332 mg/kg, 2.4% and 357.6µm, respectively. This site has EF classes of 1 for Cr, Cu and Pb and 4 for Zn. This sample, therefore, has very low heavy metal concentrations, although the very low TOC values and very high MGS results indicate that this sediment has poor suitability for heavy metal accumulation. Site 1 shows the same pattern of Zn enrichment as seen at sites in other areas of the Ashmead Channel. This site would not be considered contaminated according to the RNAL regulations.

Figure 5.30: Photograph of Site 1: the George Rex Culvert

Site 2 (Costa Sarda 1)

Site 2, named Costa Sarda after the adjacent suburb (**Figure 5.31**), is located a short distance west of Site 1, alongside a stormwater drain. This site has heavy metal concentrations of Cr: 17.2, Zn: 17, with the other metals being negligible. Al, MGS and TOC are 924mg/kg, 6.5% and 125.8µm, respectively, which are very close to their respective mean values for the catchment and therefore do not explain why the concentrations besides Cr are so low. EF classes are 1 for Cu and Pb, 3 for Cr and 4 for Zn. Besides the typical Zn contamination, Cr enrichment at this site is likely a local phenomenon. This site is non-contaminated.

Site 3 (Costa Sarda 2)

Site 3 (Costa Sarda 2), like Site 2, is located adjacent to a stormwater drain (**Figure 5.31**). H.M concentrations are Cr: 2.1mg/kg and Zn: 16mg/kg with the rest being negligible. Al, TOC and MGS are 3297mg/kg, 12.4% and 51.0µm respectively, which is a very high TOC value for the system, and a very low MGS value. This, in addition to a high Al value, indicates that the sediment is likely very suitable for the accumulation of heavy metals. EF classes are 1 for Cr, Cu and Pb and 3 for Zn. The sample appears to be highly absent of metals besides Zn. The Zn concentration is similar to that at Site 2, whereas Cr concentrations are much lower, despite this sediment being much more suitable for heavy metal accumulation. It would therefore be reasonable to assume that

the effluent discharge from this drain is minimally contaminated with heavy metals. This sediment is non-contaminated according to the RNAL.

Site 4 (Costa Sarda 3)

Site 4 (Costa Sarda 3) is located in the estuarine mudflats near the discharge point of another stormwater channel (**Figure 5.31**) and is also very clean, with negligible concentrations of all metals except Cr and Zn, with 3.3mg/kg and 16 mg/kg respectively, which are still considered to be very low according to the RNAL. Al, MGS and TOC are 1121mg/kg, 2.5% and 212.7µm respectively, which is a low Al value, a very low value for TOC and a relatively high mean GS. This indicates that the sample was not ideal for the accumulation of heavy metals, particularly since this is an estuarine site. EF Classes are 1 for all metals besides Zn, which is 3. The sample is non-contaminated.

Site 5 (Costa Sarda 4)

Site 5 (Costa Sarda 4) is located to the west of the Knysna Boat Club jetties (**Figure 5.31**) and has slightly higher overall metal concentrations than the previous sites with Cr: 3.2, Cu: 2.6, Pb: 2.3 and Zn: 15.2. Al, TOC and MGS are: 1180mg/kg, 8.4% and 71.0µm respectively. This sample is representative of an ideal site for the accumulation of metals, with its relatively high TOC % and very low average MGS. It follows that the heavy metal concentrations would be higher than those found at the previous (more riverine) sites, however, these concentrations are still very low and are indicative of non-contaminated sediment. EF classes are 1 for Cr, 2 for Cu and Pb and 3 for Zn, therefore indicating higher levels of enrichment than the previous sites.

Site 6 (Pumphouse)

Site 6, located alongside a pumphouse for the underground sewage system (**Figure 5.32**), has very similar heavy metal concentrations to Site 5, with Cr: 4.4, Cu: 2.2, Pb: 2.6 and Zn: 18.5. It does, however, have much lower TOC and higher MGS, with 3.1% and 144.3µm, respectively, therefore the conditions here are less ideal for heavy metal accumulation than Site 5, and could therefore be indicative of a slightly higher influx of metals. Al concentrations are 1861mg/kg, which is just below average for the system. EF classes are 1 for Cr, 2 for Cu and Pb and 3 for Zn, which indicates approximately the same amount of enrichment as Site 5. The heavy metal signature seen here is indicative of non-contaminated sediment.

Figure 5.31: Site images of each of the Costa Sarda sites. Clockwise; Costa Sarda 1 Costa Sarda 2 Costa Sarda 3, Costa Sarda 4.

Site 7 (Reed Bed Drain)

The last site categorized into the North-Ashmead Region is Site 7, located alongside a dense reed bed surrounding a stormwater drain (**Figure 5.32**). Nutrient enrichment from the drain is, therefore, expected at this site. This site has a similar heavy metal signature to the previous sites, with Cr: 3.6, Cu: 2.1, Pb: 2,6 and Zn: 17.4. TOC and MGS are 4.1% and 140.8µm, respectively, which are close to the mean values for the system. EF values are 1 for Cr, 2 for Cu and Pb and 4 for Zn, t indicating similar enrichment to the previous sites, albeit with higher Zn enrichment. In general, Site 7 has nearly the identical HM, TOC and MGS signature to Site 6, indicating that it is likely that there is a greater Zn input at this site than the previous few sites. This site is considered non-contaminated.

Figure 5.32: Site photographs of Site 6 (Pumphouse), left and Site 7 (Reed Bed Drain), right

5.6.7 Conclusions to be drawn from the North-Ashmead Region

The North Ashmead Region is the sampling zone that best represents the ideal deposition environment in the study area and the fact that relatively low heavy metal concentrations are found here is likely a good indicator that there is little widespread heavy metal contamination within the Knysna Estuary, due to the near-ideal conditions for the accumulation of sediment (and hence metals) in this region. This area of the channel also has less heavy metal contamination and

enrichment than the Industrial Area to the southeast and CBD to the west, indicating that the stormwater drains in this area are inputting relatively little heavy metals into the system.

5.6.8 The CBD Region

Background

The CBD Region of Knysna spans the area from the enclosed mudflats just east of the main town westwards until the intersection between the N2 and Waterfront Drive. Samples were not collected further west of this point due to the largest potential polluters likely being found in the CBD, in addition to fact that the majority of Knysna further west consists of residential suburbs and are hence unlikely to be major sources of contaminants. Finally, capacity constraints and increasing distance from the principal study area led to this sampling boundary. To facilitate comparison, the CBD has been separated into two subregions, the East CBD Region, which includes all sites east of the Thesen Island Causeway and the West CBD Region, which includes all the sites to the west of the causeway. The justification for this distinction is that the causeway allows for dramatically lower levels of circulation to its east than would have existed before its initial construction. As a result of the causeway, the flow characteristics on either side of it differ significantly, with the western zone having much greater levels of tidal flushing and circulation and the eastern zone being much more stagnant and thus more conducive to the deposition of finer-grained sediment.

5.6.9 The East CBD Region

Site 8 (CBD 1)

Site 8 is the most easterly of the CBD sites, is located in a small, isolated, wetland mostly separated from the main estuary by a pedestrian walkway (**Figures 5.33 and 5.34**). The sample was collected along the banks of the main river and tidal channel which originates in the north-eastern quadrant of the town. Site 8 has a higher heavy metal signature when compared to the more eastern sites located in the Northern Ashmead Region, with Cr: 4.1mg/kg, Cu: 4.9, Pb: 9.8 and Zn: 32.6. The site has Al, TOC and MGS values of 1225mg/kg, 2.2% and 143.9μm, respectively, which are low Al and TOC values and average MGS values for the system, thus the site has slightly below average suitability for heavy metal accumulation. EF classes are 1 for Cr, 3 for Cu and Pb and 4 for Zn. Although the heavy metal concentrations are higher here than sites further east, they are still very low in relation to the RNAL guidelines and therefore this sediment is non-contaminated.

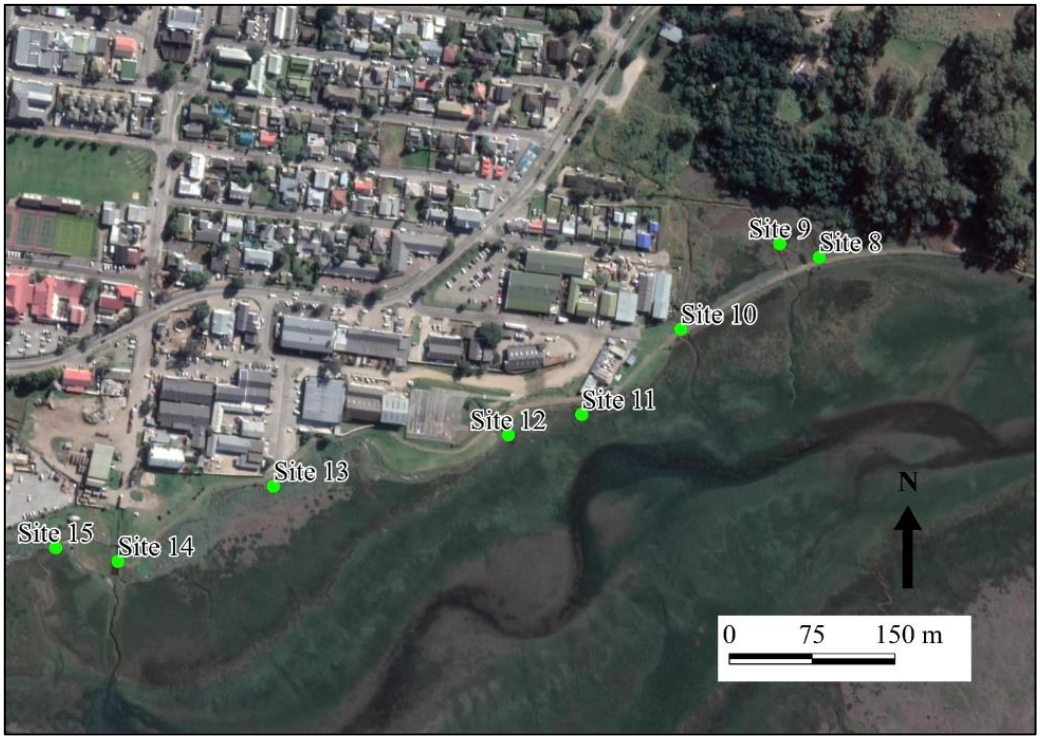

Figure 5.33: Google Earth map of the East CBD Region showing the sampling sites (Google Earth, 2020)

Figure 5.34: Site photograph of Site 8 (CBD 1)

Site 9 (CBD 2)

Site 9 is located a short distance westward of Site 8, in the isolated wetland about 100 metres to the east of the CBD (**Figure 5.35**). This site has a similar heavy metal signature to Site 8, with Cr: 3.7, Cu: 4.2, Pb: 14.7 and Zn: 30.3. Of note here is the Pb concentration of 14.7mg/kg, which is 4.9mg/kg (50%) higher than at Site 8, which may indicate that there is a greater and/ or closer Pb source. AL, TOC and MGS were 1883mg/kg, 2.2% and 182.9µm, respectively, which is a below-average Al concentration, low TOC value and a slightly above average MGS. This is expected, as the sample was collected from the banks of a riverine section. As a result, this sample has below average suitability for heavy metal accumulation. EF classes are 1 for Cr, 3 for Cu and Pb and 4 for Zn, indicating a similar degree of heavy metal enrichment to Site 8. As with Site 8, the concentrations here are higher than the Northern Ashmead Region, but still very low relative to the RNAL guidelines.

Figure 5.35: Site photographs of Site 9 (left) and Site 10 (right)

Site 10 (CBD 3)

Site 10 is located in the enclosed wetland directly adjacent to several major stormwater channels originating from the eastern edge of the CBD (**Figure 5.35**). This site has heavy metal concentrations that are higher than those seen at Site 9, with Cr: 4.9, Cu: 9.4, Pb: 17.9 and Zn: 67.2. Cu and Zn concentrations are double those seen at Sites 8 and 9. Al, TOC and MGS are 1680 mg/kg, 4.5% and 128.4µm respectively. TOC is higher here than at the previous sites, with mean

MGS being lower, indicating that this sediment is slightly more suitable for the accumulation of metals than the previous sites. Lower Al concentrations indicate lower background concentrations than Site 9. EF classes are 1 for Cr, 3 for Cu and 4 for Pb and Zn, indicating an increase in enrichment.

When comparing the sites in this band (Sites 8-10), there is a visible pattern of heavy metal concentrations and enrichment increasing with proximity to the CBD (from east to west), dispersing with distance from the CBD, which suggests that the sources of these metals are found within the CBD itself. An additional hypothesis for the higher concentrations at Site 10 is that, due to the flow being much slower than at the previous sites, more fine-grained materials are deposited and more metals precipitate from the water column. Regardless of the relatively higher concentrations found here, they are still very low and are indicative of non-contaminated sediment relative to the RNAL guidelines.

Site 11 (CBD 4)

Site 11 is located in estuarine sediment alongside the south-eastern edge of the CBD, adjacent to a stormwater channel (**Figure 5.36**). This site has significantly lower heavy metal concentrations than those seen at Sites 9 and 10, with Cr: 2.9 Cu: 2.7, Pb: 5.3 and Zn: 20.7. Al, TOC and MGS are 1558mg/kg, 2.0% and 155.1μm respectively. Generally, this site has low heavy metal concentrations, as well as low TOC levels, and average mean MGS, indicating that it has below average suitability for heavy metal accumulation. EF classes were 1 for Cr, 2 for Cu, 3 for Pb and 4 for Zn, indicating that heavy metal enrichment is lower, yet with a similar signature to that of Site 10. The increased flow within this area likely leads to a relative dilution effect when compared with Site 10. This sample is non-contaminated relative to the RNAL guidelines.

Site 12 (CBD 5)

Site 12 is located a short distance to the west of site 11, adjacent to a channel created by another stormwater drain. Site 12 has higher concentrations than Site 11 with Cr: 6.2, Cu: 6.4, Pb: 7.6 and Zn: 49.5. Al, TOC and MGS are 1683mg/kg, 9.0% and 59.1μm respectively, therefore indicating very favourable conditions for heavy metal accumulation, with anomalously low MGS and very high TOC values, which may, in part, explain why the heavy metal concentrations are higher here than at the previous site. With these conditions it is surprising that Al concentrations are so low, potentially indicating anthropogenic origins for the sediment. EF classes are 2 for Cr, 3 for Cu and Pb and 4 for Zn, with higher EF values for each metal, therefore indicating an increase in enrichment from site 11. The most noticeable difference in heavy metal concentrations is between Cr and Zn, with both of these metals being more than double those seen at site 11, however, these are still low in absolute terms and indicate that the site is not significantly contaminated with heavy metals.

Figure 5.36: Site photograph of Site 11 (CBD 4)

Site 13 (CBD 6)

Site 13 is located in an overgrown grass bed at the discharge point of a stormwater drain located directly to the south of a small business district and industrial zone (**Figure 5.37**). This site is important as it has the highest heavy metal concentrations of any of the sites in this study with Cr: 15.2mg/kg Cu: 29mg/kg, Pb: 22.3mg/kg and Zn: 345mg/kg. The sample has Al, TOC and MGS values of 2700mg/kg 18.9% and 18.5µm respectively. EF classes are 3 for Cr, 4 for Cu and Pb and 6 for Zn, therefore indicating extremely high levels of enrichment and the highest levels in this study. This site is interesting for several reasons, firstly, the concentrations of the majority of metals are higher here than what is seen anywhere else in the system, especially Zn, which has almost double the concentration of the second most contaminated site. Additionally, this site also has uncharacteristically high TOC values and extremely low mean grain size, which is much lower than what is seen even at the most pristine estuarine sites in this study. Moreover, the intense overgrowth at the site would indicate an abundance of nutrients. The sediment composition is strange, particularly the very low grain size, so the sediment has likely been artificially introduced into the system, having potentially been discarded in the industrial zone and then flushed out this drain. Another contributing explanation for this anomaly could be that, since the sediment sample is located alongside a well-maintained grass recreational strip, the sediment may be composed of artificially introduced topsoil and fertilizers, therefore partially explaining the radical differences seen between here and the other sites in this study. This could, at least partially, explain the increased concentrations of Cu, Zn and Pb, although this is just speculation (Mortvedt, 1995). In

synopsis, beyond Zn, which is found at a concentration much higher than the RNAL action level concentration guideline of 150-700mg/kg, the other metals are all found well below the RNAL action level guidelines and therefore, beyond being a single point source of Zn, this site is not significantly contaminated with heavy metals according to the RNAL, however, the relatively high concentrations and extremely high levels of Zn enrichment are concerning.

Site 14 (CBD 7)

Site 14 is located approximately 80 metres to the West of site 13, in a stormwater retention pond, with water originating from a major stormwater channel in the western edge of the industrial zone found to the north of Site 13, as well as from tidal inflows (**Figure 5.37)**. This sample was very different to the other sites along this strip in that no attempt was made to find an "estuarine sample", rather, site selection was based on the interest in what the heavy metal concentrations in the retention pond (the structure specifically designed for the deposition of sediment), would be.

Figure 5.37: Site photographs of Site 13 (left) and Site 14 (right)

Heavy metal concentrations here are similar to those seen in the majority of samples in the area, with Cr: 5.5, Cu: 1.2, Pb: 2.9, and Zn: 27. TOC and MGS are 0.5% and 341.8µm, respectively, which is both a very low TOC value and high average grain size. EF classes are 2 for Cr, Cu and Pb and 4 for Zn, which indicates much lower enrichment than at site 13, yet fairly typical enrichment for the Ashmead Channel. It is unclear why the sediment is so sandy; however, it is possible that the majority of the coarse-grained material from the stormwater channel is deposited here and hence skews the total composition in this manner (assuming that there is little fine-grained

matter in the influent). It is also likely that the sampling strategy was suboptimal for this site, with much of the fine-grained material being lost to resuspension as the trowel was drawn to the surface, hence another form of sampling, such as a Van Veen Grab Sampler, would likely have been more optimal. These reasons aside, it is evident that the sediment found in this sample is not significantly contaminated by RNAL standards.

Site 15 (CBD 8)

Site 15 is the westernmost of the sites located to the east of the Thesen Island Causeway and is found in a drainage channel originating from a stormwater drain (**Figure 5.38**). This site has a similarly low heavy metal profile to the others in the CBD region, with Cr: 2.6, Cu: 2.4, Pb: 12.1 and Zn: 27.8. Al, TOC and MGS are 3580mg/kg, 7.0% and 105.8µm respectively. This is an above-average TOC reading and below-average MGS reading, indicating that this is suitable sediment for the accumulation of metals. The Al concentration is relatively high. EF classes are 1 for Cu and Cr and 3 for Pb and Zn, showing slightly lower enrichment than other CBD sites. The heavy metal concentrations at this site are very low and are indicative of non-contaminated sediment, according to the RNAL.

Figure 5.38: Site photograph of Site 15 (CBD 8)

5.6.10 Summary of the East CBD Region

From the sites in the East CBD Region, it is clear that heavy metal contamination and enrichment increase in a westerly direction moving from the suburban Costa-Sarda area towards the more urban CBD. The enclosed wetland to the east of the CBD is possibly leading to an intensification of heavy metal concentrations due to low overall flow. Several sites to the south of the more industrial parts of the CBD are also quite concerning, with Site 13, in particular, having extremely high levels of Zn enrichment and Zn concentrations far exceeding the RNAL guidelines. Pb and Cu enrichment at this site are also significant, which is concerning. This area seems to have a similarly low Cr enrichment to the rest of the channel. Since these samples were all collected from the discharge points of stormwater drains or channels, they likely represent the worst-case scenario for heavy metal contamination in the area.

5.6.11 Analysis of the West CBD Region

Background

The West CBD Region, located to the west of the Thesen Island Causeway, includes Sites 16-21 (**Figure 5.39)**. These samples were all taken either from the discharge points of stormwater canals into the estuary, or from various distances upstream of these discharge points. Additionally, this region is important as the estuarine samples are separate from the circulation bottleneck experienced by the sites located to the east of the causeway. Finally, this western region is located a short distance from the central channel of the Knysna River and is therefore much more affected by riverine and tidal circulation than the other sites in this study (**Largier, 2000**).

Site 16 (Long Street Discharge)

Site 16 is located at the discharge point of the Long Street Canal, which drains a significant portion of CBD (**Figure 5.40**). This location was a hotspot of higher heavy metal concentrations during the 2018 study by Armitage. Heavy metal concentrations here are similar, yet slightly higher than those seen at the majority of the other CBD sites, with Cr: 7.9 Cu: 11.1, Pb: 17.5 and Zn: 92.7. Al, TOC and MGS are 9.0% and 80.9μm respectively. This is a relatively high TOC value and low MGS value, hence the sediment is suitable for the accumulation of heavy metals. EF classes are 2 for Cr and 4 for Cu, Pb and Zn, therefore indicating a high degree of enrichment for the system. Additionally, the concentrations here are comparable to those seen at the same site by Armitage (2018).

Figure 5.39: Google Earth site map of the West-CBD region (Google Earth, 2020)

Figure 5.40: Photograph of Site 16 (the Long Street Discharge)

Site 17 and 18 (Upper Long Street Canal)

Sites 17 and 18 have been grouped as they were both sampled a short distance (roughly 50 metres) up the Long Street Canal, which was approximately the furthest upstream point accessible before the canal was no longer exposed to the surface. Sample 17 was collected first, from the centre of the canal, before Sample 18 was collected 5 metres downstream, under a small bridge. The justification for this second site was that it appeared to have greater potential for the deposition of heavy metals due to the subsurface being stippled and slowing the flow of water, leading to the accumulation of finer-grained sediment. These two sites provide an insight into the difference that site selection and sample quality can make in the accumulation of heavy metals. Heavy metal concentrations at Site 17 are Cr: 1.1mg/kg, Cu: 3.7mg/kg, Pb: 3.6mg/kg and Zn 55.9mg/kg. AL, TOC and MGS are 494mg/kg, 0.8% and 420.2µm respectively. EF classes are 1 for Cr, 3 for Cu and Pb and 5 for Zn.

Heavy metal concentrations at Site 18 are Cr: 10.6mg/kg, Cu: 21.6mg/kg, Pb: 16.4mg/kg and Zn: 172mg/kg. Al, TOC and MGS at site are 1280mg/kg, 4.8% and 155.4µm respectively. EF classes are 3 for Cr, 4 for Cu and Pb and 6 for Zn.

These two sites are incredibly interesting, as, their respective heavy metal profiles would lead one to believe that the locations differed totally, yet the samples were effectively collected from the same location. To elaborate, Site 17 has very low heavy metal concentrations for the system, with the only exception being Zn which is still fairly low in concentration. Additionally, the TOC here is very low and MGS is very large, indicating that the sample was sandy and likely not suitable for heavy metal accumulation. This is in stark contrast to Site 18, which had some of the highest concentrations in the study, with the Zn concentration being found over the RNAL action level. TOC at Site 18 was not high relative to the rest of the system, however, at 4.8%, it was much higher than Site 17. Furthermore, MGS was slightly below average for the system, yet it was much lower than the MGS at Site 17. The conditions for heavy metal accumulation at Site 18 were vastly more suitable than those seen at Site 17, and this is manifested dramatically with their different contaminant profiles.

These two samples also show the usefulness of EF as a metric as, although the EF results for Site 17 are lower than Site 18, they are still high relative to the remainder of the system and show the same general trend, despite the very large differences in absolute heavy metal concentrations.

From the results of these two sites, it is evident that the Long Street Canal is highly enriched with heavy metals and that the sources likely lie within the CBD. Moreover, the difference in enrichment and concentrations between sites 17, 18 and 16 shows the relative intensification occurring in the canal and the subsequent dilution effect in the estuary. The heavy metal concentrations fall below the RNAL guidelines for all metals besides Zn, and the sediment is mostly non-contaminated.

Site 19 (Grey Street Discharge)

Site 19, located about 400 metres to the north-west of the Long Street Discharge, was chosen as it is at the discharge point of the undercover Grey Street Canal, which drains much of the western area of the CBD, including many roads and businesses. Heavy metal concentrations at this site are Cr: 14.7mg/kg, Cu: 18.4mg/kg, Pb: 20.2mg/kg and Zn: 162mg/kg. Al, TOC and MGS are 2062mg/kg, 6.5% and 140.4μm respectively, which represent typical conditions in Knysna. EF classes are 3 for Cr, 4 for Pb and Cu and 5 for Zn, indicating a high degree of enrichment for all 4 metals. The heavy metal concentrations at this site are all very high relative to the mean values for this entire sample set, with Zn being found at concentrations higher than the RNAL action level concentration of 150mg/kg. With the exception of Zn, these concentrations, although relatively high, are still considered non-threatening. As with the other sites, there is likely an intensification effect here, wherein the concentrations are higher at the discharge point due to proximity to the source of the pollution. Unfortunately, no site photograph was captured for this site.

Site 20 (Bricklebos Stream Discharge)

Site 20 is located in the estuarine channel sourced from the Bricklebos Stream, which runs through the western suburban areas of the town of Knysna and is responsible for the drainage of a large volume of the stormwater in this region (**Figure 5.41**). This site has heavy metal concentrations that are above average for the system, yet much lower than those seen at the other CBD sites, with Cr: 6.1, Cu: 7.9, Pb: 9.8 and Zn: 78. Al, TOC and MGS are 1891mg/kg, 5.0% and 143.5μm respectively, making this sample fairly typical for Knysna sediment. EF classes are 2 for Cr, 3 for Cu and Pb and 5 for Zn, indicating a similar, yet lower, degree of enrichment compared with Grey Street. This site is interesting as it indicates that, although enrichment is lower here than at Grey Street, there are still significant heavy metal inputs flowing through this stream. As previously stated, these heavy metal concentrations are above average for the system yet still low relative to RNAL guidelines.

Figure 5.41: Photograph of the Bricklebos Stream Discharge Channel (Site 20)

Site 21 (Upper Bricklebos Stream)

Site 21 is located about 100 meters upstream of Site 20, in the canalized portion of the Bricklebos Stream, near its culvert with Trotter Street (**Figure 5.42**). This site was chosen to gain insight into the state of the Western CBD Region of Knysna, without the impact of tidal and estuarine forces. Additionally, since the Bricklebos Canal drains Trotter Street, which is a fairly major roadway, and several other roads, this sample is interesting for determining whether the stormwater runoff from this region is contributing to heavy metal contamination in the estuarine sediment.

The heavy metal concentrations here are very similar, yet slightly lower than those seen at Site 20, with Cr: 5.6mg/kg Cu: 4.6mg/kg, Pb: 7.6mg/kg and Zn: 58.5mg/kg. Al, TOC and MGS are 1718mg/kg, 2.5% and 84.2µm respectively, which is below average TOC value and significantly below average MGS value. This sample is therefore above average in its suitability for heavy metal accumulation. EF classes are 2 for Cr, 3 for Cu and Pb and 5 for Zn which indicates a similar, yet slightly lower, degree of heavy metal enrichment when compared to Site 20. In summary, this site,

though enriched, has average heavy metal concentrations for Knysna. The absolute heavy metal concentrations are very low relative to the RNAL and the site is therefore uncontaminated.

Figure 5.42: Photographs of the upper Bricklebos Stream (Site 21)

Summary of the West CBD Region

The West CBD Region of Knysna has the most consistently high heavy metal concentrations and enrichment in the study area. Heavy metal enrichment is greatest towards the centre of the CBD and reduces when moving westwards. From this study, it is not clear how far west of the CBD heavy metal enrichment would no longer be considered concerning, as the lower Bricklebos Stream sites still have significant enrichment. Additionally, 2 sites (18 and 19) have Zn concentrations exceeding the 150mg/kg RNAL trace metal guidelines, with all the samples having a ZN EF class of at least 4. This area also has consistently high EF classes for Cr, Cu and Pb. The intensification effect of heavy metal concentrations and enrichment due to the samples being collected directly from the discharge points or within the canals likely causes the concentrations to be higher than in the estuary sediments as a whole as these would experience high degrees of dilution. This effect is evident between Sites 16, 17 and 18, with Sites 17 and 18 having a higher degree of enrichment than Site 16. This is likely due to the increased flow present in the estuary when compared to higher up the Long Street Canal. It is, however, clear that these canals are contributing to Cr, Cu, Pb and Zn enrichment in the estuary.

6. Chongming Island Results

6.1 Brief overview

The following section includes the results from the laboratory work on the Chongming Island samples, with many of the data tables being found in **Appendix C.**

6.2 Descriptive tables

Table 6.1: Metal concentrations and TOC results for the Chongming samples												
	Element (mg/kg)											
Site	**Al**	**Co**	**Cr**	**Cu**	**Fe**	**Mn**	**Ni**	**Pb**	**Sr**	**Zn**	**Hg**	**TOC (%)**
Xisha												
M01	24300	0.00	108	27.0	34100	251	0.00	0.00	88.6	129	0.155	5.3
M02	28800	6.00	63.4	36.7	31400	0.00	0.00	140	103	116	0.118	5.4
M03	24600	12.3	113	60.5	34400	309	0.00	0.00	92.8	121	0.150	5.8
M05	25100	0.00	159	29.3	38300	1260	74.5	0.00	87.0	143	0.185	7.3
M06	28500	3.66	140	23.0	37500	538	8.34	160	95.1	133	0.166	6.4
M07	24100	9.80	118	0.00	33900	104	32.3	0.00	87.8	135	0.147	6.3
Ganyang												
B01	32000	18.9	135	1.18	40300	475	0.00	0.00	96.7	141	0.126	8.7
B02	27700	0.00	130	23.6	37500	454	27.2	140	94.8	124	0.122	7.6
B03	29600	0.00	116	2.91	32200	105	30.1	0.00	101	106	0.0936	4.5
B04	24000	25.4	71.5	12.8	31300	210	37.1	0.00	93.7	96.4	0.086	5.6
B05	27800	36.5	121	4.22	38200	306	0.00	0.00	89.5	141	0.106	8.2
B06	27300	19.9	130	23.0	40300	332	40.1	0.00	84.1	163	0.123	10.9
B07	25200	7.26	156	0.00	43400	90.2	66.5	154	82.9	160	0.125	10.9
B08	25800	15.5	132	1.91	39300	397	0.00	0.00	89.2	132	0.109	7.2
B09	31500	31.9	168	49.1	40100	272	42.7	0.00	102	154	0.123	8.8
Basic descriptive statistics												
Mean Xisha	25900	5.30	117	29.4	34900	410	19.2	49.9	92.4	130	0.153	6.1
σ Xisha	2160	5.08	32.3	19.6	2550	455	29.8	77.6	6.08	9.80	0.0222	0.77
Mean GNG	27900	17.3	129	13.2	38100	293	27.1	32.6	92.6	135	0.113	8.1
σ GNG	2740	13.0	27.0	16.3	3950	139	23.1	64.8	6.76	23.3	0.0147	2.1
Mean Total	27100	12.5	124	19.7	36800	340	23.9	39.5	92.5	133	0.129	7.3
σ Total	2640	12.0	28.8	18.9	3710	298	25.3	68.0	6.27	18.8	0.0269	2.0
Note: All metal values are rounded to 3 significant figures												

6.3 Overview of heavy metal concentrations from Chongming

This overview only deals with the metals analysed at Knysna. The other metals listed have been included in **Table 6.1** as reference for future studies and were part of the cluster of elements analysed by the ICP-OES machine.

The results from Gangyang and Xisha have both been analysed individually and thereafter combined for the comparison between Knysna and Chongming (**Table 6.1**), with the sampling areas from opposite sides of the island forming an approximate representative sample for Chongming, and hence the Yangtze. It is important to note that the high-resolution sources and factors influencing the distributions of the heavy metals on Chongming Island are not important for the purposes of this dissertation and the above results, therefore, stand as a broad, low-resolution snapshot of Chongming Island and the Yangtze Estuary.

The total heavy metal concentrations at the two sites are comparable, which is an interesting result and, therefore, they have been combined into a single dataset. Al concentrations ranged from 24100mg/kg to 32000mg/kg, Cr ranged from 63.4mg/kg to 168mg/kg, Cu ranged from 0mg/kg to 60.5mg/kg, Pb ranged from 0mg/kg ton 154mg/kg and Hg ranged from 0.086mg/kg to 0.185mg/kg. It is important to note that, where the ICP reported 0mg/kg for a metal, this likely represents machine error when detecting metals in low concentrations. The results for Pb are particularly interesting as the concentrations are either very high or 0, which could indicate that the Pb results are not very reliable due to machine error.

6.4 TOC results

The TOC results from the loss on ignition process show a mean TOC of 7.3% for the whole Chongming sample, with 6.1% for Xisha and 8.1% for Gangyang (**Table 6.1**). These TOC results show that the sediments surrounding Chongming Island have high organic matter contents and should therefore have many absorption sites for heavy metals. Additionally, the sediments from Gangyang have greater amounts of organic matter than sediment from Xisha, although the small sample size means that this is not necessarily a significant trend.

6.5 Grain size data for Chongming

6.5.1 Tables and figures

The following section includes the tables and figures for the Chongming Island grain size results. **Tables 6.5** and **6.6** are found in **Appendix C.**

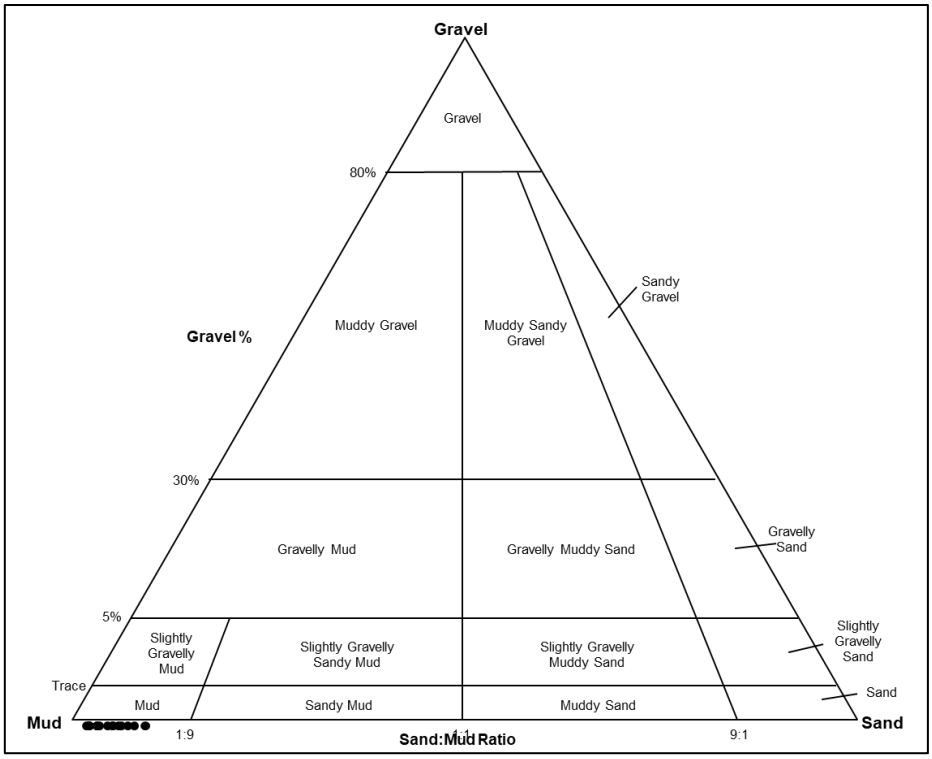

Figure 6.1: Gravel-Sand-Mud diagram for Chongming

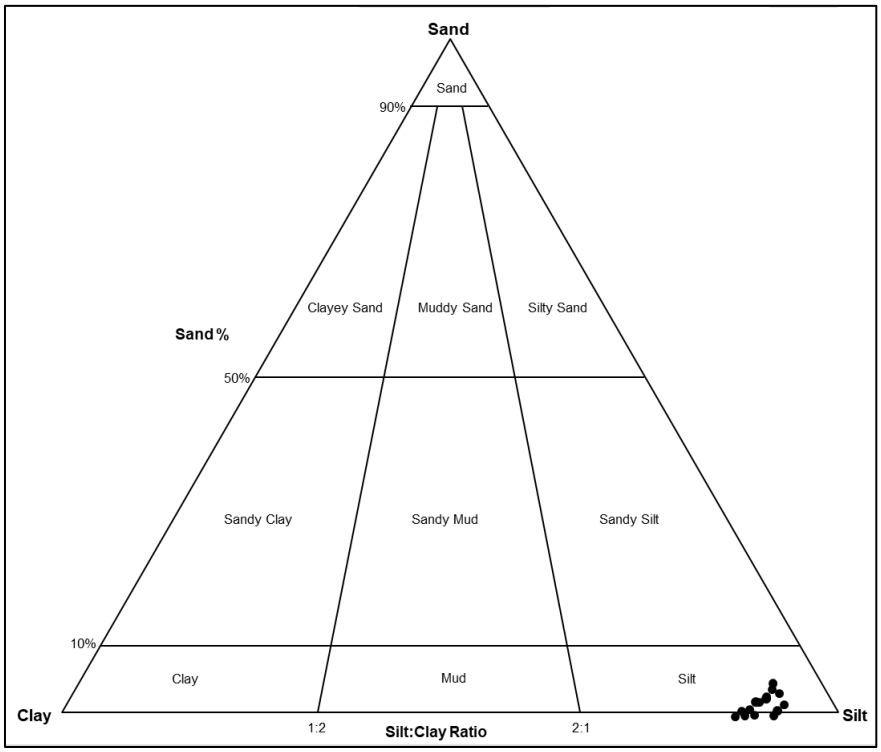

Figure 6.2: Sand-Silt-Clay Diagram for Chongming

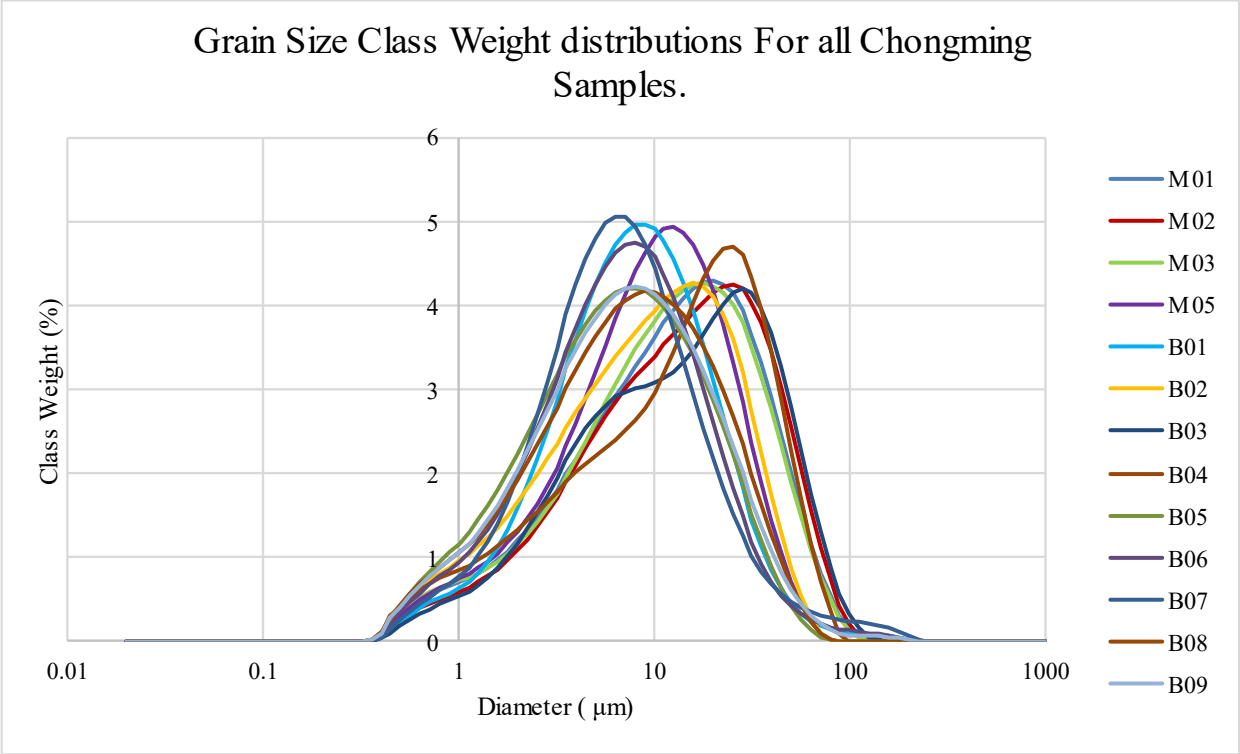

Figure 6.3: Grain size class weight distribution graphs for the entire Chongming Island sample set

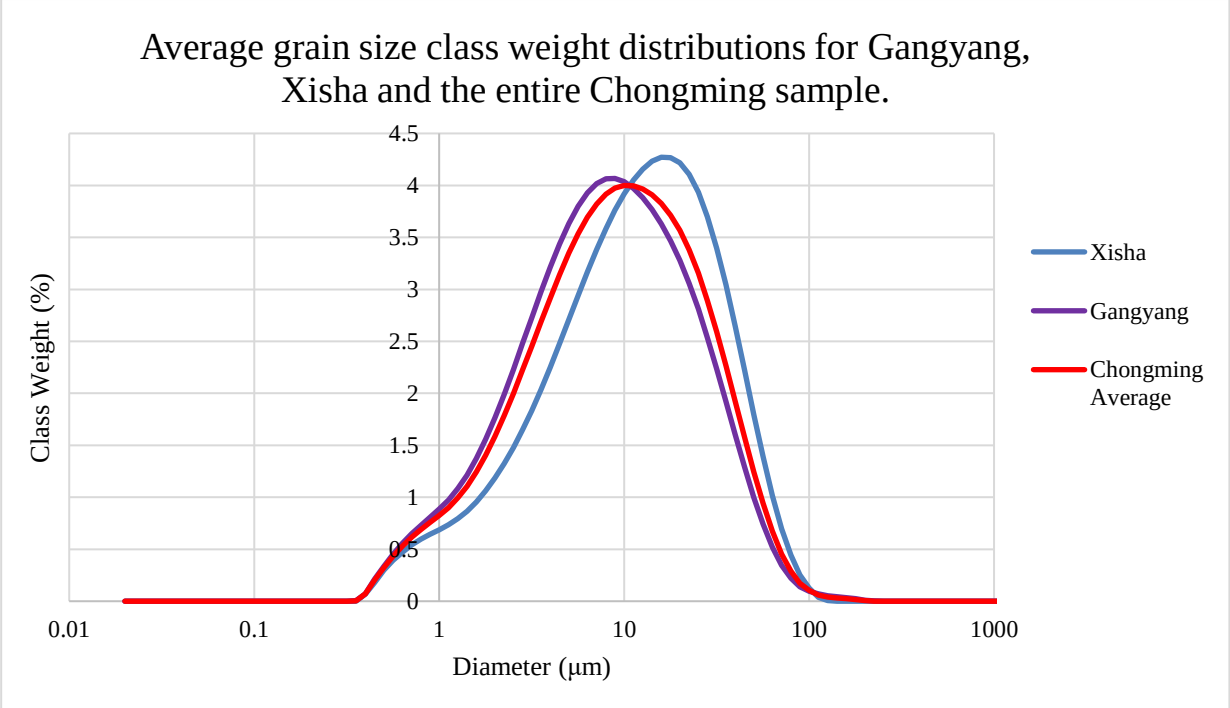

Figure 6.4: Average grain size class weight distributions for Gangyang, Xisha and the entire Chongming sample set

6.5.2 Overview of Chongming grain size data

The GS data highlighted in **Figures 6.1-6.4** and **Tables 6.5, 6.6** (**Appendix C**) show that the grain size at Chongming Island is predominantly unimodal, with the majority (>90%) of the class weights of the samples being found in the mud portion of the grain size spectrum (<68μm), of which the largest constituents are medium and coarse silt. The sediments have a mean grain size of 9.52μm across all the sites, with 11.17 at Xisha and 8.41 at Gangyang. The Chongming Island sediments are mostly homogenous and are highly suitable for heavy metal accumulation due to their low mean grain size as well as their large mud percentage.

6.6 Enrichment factor results

6.6.1 Descriptive tables

Table 6.7, which contains the enrichment factor results and classes for the Chongming Island samples, can be found in **Appendix C.**

6.6.2 EF intensity maps for Chongming Island

The following pages display red-scale intensity maps representing the EF data for Chongming Island.

Figure 6.5: Pb EF classes for Xisha

Figure 6.6: Cr EF Classes for Xisha

Figure 6.7: Cu EF classes for Xisha

Figure 6.8: Zn EF classes for Xisha

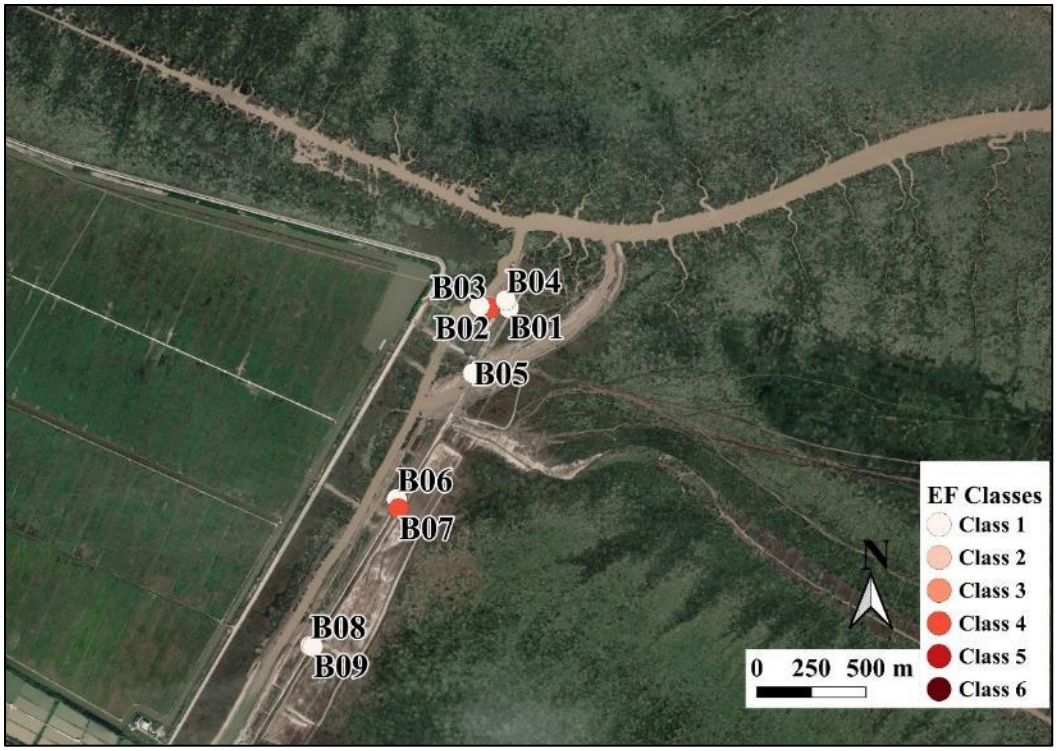

Figure 6.9: Pb EF classes for Ganyang

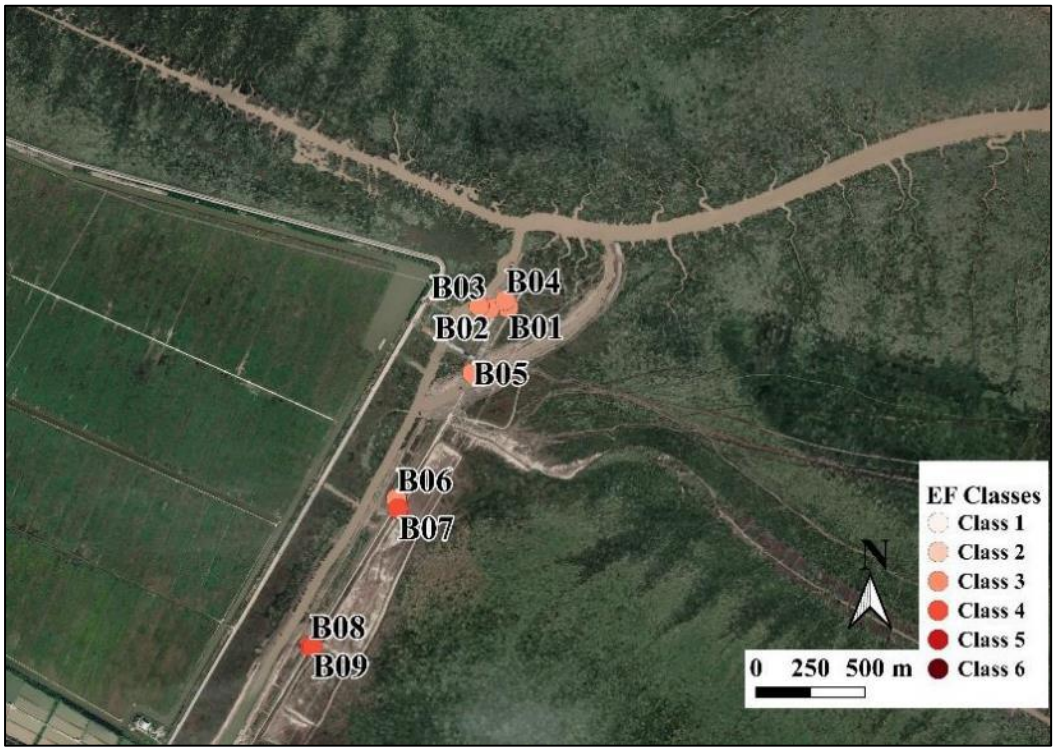

Figure 6.10: Cr EF classes for Ganyang

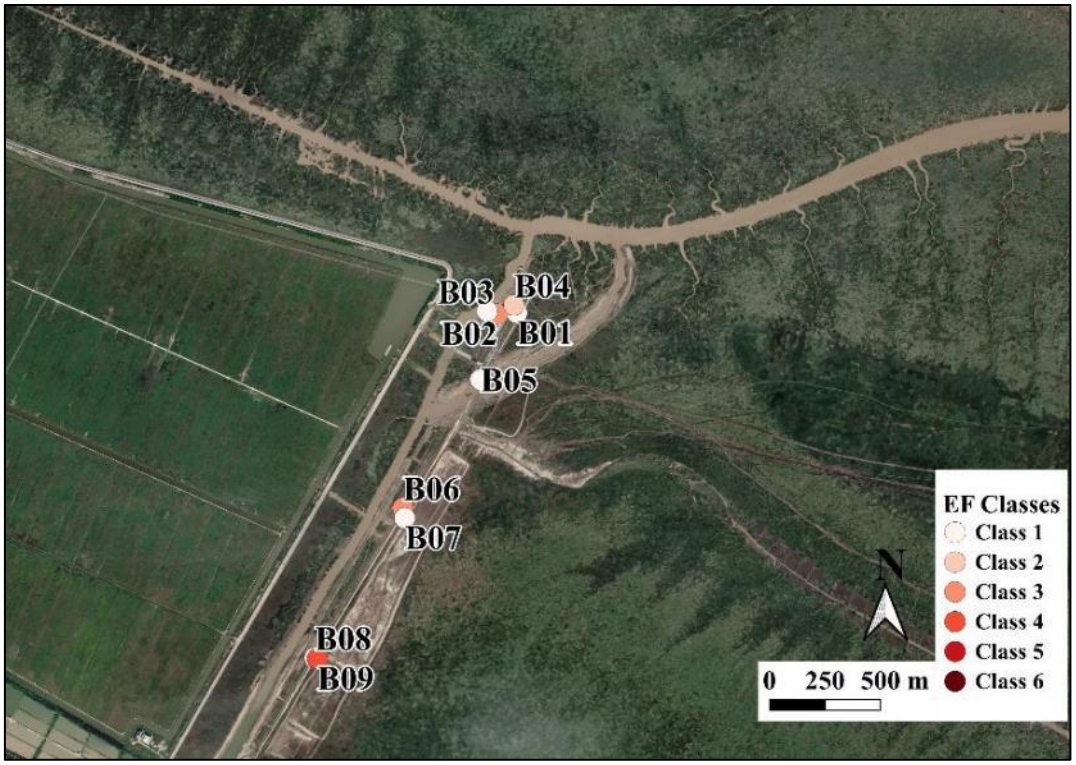

Figure 6.11: Cu EF classes for Gangyang

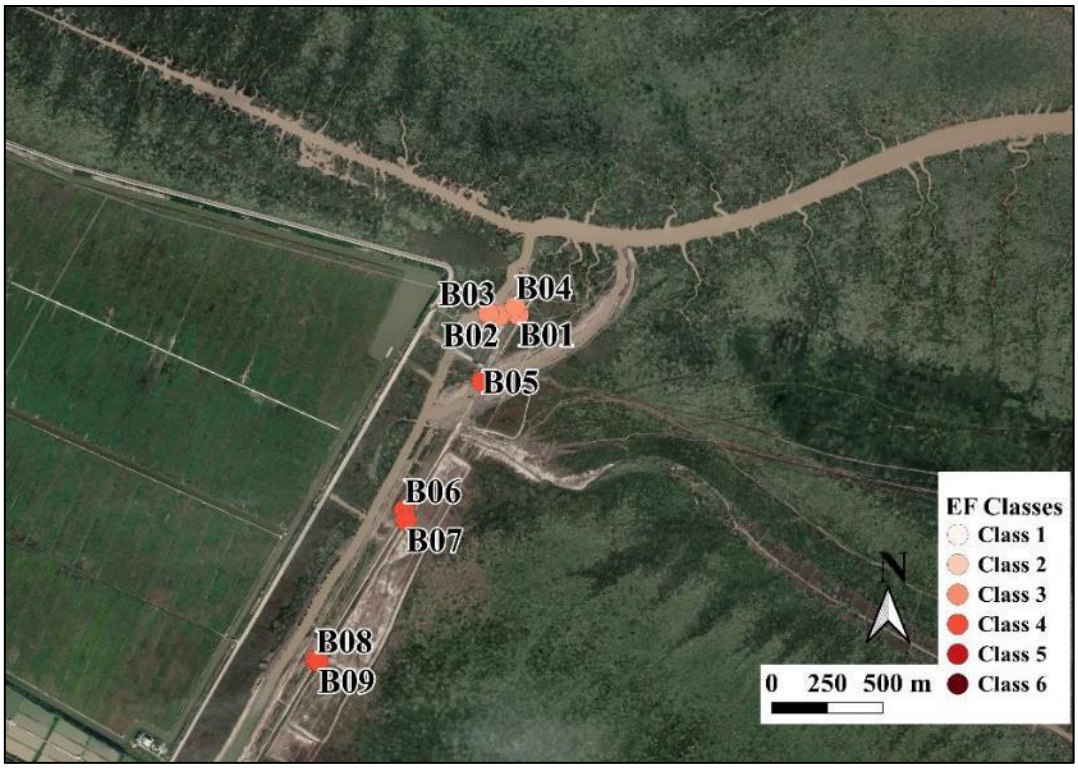

Figure 6.12: Zn EF classes for Gangyang

6.6.3 Overview of Chongming EF results

EF results for the Chongming sites vary between the metals (**Figures 6.5-6.12, Table 6.7**). Cr is either class 3 or 4 for every site, with a mean of 3.27, indicating moderate to significant enrichment. Cu varies more greatly, with higher values at Xisha than Ganyang, with a mean EF class of 2.83 and 1.89, respectively. All the classes at Xisha are either 3 or 4 except for Site 1, whereas Ganyang predominantly has EF classes of 1, with a few cases of higher classes at other sites, therefore indicating a greater spatial variability at Ganyang. The EF classes for Pb seem to be highly point-specific on Chongming Island and therefore non-uniform, with most sites having an EF class of 1, except for 3 sites that have an EF class of 4, indicating that most of the sediment is non-enriched with Pb, yet a few sites fall into the significant enrichment category, however, the Pb concentrations might be skewed to due machine error. Zn is the element with the most consistently high degree of contamination, with all the sites having either an EF class of 3 or 4, indicative of moderate-to-significant enrichment. It is also interesting to note that, for Gangyang, Zn enrichment is greatest further inland, and decreases as the reclaimed land becomes more recent, with this trend also being visible for Cr.

6.7 Summary of correlations from the Chongming Island data

The correlation matrix of the Chongming Island samples is included in **Table 6.8**. This matrix has been conducted for the entire sample, rather than being subdivided for Gangyang and Xisha, both to try to attain a surface level understanding of the correlations between these variables for Chongming as a whole, as well as to increase the sample size (N) and therefore the statistical accuracy of the correlations. Of particular interest is the fact that Cr, Zn and TOC % all have negative correlations with MGS, (R= -0.684, -0.767 and -0.855), which are significant at the 1% level, therefore suggesting that, as grain size increases, these variables will decrease, which is consistent with the literature. Zn and Cr also have a strong positive correlation, which is significant at the 1% level, suggesting that if a site has a high Zn concentration, it will also have a high Cr concentration. Zn also has a strong positive correlation with TOC, which is significant at the 1% level. Cr and TOC also have a moderate positive correlation, with R=0.618, which is significant at the 5% level. From this data, it appears that Zn, Cr, TOC, and MGS are all interrelated, whereas the other elements appear to occur with less of a pattern.

7. Discussion

The discussion begins by determining the implications and significance of the various study metrics for the Knysna Estuary. The results from Knysna are then compared to the results from other similar studies from both South Africa and from other global localities to determine how the Knysna concentrations vary from those of these studies. The results from Knysna and the Yangtze are then compared, and the relevant commonalities and differences are ascertained.

7.1 Implications of the EF results

The EF results presented in **Section 5.5** show a slightly different signal for each metal. It is clear that Cr contamination in Knysna is not currently a concern as the concentrations are low, both on absolute and enrichment scales. Cu and Pb enrichment in the Ashmead Channel is more concerning, as their enrichment level appears to have increased by a substantial degree (from EF classes of roughly 1-2 in 2000 to classes of 2-5 currently). This prompts questions regarding which behaviours could be leading to the increase in enrichment. Although concerning, the fact that the absolute concentrations of Pb and Cu in the channel are still relatively low indicates that the present threats associated with this contamination remain low. It is, however, important that this trend be curbed in the future.

Zn is the metal of most concern in the Ashmead, with the highest relative concentrations, as well as consistently the highest enrichment levels in the area. Furthermore, Zn concentrations and enrichment seems to have amplified in the last 20 years, suggesting a large increase in the amount of Zn contaminants entering the system. Most sites are still found to be within safe concentrations for Zn according to the RNAL, however, it is probable that, should Zn enrichment in Knysna continue to be high, concentrations could reach concerning levels in the coming decades.

It is likely that the tidal conditions and limitations in flushing present within the Ashmead Channel and the heavy metal inputs from many of the largest polluting areas in Knysna are resulting in a relative intensification of Cu, Pb and Zn. Enrichment in the area is increasing at a concerning rate and needs to be addressed before it becomes a risk to plant and animal life in the future. It is not possible to infer what the heavy metal concentrations are like in the rest of the estuary without further study, however, it is likely that regions with higher degrees of tidal flushing and fewer drain inputs have lesser degrees of contamination than the Ashmead, which likely represents the worst-case scenario. The EF results from this study should therefore stand as a warning against further contamination within the Knysna Estuary, notable for holding the highest conservation status in South Africa (Turpie *et al*., 2002).

7.2 Summary of findings for the Ashmead Channel

The previous sections show that, overall, as of the 2018 and 2019 sampling periods, the total heavy metal concentrations within the Ashmead Channel and surrounding tributaries do not exist in high levels.

It is, however, clear that Zn enrichment in Knysna is a major concern, with EF classes of 3 or higher for most of the system. This is indicative of a widespread moderate-to-high degree of enrichment. Additionally, several sites, namely those found adjacent to the Industrial Area or CBD, have Zn concentrations exceeding the 150mg/kg RNAL guideline. These likely represent local hotspots.

Cu and Pb enrichment is also a concern in Knysna, albeit to a lower extent, with EF classes of 2-4 being prevalent throughout the more contaminated areas of the system. On a more positive note, the results of this study show minimal As, Hg and Cd contamination with concentrations of <1mg/kg across the study area. This is encouraging as they are some of the most concerning metals from a health perspective. It must be noted that, since the ICP-OES struggles to quantify very low concentrations, it is not possible to know exactly what the concentrations of these metals are, which is an important consideration since these metals can be harmful even in fairly low concentrations.

The concentrations of the metals in this study and their distributions are not uniform. The extent of contamination varies across space, and it appears that there are several hotspot areas of heavy metal contamination within the Ashmead Channel. The highest levels of enrichment are present in the CBD area in the north-west of the study area and all the stormwater drains and canal sites having similarly high degrees of enrichment. Several hotspot sites have Zn concentrations exceeding the 150mg/kg RNAL action level threshold concentration.

Heavy metal concentrations and enrichment decrease with distance from the centre of the CBD, towards the Costa-Sarda area, indicating that the main sources of these contaminants are within the CBD. The estuarine sites to the south of the Costa-Sarda residential area appear to be relatively non-enriched. There is a small, localized increase in heavy metal contamination in proximity to the George-Rex Drive Culvert. Heavy metal concentrations in the northeast of the channel are consistently low, with the cross-channel transect having minimal enrichment, apart from Zn.

The Eastern Ashmead Region and Bongani Stream Outlet have higher heavy metal concentrations and enrichment than the north-east sites. The concentrations and degree of enrichment at these sites are somewhat lower than one might expect, given the presence of the outlet of the Bongani Stream, WWTW and Industrial Area, however, some of this can potentially be attributed to sample quality, as mentioned in **Section 5.6.5**. The Vigilance Drive Canal also appears to be a hotspot for heavy metals in this study, due to its proximity to the Industrial Area, with a Zn EF class of 6, and

4 for Cu and Pb, however, the high concentrations and enrichment are likely intensified by the proximity to contaminating bodies, coupled with the low total volume of water in the canal. The subsequent dilutions with the Bongani and Ashmead likely lead to the lower enrichment found in the Eastern Ashmead Channel.

The Bongani Stream appears to have some degree of Zn enrichment through its course, with EF classes of 3 or 4 throughout its course, indicating a local source of Zn in the upper courses of the stream. The Upper Bongani site also has EF classes of 3 for Pb and Cu, yet both metals only have an EF class of 2 in the lower courses of the river, until the Bongani passes the Industrial Area, and the EF classes increase to 3 again. It is therefore evident that there is some degree of heavy metal mobilization through the Bongani Stream, however, the extent of contamination is lower than in the CBD.

The Bigai Spring was sampled less intensively than the Bongani, however, it appears to be less contaminated, with EF classes of 3 for Zn in the upper catchment. Interestingly it seems that the Upper Bigai site (Site 36), is more contaminated than the site further downstream (Site 32), with Site 36 having an EF class of 3 for Pb and 2 for Cu, whereas Site 32 only has EF classes of 1 for Pb and Cu. This may occur as a result of local contamination in the upper Bigai and/or a dilution effect due to the increased volume of water at Site 32. The Bigai Mountain Spring Tributary (Site 29) has negligible concentrations of all the metals and appears to be uncontaminated by litter or waste, which may be due to the community incentives to keep this stream clean.

Finally, the area to the south of Thesen Island, where 3 samples were collected in 2018, was the least contaminated part of the Ashmead, with low total HM concentrations and EF classes of 1 or 2 for all metals.

7.2.1 Potential causes of this contamination

Determining the causes of the enrichment of Zn, Cu and Pb is challenging, and it is not possible to directly attribute causation within this dissertation. Several possible sources should be considered; however, this is mostly speculation.

Zn

There are several likely sources of Zn in the system, with the use of Zn sacrificial anodes on boats to prevent the corrosion of the steel structures being a likely contributor, due to the popularity of motorboats in Knysna (Mathiessen *et al*., 1999; Rees *et al.*, 2017; Rees *et al*., 2020). This form of contamination would also make sense in the study area of the Ashmead Channel, due to the presence of the Knysna Harbour and the Knysna Boat Club in the channel, in addition to the Thesen Island residential area. There is therefore a large motorboat presence in this region of the Knysna Estuary. This could, in part, explain the enrichment present in the estuarine sites and the lower-

canal sites as tidal flushing leads to backwash up these canals. Zn contamination can also be attributed to runoff from roads, with the breakdown of tyres being the largest culprit and the N2 National Road and surrounding roads of Knysna being possible contributors (Adachi and Tainosho, 2004; Dierkes *et al*., 2006). The high degree of enrichment present in the Vigilance Drive Canal would also suggest that the industrial activities occurring in the Industrial Area are also contributing to the Zn enrichment in the estuary. A final potential source of Zn could be runoff from corrugated metal roofs in the semi-formal and informal settlements found in the upper catchments of the Bongani and Bigai streams, which could partially explain the degree of enrichment present in the riverine sites (Dierkes *et al*., 2006).

Cu

There are many potential sources of Cu in the Knysna system and these could include the corrosion of antifouling paints present on the surface of the many boats in the estuary, runoff from industrial activities and the corrosion of copper pipes and fittings in the urban areas of Knysna. Cu has also been linked to vehicle emissions and the breakdown of tyres, which could also be contributing to Cu enrichment in Knysna (Adachi and Tainosho, 2004; Gupta, 2020). Additionally, Cu can be found in the chemicals used to treat timber, a process closely linked to the area's history (Monteiro *et al*., 2000).

Pb

Pb has many possible sources in Knysna, including emissions from vehicles and the breakdown of their tyres, the corrosion of old batteries, runoff from Pb-based paints, as well as from industrial activities (Adachi and Tainosho, 2004). It is also possible that runoff from the maintenance of vehicles in the upper Bongani and Bigai could be contributing to the degree of enrichment present in these areas. Finally, it is possible that runoff from old Pb piping could be contributing to the enrichment, however, this would not explain why enrichment is worse in the last 20 years.

7.3 The state of heavy metal contamination in Knysna compared with past studies and other similar environments

7.3.1 Heavy metals in Knysna in relation to past studies

When comparing the state of heavy metal contamination in Knysna with the findings of Watling & Watling (1977, 1982) and Monteiro *et al*. (2000), it is clear that the degree of heavy metal enrichment has increased dramatically throughout the system for Cu, Zn and Pb, which is shown in the EF results present in **Section 5.5.** The EF classes within the Ashmead Channel have increased from mainly 1-2 to 3-5 for Cu and Pb and from mainly 1-2 to 4-6 for Zn since 2000. This indicates that the rates of input of these metals into the system have increased dramatically in the last 20 years, which is very concerning. It is possible to directly compare the concentrations of these studies as Watling & Watling (1977, 1982), as well as Monteiro *et al*. (2000) utilised Varian Flame Atomic Absorption Spectrometers to quantify heavy metal concentrations. This method, although less sensitive than the ICP-OES method used to quantify heavy metal concentrations used for the samples from the current study, ensures that the results have sufficient accuracy (Olesik, 1991).

It is interesting to consider that Monteiro *et al*. (2000) noted that the heavy metal contamination in Knysna had not increased significantly since the Watling reports, and this is reflected in the EF analysis (**Section 5.5.2**). EF results from the two studies were very similar and indicate a possible small reduction in heavy metal enrichment between 1977 and 2000. Human activities, such as increased urban development and industrial activities must, therefore, have increased by a large margin in the areas feeding the Ashmead Channel to account for this subsequent increase in enrichment. On a positive note, Cr enrichment in the channel has not increased and the total concentrations of other toxic metals studied (Cd, Hg and As) have either decreased or had no noticeable increase (**Table 5.2)**. It must be reiterated that the ICP-OES did not have sufficient sensitivity at low concentrations to fully determine the extent of Hg, As and Cd contamination, although it can be confirmed that there are not high concentrations of these metals in the channel.

Total concentrations of the metals show that mean Cr concentrations have decreased from 13.21mg/kg in 2000 to 7.37mg/kg in 2019. Mean Cu concentrations have increased from 3.62mg/kg in 2000 to 6.43mg/kg in 2019. Pb has also increased from <5mg/kg in 2000 to 7.43mg/kg in 2019. Finally, and most strikingly, Zn concentrations have increased from 16.35mg/kg in 2000 to 57.4mg/kg in 2019. It must be noted that the comparison of these absolute concentrations will be influenced by the sampling factors mentioned in Section 4.1.3. Despite these limitations, it is clear that the concentrations of Pb, Cu and Zn have all increased in the last 20 years.

When comparing the EF and total heavy metal concentration results from the current study with those from the previous benchmark studies (1977 and 2000), it can be concluded that the most concerning heavy metals in Knysna are Zn, Cu and Pb which have increased in contamination over the past 20 years. Furthermore, future analysis into the causes and potential remediation of this extreme Zn enrichment will be necessary to curb this increasing trend and prevent future contamination.

7.3.2 Comparing heavy metal concentrations in Knysna with similar estuarine environments

Comparison with South African estuaries

Scientific work covering heavy metal concentrations in surface sediments from South African estuaries is scarce in recent years. Furthermore, much of the recent research on surface sediments are from mining/ farming areas in South Africa and therefore have limited similarities with Knysna. The following section therefore compares the available literature from South African estuaries with Knysna, with the heavy metal concentrations results being found in **Table 7.1**.

From the available literature, it is interesting to note that the heavy metal concentrations present in the current study are comparable to those seen in a 2001 study from the Swartklops Estuary, located about 250km to the east of Knysna (Binning and Baird, 2001). The Swartklops had higher Cr and Pb concentrations than Knysna, with a mean Cr concentration of 20.3mg/kg and 7.37mg/kg respectively. and respective mean Pb concentrations of 32.9mg/kg and 7.43mg/kg. at Knysna and in the Swartklops. The mean Cu and Zn concentrations in the Swartklops are very similar to those seen in Knysna, with Cu concentrations of 6.8mg/kg in the Swartklops vs 6.43mg/kg in Knysna and Zn concentrations of 35.9mg/kg in the Swartklops vs 57.4mg/kg in Knysna. These results may indicate that Zn contamination is widespread in the greater region. The qualification must be stated that the concentrations from the Swartklops study are 20 years old and therefore likely do not represent the current condition of the system. Additionally, the study does not have enrichment factor data and, therefore, this comparison can only be made with total heavy metal concentrations.

An unpublished paper from 2010, concerning the heavy metal concentrations in the St. Lucia Estuary in Kwazulu Natal showed that the estuary had much higher heavy metal concentrations than those seen at Knysna, with Cr: 123.89mg/kg, Cu: 47mg/kg and Pb: 16mg/kg (Agjee *et al*., 2010). Zn was the exception, with concentrations in the St Lucia Estuary being analogous to those seen in Knysna with a mean concentration of 46.89mg/kg vs 57.4mg/kg at Knysna. Once again, background heavy metal concentrations likely underlie the difference, and since this research is unpublished, further validity cannot be given to these results.

A recent study on heavy metal concentrations from the Mvoti River and Estuary in KwaZulu Natal shows negligible concentrations of Cr, Pb and Zn, with all mean concentrations being 0-1mg/kg,

which is much lower than the concentrations seen at Knysna (Sukdeo *et al*., 2012). It must, however, be stated that the study only had 8 samples from various locations on the river and therefore it is likely that the results would be much different with greater sample densities. It is also possible that the Mvoti River system has much lower inputs of heavy metals than Knysna. The very low concentrations of Al present in the sediment samples from this study (<100mg/kg) may also indicate that the sediment has extremely low background concentrations of heavy metals (Sukdeo *et al*., 2012).

A recent PhD thesis, which covered the topic of heavy metal contamination in the Berg River and Estuary, showed that the Berg River Estuary has much higher As, Cd, Cr and Pb concentrations than what is present at Knysna, with mean values of 21.17mg/kg for As, 1.88mg/kg for Cd, 98.76mg/kg for Cr and 386.45mg/kg for Pb (Benamer, 2014). Cu concentrations were comparable to those seen at Knysna with 5.26mg/kg in the Berg River and 6.43mg/kg in Knysna. Surprisingly, Zn concentrations were significantly lower than those in the Knysna Estuary, with mean surficial Zn concentrations of 26.95mg/kg vs 57.4mg/kg in Knysna. Furthermore, the author conducted enrichment factor analysis which also showed that the degree of enrichment in the Berg River was much higher for Cd, Pb and Cr than what is seen at Knysna, with mean EF values of 60 for Cd, 298.42 for Pb and 199.86 for Cr. These results show that the Berg River Estuary has far higher levels of heavy metal contamination than what is seen at Knysna, which can probably be explained by differences in land use, due to the relatively large degree of urban, industrial, and agricultural activity present along the Berg River Catchment. The author did not, however, directly attribute the high degree of contamination to any specific source, but rather to anthropogenic activity as a whole. The more intensive forms of land use present in the Berg River, therefore, seem like the logical cause of the disparity in contamination between the systems.

Finally, the most recent study, conducted on the Mhlathuze Estuary in KwaZulu-Natal showed higher heavy metal concentrations than Knysna, with the exception of Zn (Izegaegbe *et al*., 2020), with mean Cr concentrations of 53.3mg/kg vs 7.37mg/kg at Knysna, Pb concentrations of 13.6mg/kg vs 7.43mg/kg at Knysna, Cu concentrations of 14.3mg/kg vs 6.43mg/kg at Knysna, Zn concentrations 18.8mg/kg vs 57.4mg/kg at Knysna. Mean Al concentrations were much higher in the Mhlathuze, with 12668mg/kg vs 2138 at Knysna. The authors also conducted EF analysis and acquired mean EF results of 1.6 (class 2) for Pb, 2.9 (Class 3) for Cr, 1.4 (class 2) for Cu and 0.7 (class 1) for Zn. These EF results therefore indicate that the Mhlathuze is less enriched than Knysna with Pb, Cu and Zn, despite having higher Pb and Cu concentrations. The high level of Zn enrichment in Knysna compared to the negligible enrichment in the Mhlathuze, in addition to the relatively low Cr enrichment in Knysna compared to the higher Cr enrhichment in the Mhlathuze is interesting and indicative of very different forms of contamination between the systems.

Despite the relative lack of recent literature, it would appear from the above studies that the Knysna Estuary has relatively low heavy metal concentrations when compared to other estuarine

environments along the coast of South Africa. The notable exception is once again Zn, which seems to exist in comparable, or higher, concentrations in Knysna than these in other environments and further poses the challenge to manage Zn enrichment in Knysna in future years. Future research, in which sediment samples are collected along the course of the Knysna River and Estuary, would also be highly beneficial, as this would provide a more useful comparative data set when looking at results from other river systems in South Africa, and negate the effect that the locality-specific factors present within the Ashmead Channel have had on this comparison.

Comparison with similar sized estuaries around the globe

When the Knysna results are compared to those from similar-sized estuaries from around the globe, the concentrations are placed in more context (**Table 7.1**). The concentrations of all the metals seem low in relation to other estuaries, with the notable exception of Zn, which is similar to or higher than a number of estuaries. The Derwent Estuary in Australia and Seine estuary in France have much higher concentrations of all metals, including Zn (which is 44.6 times higher in the Derwent and 7.8 times higher the Seine). Despite differences in sediment composition likely explaining much of this extreme disparity in heavy metal concentrations, it is clear that even the highest heavy metal concentrations in Knysna are low in relation to systems with very high heavy metal concentrations.

Table 7.1 Mean heavy metal concentrations (mg/kg) from other estuarine environments

	Cr	Cu	Pb	Zn	Cd	As	Reference
South Africa:							
Knysna Estuary	7.37	6.43	7.43	57.4	Neg	Neg	Current Study
Swartklops Estuary	20.3	6.8	32.9	35.9	N.A	N.A	Binning & Baird, 2001
St. Lucia Estuary	123.89	47	16	46.89	N.A	N.A	Agjee *et al*., 2010
Mvoti River and Estuary	0-1	N.A	0-1	0-1	N.A	N.A	Sukdeo *et al*., 2012
Berg River Estuary	98.76	5.26	386.45	26.95	1.88	21.17	Benamer, 2014
Mhlathuze Estuary	53.3	14.3	13.6	18.8	0.2	N.A	Izegaegbe et al., 2020
Rest of the world:							
Sangu River Estuary, Bangladesh	25.15	29.42	19.58	88.97	Neg	2.58	Hossain *et al*., 2019
Meghna River Estuary, Bangladesh	10.59	6.22	12.48	42.41	0.28	N.A	Siddique *et al*., 2021
Klang Estuary, Malaysia	N.A	9.38	37.39	22.46	NA	N.A	ELTurk *et al*., 2019
Derwent Estuary, Australia	N.A	130	509	2557	18	56	Coughanowr *et al*., 2015
Seine Estuary, France	98	N.A	138	448	6.2	N.A	Hamzeh et al., 2014
Yangtze Estuary, PRC	124	19.7	39.5	133	N.A	N.A	Current Study

7.4 Comparative analysis between Knysna and Chongming

7.4.1 Forward

Before comparing the Ashmead Channel and Chongming Island, it must once again be reiterated that the two systems are orders of magnitude different in size, located on opposite sides of the planet, experience dramatically different forms and scales of contamination, and have different land-use practices, flow volumes and sediment volumes. This comparison therefore takes a high-level view of the differences in sediment characteristics and degrees of contamination between the two localities and does not go into a high degree of depth as it is simply not possible due to the constraints present within this dissertation. The statistics used in this discussion use only the 36 samples collected from Knysna in 2019, except for EF, which includes the results from the 2018 study. The comparison is structured into broad categories to best interpret the data.

7.4.2 Sediment characteristics

Sediment characteristics vary greatly between each system, with the Chongming Island sediment being composed of much finer sediment particles (**Figure 7.2**), with a much lower average mean size than what is seen at Knysna, with 9.51μm at Chongming and 173μm for Knysna. The grain size distribution at Chongming appears to be more uniform and unimodal than what is seen at Knysna, with each sample having approximately the same grain size distribution. The Knysna sediment appears to be slightly bimodal, with a silt component and a sand component. The sediment samples from Knysna also vary greatly based on location and depositional environment. The mud component (<63um) is therefore much greater in the Chongming Island sediment than at Knysna.

The Chongming samples have vastly higher Al concentrations than Knysna, with a mean value of 27100mg/kg at Chongming as opposed to 2138mg/kg at Knysna, which is in excess of an order of magnitude greater (**Table 7.2**).

The TOC present at each locality is also different, with a mean value of 5.3% for Knysna and 8.1% for Chongming, indicating that the Chongming Island sediment has a greater organic matter component. These results indicate that the sediment surrounding Chongming is much more conducive for the accumulation of heavy metals and would be expected to have much higher background heavy metal concentrations due to the large Al component (Newmann & Watling, 2007).

Table 7.2: Mean values of important parameters from the Ashmead Channel and Chongming Island								
	Al (mg/kg)	**Cr (mg/kg)**	**Cu (mg/kg)**	**Pb (mg/kg)**	**Zn (mg/kg)**	**Hg (mg/kg)**	**TOC (%)**	**Grain Size (μm)**
Xisha	25900	117	29.4	49.9	130	0.153	6.1	11.17
Gangyang	27900	129	13.2	32.6	135	0.113	8.1	8.41
Mean Chongming	27100	124	19.7	39.5	133	0.129	7.3	9.52
Knysna	2138	7.37	6.43	7.43	57.4	<0.5	5.3	157.6
Difference	24962	117	13	32	76	N.A	2	-148

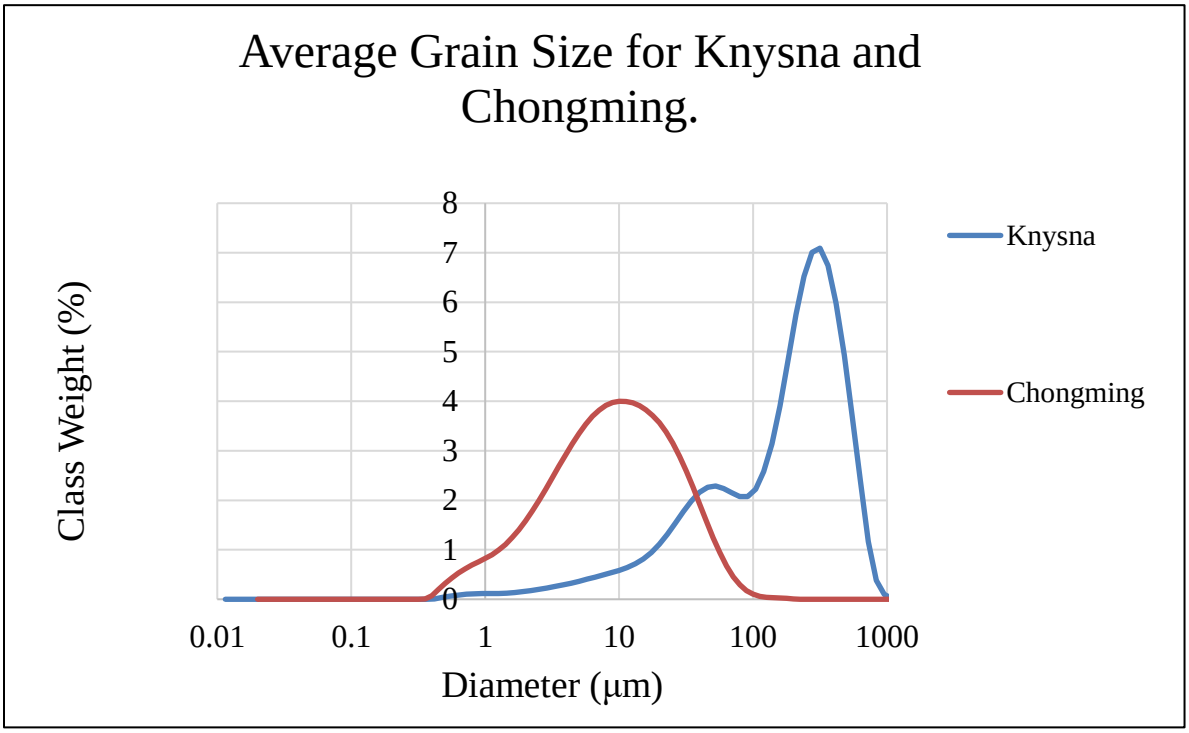

Figure 7.1: Cumulative frequency line graphs depicting the MGS distribution at Chongming Island and the Ashmead Channel

7.4.3 Absolute heavy metal concentrations

The absolute heavy metal concentrations on Chongming Island appear to be much higher than those seen at Knysna (**Table 7.2**). The difference varies significantly between metals, with Cr being, on average, 16.8 times higher at Chongming than at Knysna, Pb: 5.32 times, Cu: 3.06 times and Zn: 2.32 times. It was not possible to compare Cd concentrations as there was an error with the machine results pertaining to the Cd from Chongming Island.

It is not possible to determine the difference in anthropogenic contamination from the comparison of total heavy metal concentrations alone, due to the differences in sediment background concentrations based on local environmental characteristics. It is, however, interesting to see that Zn concentrations are relatively similar, despite the large difference in environmental characteristics. The absolute heavy metal concentrations also seem to vary more greatly with space in Knysna than at Chongming, which appears to be more uniform. This, however, may be attributed to the differences in depositional environments and local contaminants at Knysna in contrast to the conditions experienced at the Chongming island sites which are likely very similar to each other as they all lie within the same part of the Yangtze system.

The heavy metal concentrations on Chongming appear to be similar at both Gangyang and Xisha, however, concentrations do seem to be higher at the older reclaimed land at Gangyang than the more recently deposited sediment.

7.4.4 Enrichment factor comparison

A more informative comparative topic than absolute heavy metal concentrations is enrichment factor, since the normalization of heavy metal concentrations with baseline ratios allows for an apples-to-apples comparison between the two systems and removes much of the effect of the huge disparity in Al concentrations (Barbieri, 2016; Newman & Watling, 2007).

A comparison of EF values from both sites is interesting as it indicates a much more similar degree of enrichment than what would be assumed from the differences in heavy metal concentrations. **Table 7.3** shows a comparison between the mean EF classes in both systems and is interesting as it suggest that, while Cr contamination is much more significant in Chongming, Zn and Cu enrichment are similar and Pb enrichment may be higher in the Ashmead Channel. This does not necessitate that the Knysna Estuary is more contaminated that the Yangtze Estuary, which is infamously one of the most contaminated river systems globally in terms of contaminant volume. There are, instead, several possible explanations for this apparently shocking result.

Table 7.3: Average EF classes for both Estuaries				
	Cr	Zn	Pb	Cu
Chongming	3.27	3.67	1.8	2.27
Knysna	1.69	3.89	2.56	2.33
Difference	1.58	-0.22	-0.76	-0.06

The principal explanation for the similarity in results has to do with factors relating to scale and dilution effects arising from differences in sediment accumulation rates. The small scale of the Ashmead Channel and surrounding rivers, combined with the low water and sediment flow rates and presence of several local contaminant sources, causes a relative intensification of heavy metals in the sediment. Chongming Island represents the other end of the spectrum, with the Yangtze River being one of the largest rivers in the world. The enormous volumes of both sediment and water, therefore, result in huge dilution effects through the rapid rates of sediment accumulation (Chen *et al*., 2004; Chen & Wang, 2008; Wu *et al*., 2019). These rapid sediment accumulation rates therefore means that the period represented by the Chongming sites likely only represents a few years of accumulation, whereas the equivalent sediment depth in Knysna may represent several decades of accumulation. As a result, despite the enormous scale of the heavy metal inputs into the Yangtze River, the total extent of heavy metal enrichment in the sediment is much lower than it would otherwise be.

The second major issue is that of site selection. Most of the Knysna samples were deliberately collected from sites that were likely exposed to the highest degree of contaminants. Furthermore, many of the Ashmead Channel sites had more favourable conditions for sediment deposition and heavy metal accumulation than would be typical in the remainder of the estuary (Watling & Watling, 1978; Largier, 2000; Maree, 2000). This, in conjunction with the low levels of circulation present in the Ashmead, the relatively high numbers of contaminant sources and the intentional site selection mean that the results from Knysna likely represent the worst case scenario for the Knysna system as a whole. This is evident when considering the results from the 2018 samples collected from the south of Thesen Island, which have minimal heavy metal enrichment. This contrasts with the Chongming Island samples, which were collected from sites with no specific localized metal sources. The samples were instead collected from both Gangyang and Xisha so as to get the most representative result for the two sites. The results from Chongming should therefore likely be a passable representation of other sites in the Yangtze Estuary and, therefore the contamination present in the sediment is likely widespread in the system.

Subsequently, it is suggested that although the EF results are fairly similar, this is not an indication that the Knysna estuary is similarly contaminated to the Yangtze. Rather, even at the most contaminated sites, under most pressing conditions, the degree of enrichment present in the

sediments at Knysna appears to be comparable for at least Zn, Pb and Cu. The fact that this comparison can even be made should be a cause for some concern in Knysna, particularly due to the trajectory of heavy metal contamination in the system since the Monteiro *et al*. (2000) report.

7.4.5 Key points from the comparison

Despite the immense difference in scale between the Knysna and Yangtze estuaries, this small overview of two regions in each system has led to several important conclusions and observations.

It is evident that the sediment on Chongming is composed of much finer-grained particles and has far higher Al content and higher TOC values than Knysna, which can explain much of the disparity in total heavy metal concentrations when compared to the Ashmead Channel. Enrichment factor proves to be the most informative comparative tool and has shown that the degree of enrichment in the Ashmead Channel is more similar to that seen at Chongming than one might expect when conducting a literature review of the two systems.

This form of comparison between estuarine systems is useful for assessing the degree of human impact on estuarine environments and can lead to both interesting conclusions and encourage knowledge transfer between researchers working in and around such systems. It should be noted that a comparison between the Knysna and Yangtze estuaries is likely not completely ideal in terms of the immense environmental differences mentioned in the above paragraphs and the differences in culture and land use. This significantly limits the usefulness of such a study when considering estuarine management, or determination of the origins of the contaminants in each system.

A further limiting factor is that, due to the scale of the Yangtze and scope of this dissertation, it is not possible to directly compare contaminant sources with any meaningful detail, whereas, if a smaller, more similar system had been chosen, it would have been possible to conduct a more direct comparison, rather than a high-level overview.

In future, a more practical comparative study may be conducted between Knysna with other African estuaries, or with estuaries from areas of the world with similar socio-economic conditions to Knysna.

8. Conclusions

8.1 Assessment of the accomplishment of aims and objectives of the study

This study has been largely successful in accomplishing the primary aim of determining the extent of recent heavy metal contamination in the Ashmead Channel. Comparative analyses between the 2018 and 2019 results and those of the two prior studies provide an indication of the trajectory of heavy metal enrichment in the Ashmead Channel over the past 40 years. The results indicate that Zn, Cu and Pb are the key metals which have increased in concentration and enrichment level in recent decades.

The second component of the aim, which comprised a low-resolution comparative analysis between the Knysna and Yangtze estuaries, has also a been achieved. The means by which this project attempted to accomplish the objectives as listed in **Section 1.2** are detailed directly

Objective a, which entailed sampling surface sediments from representative localities in the Ashmead Channel and surrounding rivers and canals was predominantly accomplished. Ideally, further samples should be collected from the lower reaches of the Bigai Stream and Estuary, as this represents a hole in the data. Future studies should also sample a wider area of the Knysna Estuary in order to form a more representative dataset that is less influenced by the somewhat unique factors affecting the Ashmead Channel and surrounds. Future studies should also consider addressing the access issues which prevented sampling in some areas in 2019. The sampling conducted in this dissertation nevertheless represents a sufficient worst case scenario for heavy metals in Knysna and includes sediment influenced by many of the potential contaminant sources in the system. The results, therefore, provide valuable information to stakeholders and decision-makers in the area.

This study also mostly succeeded in sampling surface sediments in representative localities on Chongming Island, as highlighted in **Objective b**. This sampling covered only a fraction of the Yangtze Estuary yet was sufficient to form the high-level comparison that was intended within this project. Had the comparison formed a larger component of the dissertation, a larger number of sites with a wider distribution would have been more ideal., The sites chosen for this study were a good optimization given the time and logistical constraints present during the fieldwork excursion in the Yangtze.

Objective c, which covers the laboratory analysis component of the dissertation, was very successful and included a good suite of tests for the desired aim, while not requiring excessive

time or funding. The fact that the Knysna Municipality funded and hired a laboratory to conduct the ICP-OES heavy metal quantification allowed for a much larger number of samples to be collected and, therefore, a much richer body of data to be used for developing this dissertation.

Objective d, pertaining the statistical analyses and graphing of the data, was carried out successfully. The data were effectively organised in order to facilitate comparison between previous studies in Knysna and the results from the Yangtze. The analysis would likely have benefitted from more advanced statistics, such as Principal Component Analysis, to further determine commonalities in heavy metal sources, however, the suite of statistics used did a sufficient job in fulfilling the aim.

Objective e entailed mapping the contaminant concentrations. This was modified to include the mapping of enrichment factor values classes, as they represent a more holistic picture of the state of contamination in the two systems, and was successful. The use of red scale intensity maps allows for easy interpretation of the enrichment factor data, which fulfils the objective effectively. Furthermore, the many maps throughout the dissertation enable visualisation of the locality and conditions present at each site in Knysna, which, together with site descriptions and photographs make the content accessible.

Objective f, which entailed comparing the current state of heavy metal contamination in Knysna to that in prior studies, was achieved. The similarities between the sampling sites, coupled with the calculation of enrichment factor both on the current and previous results allowed for a good apples-to-apples comparison and thus for strong conclusions to be drawn. The comparison between the Knysna Estuary and other South African estuarine environments was somewhat less successful, predominantly due to the sparse research available for the last two decades. This comparison allowed for some tentative conclusions to be drawn, although the lack of recent comparative studies does mean these conclusions are not very strong.

Finally, this dissertation has been somewhat successful in accomplishing **Objective g**, which involved comparing the geochemical composition and extent of heavy metal contamination between the Knysna and Yangtze estuaries. This was predominantly a surface-level comparison, and no attempt was made to directly compare the sources of contamination in these systems, however, the suite of results did allow for comparison of the basic sediment composition between the systems. The total HM concentrations and enrichment factor results also allowed for comparison between the extent of contamination in these two systems. Many caveats had to be made when considering the comparative results, however, the comparison itself was largely a success.

8.2 Key conclusions to be drawn from this research

From this research, it is possible to draw several key conclusions for the state of heavy metal contamination within the Knysna system. It is evident that, at present, the absolute heavy metal concentrations within the channel should not be a threat to human and animal life, with the majority of the sediment samples having concentrations below the RNAL guidelines for these metals, with the exception of Zn at a few isolated sites. It is also clear that of the metals sampled, the most concerning with regards to continued enrichment are Zn, Cu and Pb, with Cr being found within baseline concentrations and Hg, Cd and As being negligible.

The trend in heavy metal enrichment in the Ashmead Channel observed by analysing the enrichment factor results is highly concerning. There is a small reduction in enrichment from the Watling & Watling (1978) study until the baseline study of Moneteiro *et al*. (2000) and then a dramatic increase in enrichment between 2000 and the 2018-2019 sampling period of this dissertation, in which EF classes of 3-5 for Zn and 2-4 for Cu and Pb are observed.

The recent increased levels of enrichment of Zn, Cu and Pb is concerning and seems to be most intense in three regions: the Knysna CBD, the Industrial Area and the East Ashmead Region, which drains the Bongani Stream and the Industrial Area. The Costa Sarda region and south Thesen Island are the areas in the study area with the least enrichment. This study is not able to directly ascertain source-sync relationships, however, continued urban development in the area can likely be identified as a cause of the increase in enrichment in the Ashmead. The very high levels of enrichment and HM concentrations present in the Vigilance Drive Canal would suggest that the industrial activities present in this zone are also contributing to the progressive enrichment of Zn, Cu and Pb in the Ashmead Channel. From the high levels of enrichment present in the CBD area, it is likely that urban runoff and possibly increasing runoff from the N2 national road, linked to vehicle emissions, are also increasing the concentrations of these metals in the stormwater drains and canals. Furthermore, corrosion of the corrugated metal roofs present in the semi-formal settlements in the eastern areas of Knysna may be continuously leeching Zn into the environment, with the growth in these settlements increasing the rate of this process. Finally, it is also highly likely that the use of Zn in the sacrificial anodes of boats is contributing to the enrichment present in the estuary (Mathiessen *et al*., 1999).

Despite the low absolute concentrations of these metals, it is important to consider that, due to the high enrichment factor of these sediments, a large portion of these metals likely exists in the bioavailable, mobile fraction of the sediment and can therefore be assimilated into the tissues of the local biota (Barbieri, 2016).

Finally, it should again be noted that the enrichment present within the Ashmead Channel likely represents an intensification of the polluting factors in Knysna, with many of the key polluting

entities discharging effluent into a relatively small area which has constrained tidal flushing, and therefore the remainder of the estuary likely has a reduced degree of enrichment when compared to the Ashmead.

When the results from Knysna were compared with those from Chongming Island, it was found that the total heavy metal concentrations in Knysna are much lower than those present in the Yangtze. The degree of heavy metal enrichment was, however, quite similar for the two systems despite the large disparity in absolute heavy metal concentrations. The large (sometimes an order of magnitude) difference in absolute concentrations occurs predominantly as a result of differences in sediment composition linked to vastly higher Al concentrations (by approximately an order of magnitude), and therefore clay minerals in the Yangtze samples, which leads to far higher concentrations of non-bioavailable lattice-bound metals (Newman & Watling, 2007; Barbieri, 2016). The similarities in EF results can be largely explained by the vast differences in sediment accumulation rates between the systems, resulting in large scale dilution within the Yangtze and relative intensification effects. Despite this dilution effect, it is still concerning that the degree of enrichment is comparable between Knysna and one of Earth's most-contaminated systems (by volume of pollutant input) (Chen et al., 2004; Chen & Wang, 2008; Wu et al., 2019). In future, the sedimentation rate difference that influences the heavy metal results could be resolved through the development of a robust age model, however this falls beyond the scope of this dissertation.

When comparing the results from Knysna with those from other South African estuaries, it is evident that the heavy metal concentrations in Knysna are relatively low, with the exception of Zn, which is significantly higher than all but the St. Lucia Estuary, and Cu, which values are similar to those of most of the other systems. The heavy metal concentrations from Knysna are also shown to be low relative to other similarly sized estuaries from around the globe, once again with the exception of Zn, which values are in the range of, or higher than a number of other estuaries. Comparison reveals that a number of systems, namely the Derwent Estuary in Australia and Seine Estuary in France, have substantially higher mean Zn concentrations than Knysna, with concentrations 2257mg/kg and 448mg/kg respectively, with Knysna having a mean concentration of 57.4mg/kg These results therefore show that, while the increasing Zn concentrations in Knysna are concerning, they are not especially high on a global scale.

In closing, considering that Knysna is the estuary with the highest degree of ecological significance in South Africa, with many species depending on the health of the estuary for their continued existence, in addition to the many people dependent on the estuary for their livelihoods, it is, therefore, crucial that the trend of increasing heavy metal concentrations in Knysna be curbed (Turpie *et al.*, 2002). It is not within the scope of this dissertation to quantify exactly when heavy metal contamination in Knysna will reach a threshold that poses a risk to the health of the system, however, it is clear that the current rate of contamination needs to be slowed in order to preserve the pristineness of the system. Siltation and nutrient pollution are already leading to serious habitat

disruption in Knysna, with heavy metal pollution looming as a future threat should this trend continue (Maree, 2000; Human et al., 2016; Harvey 2019). The maintenance of the health of the estuary as a fish nursery ground and bird sanctuary, coupled with the prevention of heavy metal bioaccumulation within fish species, will also act to protect the fisheries of the southern coast of South Africa and, in turn, preserve the local ecology for current and future generations. The results of this dissertation should therefore be considered an early warning of a problem that has the potential to become more serious in the future.

9. References

Adachi, K. and Tainosho, Y., 2004. Characterization of heavy metal particles embedded in tyre dust. *Environment International*. 30(8): 1009-1017.

Agjee, N., Pillay, K. and Pillay, S. 2010. An assessment of sediment heavy metal concentrations in the lower St. Lucia Estuary, KwaZulu Natal, South Africa. *Unpublished manuscript cited by Sudkeo et al.*

Allanson, B.R. 2000a. The Knysna Basin project reviewed—research findings and implications for management. *Transactions of the Royal Society of South Africa*. 55(2): 97-100.

Allanson, S. 2000b. Bibliography of scientific and environmental literature (published and unpublished), relating to the Knysna Basin: lagoon, estuary, river and catchment. *Transactions of the Royal Society of South Africa*. 55(2):223-237.

A.l. Abbott and Associates. 2016. ICP-OES Laboratory Test Method no. 5.4.2/1/92 Rev 4. 1-28.

Alloway, B.J. 2013. Sources of Heavy Metals and Metalloids in Soils. In *Heavy Metals in Soils: Trace Metals and Metalloids in Soils and their Bioavailability.* B.J. Alloway, Ed. Dordrecht: Springer Netherlands. 11-50.

American Public Health Association. 1998. *WEF Standard methods for the examination of water and wastewater 20th edition.* L.S. Clesceri, A.E. Greenberg, A.D. Eaton, Eds. Washington DC: American Public Health Association.

Armitage, M.P.A. 2018. A Current Analysis of the Heavy Metal Load in the Ashmead Channel (Knysna Lagoon) Sediments. Unpublished BSc Honours Dissertation. The University of Cape Town.

Bao, J. and Gao, S. 2021. Wetland utilization and adaptation practice of a coastal megacity: a case study of Chongming Island, Shanghai, China. *Frontiers in Environmental Science*. 9

Barbieri, M. 2016. The importance of enrichment factor (EF) and geoaccumulation index (Igeo) to evaluate the soil contamination. *Journal of Geology & Geophysics* 5(1): 1-4.

Bateman, C. 2009. Up to its eyeballs in sewage: Government pleads for help. *SAMJ: South African Medical Journal*. 99(8): 556-560.

Bellucci, L.G., Frignani, M., Paolucci, D. & Ravanelli, M. 2002. Distribution of heavy metals in sediments of the Venice Lagoon: the role of the industrial area. *Science of the Total Environment.* 295 (1-3): 35-49.

Benamer, M. 2014. Chemical speciation and spatial distribution of heavy metals and their adsorption onto sediments of the Berg River, Western Cape, South Africa. PhD thesis: University of Cape Town.

Binning, K. and Baird, D. 2001. Survey of heavy metals in the sediments of the Swartkops River Estuary, Port Elizabeth, South Africa. *Water SA.* 27(4): 461-466.

Blankworldmap.net. 2021. Printable Blank South Africa Map with Outline, Transparent Map. Available: https://blankworldmap.net/tag/blank-map-of-south-africa/.

Blott, S.J. and Pyre, K. 2001. Gradistat: a grain size distribution and statistics package for the analysis of unconsolidated sediments. *Earth Surface Processes and Landforms*. 26(11): 1237-1248.

Bonanno, G. & Giudice, R.L. 2010. Heavy metal bioaccumulation by the organs of Phragmites australis (common reed) and their potential use as contamination indicators. *Ecological Indicators*. 10(3: 639-645.

Bradl, H. B. 2005. *Heavy metals in the environment: origin, interaction and remediation, 1st edition*. H.B. Bradl, Ed. Elsevier Academic Press, London. 1-288.

Bryan, G.W. & Langston, W.J. 1992. Bioavailability, accumulation and effects of heavy metals in sediments with special reference to United Kingdom estuaries: a review. *Environmental Pollution*. 76(2):89-131.

Chen, Z., Kostaschuk, R. & Yang, M. 2001. Heavy metals on tidal flats in the Yangtze Estuary, China. *Environmental Geology*. 40(6): 742-749.

Chen, Z., Saito, Y., Kanai, Y., Wei, T., Li, L., Yao, H. & Wang, Z. 2004. Low concentration of heavy metals in the Yangtze estuarine sediments, China: a diluting setting. *Estuarine, Coastal and Shelf Science*. 60(1):91-100.

Chen, G.G., Xi, X.H., Liang, X.H., Liu, H.Y., Zhang, M., Tian, F.J. 2008. Soil geochemical baselines of the Yangtze River Delta and their significances. *Geoscience.* 22 (6): 1041–1048.

Chen, B. & Wang, K. 2008. Suspended sediment transport in the offshore near Yangtze Estuary. *Journal of Hydrodynamics, Series B.* 20(3):373-381.

Claassens, L., Barnes, R.S.K., Wasserman, J., Lamberth, S.J., Miranda, N.A.F., Van Niekerk, L. & Adams, J.B. 2020. Knysna Estuary health: ecological status, threats and options for the future. *African Journal of Aquatic Science*. 45(1-2): 65-82.

Coughanowr, C., Whitehead, S., Whitehead, J., Einoder, L., Taylor, U., Weeding, B. 2015. State of the Derwent estuary: a Review of Environmental Data from 2009 to 2014. In: Derwent Estuary Program.

CSIR. 1991. *Exploratory investigation of the dump sites on Thesen Island with reference to potential impact on the water quality in the lagoon and proposed marina*. CSIR Report EMA-C 918. Stellenbosch.

Day, J.H., Millard, N.A.H. & Harrison, A.D. 1952. The ecology of South African estuaries. Part III. Knysna: a clear open estuary. *Transactions of the Royal Society of South Africa*. 33(3): 367-413.

Department of Environmental Affairs. 2019. *Review And Update Of South Africa's National Action List For The Screening Of Dredged Sediment Proposed For Marine Disposal*. South Africa: Department of Environmental Affairs.

Dierkes, C., Göbel, P., Lohmann, M. & Coldewey, W.G. 2006. Development and investigation of a pollution control pit for treatment of stormwater from metal roofs and traffic areas. *Water Science and Technology*. 54(6-7): 291-298.

ELTurk, M., Abdullah, R., Zakaria, R.M. and Bakar, N.K.A. 2019. Heavy metal contamination in mangrove sediments in Klang estuary, Malaysia: implication of risk assessment. *Estuarine, Coastal and Shelf Science*. 226: 106266

Gao, W., Du, Y., Gao, S., Ingels, J. & Wang, D. 2016. Heavy metal accumulation reflecting natural sedimentary processes and anthropogenic activities in two contrasting coastal wetland ecosystems, eastern China. *Journal of Soils and Sediments*. 16(3):1093-1108.

Google Earth Pro 7.3 .2019a. The Knysna Estuary [Map, July 2019]. 34° 02' 53.42"S, 23° 05' 03.14"E, Eye alt 6.32km. AfriGIS (Pty) Ltd., DigitalGlobe, Google. 2019. Viewed 10 July 2019

Google Earth Pro 7.3 .2019b. The Yangtze Estuary [Map, July 2019]. 31° 38' 43.63"N, 121° 28’ 43.85"E, Eye alt 159.24km. Data SIO, NOAA, U.S. Navy, NGA, GEBCO Image Landsat/ Copernicus, TerraMetrics .2019. Viewed 10 July, 2019.

Google Maps. 2019. Map of the Eastern hemisphere. Available: https://www.google.com/maps/@1.0572231,47.7881847,3.08z [2019, July 11].

Gopal, B. 1999. Natural and constructed wetlands for wastewater treatment: potentials and problems. *Water Science and Technology*. 40(3): 27-35.

Gupta, V. 2020. Vehicle-generated heavy metal pollution in an urban environment and its distribution into various environmental components. *Environmental Concerns and Sustainable Development* .113-127. Springer, Singapore.

Hamzeh, M., Ouddane, B., Daye, M., & Halwani, J. (2014). Trace metal mobilization from surficial sediments of the Seine River Estuary. *Water, Air, & Soil Pollution*. 225(3): 1-15.

Harris, D., Horwáth, W.R. and Van Kessel, C. 2001. Acid fumigation of soils to remove carbonates prior to total organic carbon or carbon-13 isotopic analysis. *Soil Science Society of America Journal*. 65(6): 1853-1856.

Harvey, A. 2018. An investigation of the pollution contribution of catchments surrounding the Knysna Estuary, with implications for stormwater management. MSc ENG Dissertation. The University of Cape Town.

He, Z., Li, F., Dominech, S., Wen, X. and Yang, S. 2019. Heavy metals of surface sediments in the Changjiang (Yangtze River) Estuary: distribution, speciation and environmental risks. *Journal of Geochemical Exploration*. 198: 18-28.

He, W., Wallinder, I.O. and Leygraf, C. 2001. A comparison between corrosion rates and runoff rates from new and aged copper and zinc as roofing material. *Water, Air and Soil Pollution: Focus*. 1(3): 67-82.

Heiri, O., Lotter, A.F. & Lemcke, G. 2001. Loss on ignition as a method for estimating organic and carbonate content in sediments: reproducibility and comparability of results. *Journal of Paleolimnology*. 25(1):101-110.

Hossain, M.B., Shanta, T.B., Ahmed, A.S., Hossain, M.K. and Semme, S.A. 2019. Baseline study of heavy metal contamination in the Sangu River estuary, Chattogram, Bangladesh. *Marine pollution bulletin*. 140: 255-261.

Human, L.R.D., Adams, J.B. and Allanson, B.R., 2016. Insights into the cause of an Ulva lactuca Linnaeus bloom in the Knysna Estuary. *South African Journal of Botany*. 107: 55-62.

Hseu, Z., Chen, Z., Tsai, C., Tsui, C., Cheng, S., Liu, C. & Lin, H. 2002. Digestion Methods for Total Heavy Metals in Sediments and Soils. *Water, Air, and Soil Pollution*. 141(1):189-205.

Impellitteri, C.A., Saxe, J.K., Cochran, M., Janssen, G.M. and Allen, H.E. 2003. Predicting the bioavailability of copper and zinc in soils: Modeling the partitioning of potentially bioavailable copper and zinc from soil solid to soil solution. *Environmental Toxicology and Chemistry: An International Journal*. 22(6): 1380-1386.

Izegaegbe, J.I., Vivier, L. and Mzimela, H.M. 2020. Trace metal contamination in sediment in the Mhlathuze Estuary, northern KwaZulu-Natal, South Africa: effects on the macrobenthic community. *Environmental monitoring and assessment*. 192: 1-18.

Kennish, M.J. 2018. *Ecology of estuaries volume 2: Biological Aspects*. CRC Press, Boca Raton, Florida. 1-245

Kim, K.R., Owens, G., Naidu, R. & Kim, K.H. 2007. Assessment techniques of heavy metal bioavailability in soil-A critical review. *Korean Journal of Soil Science and Fertilizer*. 40(4): 311-325.

Largier, J.L., Attwood, C. & Harcourt-Baldwin, J. 2000. The hydrographic character of the Knysna Estuary. *Transactions of the Royal Society of South Africa*. 55(2):107-122.

Levin, L.A., Boesch, D.F., Covich, A., Dahm, C., Erséus, C., Ewel, K.C., Kneib, R.T., Moldenke, A., Palmer, M.A., Snelgrove, P. & Strayer, D. 2001. The function of marine critical transition zones and the importance of sediment biodiversity. *Ecosystems*. 4(5): 430-451.

Lu, J., Yuan, F., Zhang, F. & Zhao, Q. 2016. The study on heavy metal distribution in the sediment of middle tidal flat in Yangtze Estuary, China. *Environmental Earth Sciences*. 75(7):1-12.

Lu, J. & Yuan, F. 2019. The distribution of heavy metals in the sediment of low tidal flat, eastern Chongming Island, China. *IOP Conference Series: Materials Science and Engineering.* 472 (12091): 1-7.

Ma, C., Zheng, R., Zhao, J., Han, X., Wang, L., Gao, X. & Zhang, C. 2015. Relationships between heavy metal concentrations in soils and reclamation history in the reclaimed coastal area of Chongming Dongtan of the Yangtze River Estuary, China. *Journal of Soils and Sediments*. (1):139-152.

Ma, Z., Li, B., Zhao, B., Jing, K., Tang, S. & Chen, J. 2004. Are artificial wetlands good alternatives to natural wetlands for waterbirds? – A case study on Chongming Island, China. *Biodiversity and Conservation*. 13(2):333-350.

Mahbub, P., Ayoko, G.A., Goonetilleke, A., Egodawatta, P. & Kokot, S. 2010. Impacts of traffic and rainfall characteristics on heavy metals build-up and wash-off from urban roads. *Environmental Science & Technology*. 44(23): 8904-8910.

Maree, B. 2000. Structure and status of the intertidal wetlands of the Knysna Estuary. *Transactions of the Royal Society of South Africa*. 55(2):163-176.

Matthiessen, P., Reed, J. and Johnson, M. 1999. Sources and potential effects of copper and zinc concentrations in the estuarine waters of Essex and Suffolk, United Kingdom. *Marine Pollution Bulletin*. 38(10): -920.

Mikutta, R., Kleber, M., Kaiser, K. and Jahn, R., 2005. Organic matter removal from soils using hydrogen peroxide, sodium hypochlorite, and disodium peroxydisulfate. *Soil Science Society of America Journal*. 69(1): 120-135.

Mortvedt, J.J. 1996. Heavy metal contaminants in inorganic and organic fertilizers. In *Fertilizers and Environment: Proceedings of the International Symposium "Fertilizers and Environment", held in Salamanca, Spain, 26–29, September, 1994*. C. Rodriguez-Barrueco, Ed. Dordrecht: Springer Netherlands. 5-11.

Monteiro, P.M.S., Scott, D. & Taljaard, S. 2000. Knysna Lagoon - Thesen Island development water quality baseline study: 2000 & monitoring plan (Report No. ENV-S-C 2000 046). Stellenbosch: CSIR Environmentek.

Monachese, M., Burton, J.P. & Reid, G. 2012. Bioremediation and tolerance of humans to heavy metals through microbial processes: a potential role for probiotics? *Applied and Environmental Microbiology*. 78(18): 6397-6404.

Pavlovich Muranov, A. 2021. Yangtze River. In Encyclopaedia Britannica. Available: https://www.britannica.com/place/Yangtze-River.

Newman, B.K. and Watling, R.J., 2007. Definition of baseline metal concentrations for assessing metal enrichment of sediment from the South-Eastern Cape coastline of South Africa. *Water SA*. 33(5): 675-692.

Niu, Y., Chen, F., Li, Y. & Ren, B. 2021. Trends and sources of heavy metal pollution in global river and lake sediments from 1970 to 2018. In *Reviews of Environmental Contamination and Toxicology Volume 257*. P. de Voogt, Ed. Springer International Publishing. 1-35.

Olesik, J.W. 1991. Elemental analysis using ICP-OES and ICP/MS. *Analytical Chemistry*. 63(1): 12A-21A.

Puth, M.T., Neuhäuser, M. and Ruxton, G.D., 2014. Effective use of Pearson's product–moment correlation coefficient. *Animal Behaviour*. 93: 183-189.

Rees, A.B., Gallagher, A., Comber, S. and Wright, L.A., 2017. An analysis of variable dissolution rates of sacrificial zinc anodes: a case study of the Hamble estuary, UK. *Environmental Science and Pollution Research*. 24(26): 21422-21433.

Rees, A.B., Gallagher, A., Wright, L.A., Wood, J., Cathery, T., Harrison, B., Down, C. and Comber, S., 2020. Leisure craft sacrificial anodes as a source of zinc and cadmium to saline waters. *Marine Pollution Bulletin*. 158: 111433.

Ryżak, M. and Bieganowski, A. 2011. Methodological aspects of determining soil particle-size distribution using the laser diffraction method. *Journal of Plant Nutrition and Soil Science*. 174(4): 624-633.

SABS, 2008. South African National Standard Water quality - determination of selected elements by inductively coupled plasma optical emission spectrometry (ICP-OES).

Schumacher, B.A. 2002. *Methods for the determination of total organic carbon (TOC) in soils and sediments* (Report no. NCEA-C- 1282 EMASC-001). Las Vegas: United States Environmental Protection Agency Environmental Sciences Division National Exposure Research Laboratory.

Siddique, M.A.M., Rahman, M., Rahman, S.M.A., Hassan, M.R., Fardous, Z., Chowdhury, M.A.Z. and Hossain, M.B., 2021. Assessment of heavy metal contamination in the surficial sediments from the lower Meghna River estuary, Noakhali coast, Bangladesh. *International Journal of Sediment Research*. 36(3): 384-391.

Simon, C., Du Toit, A.N., Smith, M.K.S., Claassens, L., Smith, F. & Smith, P. 2019. Bait collecting by subsistence and recreational fishers in Knysna Estuary may impact management and conservation. *African Zoology*. 54(2):91-103.

Sinex, S.A. & Wright, D.A. 1988. Distribution of trace metals in the sediments and biota of Chesapeake Bay. *Marine Pollution Bulletin*. 19(9):425-431.

Soon, Y.K. & Bates, T.E. 1982. Chemical pools of cadmium, nickel and zinc in polluted soils and some preliminary indications of their availability to plants. *Journal of Soil Science*. 33(3):477-488.

SSI. 2012. Knysna estuary pollution study final report July 2012 (Report No. W01.grj.000203). SSI Engineers & Environmental Consultants.

Sukdeo, P., Pillay, S. and Bissessur, A. 2012. An assessment of the presence of heavy metals in the sediments of the lower Mvoti River system. *African Journal of Science and Technology*. 12(1): 51-58.

Switzer, A.D. & Pile, J. 2015. Grain size analysis. In *Handbook of Sea-Level Research*. I. Shennan, A.J. Long & B.P. Horton, Eds. John Wiley & Sons. 331-346.

Thorne, L.T. & Nickless, G. 1981. The relation between heavy metals and particle size fractions within the Severn Estuary (U.K.) inter-tidal sediments. *Science of the Total Environment*. 19(3):207-213.

Thornton, I., Watling, H. & Darracott, A. 1975. Geochemical studies in several rivers and estuaries used for oyster rearing. *Science of the Total Environment*. 4(4): 325-345.

Turpie, J.K., Adams, J.B., Joubert, A., Harrison, T.D., Colloty, B.M., Maree, R.C., Whitfield, A.K., Wooldridge, T.H., Lamberth, S.J., Taljaard, S. & Van Niekerk, L. 2002a. Assessment of the conservation priority status of South African estuaries for use in management and water allocation. *Water SA*. 28(2): 191-206.

Turpie, J.K., Adams, J.B., Colloty, B.M., Joubert, A.J., Harrison, T.D., Maree, R.C. & Mackay, H. 2002b. *Classification and prioritization of South African estuaries on the basis of health and conservation priority status for determination of the estuarine water reserve (3rd edition).* Pretoria: Department of Water Affairs.

Vaasma, T. 2008. Grain-size analysis of lacustrine sediments: a comparison of pre-treatment methods. *Estonian Journal of Ecology*. 57(4):231.

Verhoeven, J.T. and Meuleman, A.F. 1999. Wetlands for wastewater treatment: opportunities and limitations. *Ecological Engineering*. 12(1-2): 5-12.

Vinodhini, R. & Narayanan, M. 2008. Bioaccumulation of heavy metals in organs of fresh water fish Cyprinus carpio (Common carp). *International Journal of Environment Science and Technology*. 5(2):179-182.

Watling, R.J. and Watling, H.R., 1977. *Metal concentrations in surface sediments from Knysna Estuary*. Pretoria: National Physical Research Laboratory, CSIR. Special Report FIS, 122:38.

Watling, RJ & Watling, H.R. 1982. Metal Surveys in South African Estuaries II. Knysna River. *Water SA*. 8(1): 36-44.

Weltje, G.J. & von Eynatten, H. 2004. Quantitative provenance analysis of sediments: review and outlook. *Sedimentary Geology*. 171(1-4): 1-11.

World Wildlife Fund. 2021. Living Yangtze. Available: https://en.wwfchina.org/en/what_we_do/living_yangtze/

Wu, S., Chen, R. & Meadows, M.E. 2019. Evolution of an estuarine island in the Anthropocene: complex dynamics of Chongming Island, Shanghai, PR China. *Sustainability*. 11(24): 6921.

Ying, M., Li, J.F., Wan, X.N. & Shen, H.T. 2005. Study on time series of sediment discharge at Datong station in the Yangtze River. *Resources and Environment in the Yangtze Basin*. 14(1): 87-92.

Yongming, H., Peixuan, D., Junji, C. & Posmentier, E.S. 2006. Multivariate analysis of heavy metal contamination in urban dusts of Xi'an, Central China. *Science of the Total Environment*. 355(1-3): 176-186.

Yu, T., Zhang, Y. and Zhang, Y., 2012. Distribution and bioavailability of heavy metals in different particle-size fractions of sediments in Taihu Lake, China. *Chemical Speciation & Bioavailability*. 24(4): 205-215.

Zhang, W., Yu, L., Hutchinson, S.M., Xu, S., Chen, Z. & Gao, X. 2001. China's Yangtze Estuary: I. Geomorphic influence on heavy metal accumulation in intertidal sediments. *Geomorphology*. 41(2):195-205.

Zhang, J. & Liu, C.L., 2002. Riverine composition and estuarine geochemistry of particulate metals in China - weathering features, anthropogenic impact and chemical fluxes. *Estuarine, Coastal and Shelf Science*. 54(6): 1051-1070.

Zhang, W., Feng, H., Chang, J., Qu, J., Xie, H. & Yu, L. 2009. Heavy metal contamination in surface sediments of Yangtze River intertidal zone: an assessment from different indexes. *Environmental Pollution*. 157(5): 1533-1543.

Zhao, B., Kreuter, U., Li, B., Ma, Z., Chen, J. & Nakagoshi, N. 2004. An ecosystem service value assessment of land-use change on Chongming Island, China. *Land use Policy*. 21(2):139-148.

Zheng, R., Zhao, J., Zhou, X., Ma, C., Wang, L. & Gao, X. 2016. Land use effects on the distribution and speciation of heavy metals and arsenic in coastal soils on Chongming Island in the Yangtze River Estuary, China. *Pedosphere.* 26(1):74-84.

10. Appendices

Appendix A: Detailed Laboratory Methodology

4.2 Laboratory Work for Knysna Samples

4.2.1 Initial sample preparation for loss on ignition and grain size analysis

The 36 samples were removed from the freezer and allowed to thaw for 48 hours. Heat-resistant crucibles were cleaned with a brush and water, then dried in an oven at 105°c for one hour, with two extra crucibles being prepared as spares in the event of one of the others breaking. The crucibles were then filled with sample using a small teaspoon and placed in a drying oven at 105°c for 24 hours to remove any moisture from the sample while retaining the dried organic matter (**Figure 4.1**). The spoon was cleaned between samples to prevent contamination. Once dry, the samples were poured into zip-seal bags for storage before further analysis. Samples were later removed from the bags and lightly ground in a pestle and mortar to disaggregate the particles which had formed a cake, without reducing the size of the sediment particles. The sediment was thereafter returned to the bag and sealed.

4.2.2 Loss on ignition

The loss on ignition process took place in the Biological Sciences Department at UCT (**Figure 4.2**). Two LOI runs were needed per sample to increase the accuracy of the experiment, therefore 72 crucibles were cleaned with soap and water and dried. The crucibles were weighed while empty, which was recorded in a document, and numbered from 1-72 in pencil on the base. Each crucible was then filled with roughly 5 grams of the dry sediment sample and the combined weight of sediment and crucible was recorded using an AND HT-120 scale. It is important to note that, due to several of the sediment samples initially being composed largely of water, some of the sediment samples did not have enough sediment for two full runs of 5 grams. Crucible 6 (Sample 3) lacked enough sediment for a second LOI run. Sample 28 also had very little sediment mass and as a result, the first run was composed of only 3.13grams of sediment, with no second run being possible, which is not ideal, however, 3.13 grams was sufficient for a reasonable result.

The crucibles were thereafter placed on three furnace trays filled with sand to stabilize the crucibles before being placed in two muffle furnaces which were allowed to reach a heat of 550°c and were left at this temperature for 3 hours to ignite, and hence remove, the organic matter in the sediment samples. The samples were then allowed to slowly cool overnight in the furnaces, which allowed for the stabilization of mass and prevention of the rapid water gain which happens when exposing

extremely hot sediment to far cooler, more moist, ambient air. The trays were removed from the furnaces the following morning and the crucibles were weighed to ascertain the final weights for the IOI analysis, which was recorded in a document. The sediment was thereafter placed in labelled zip-seal bags in preparation for grain size analysis.

4.2.3 Preparation for grain size analysis

The post-LOI samples were sieved through a 1mm tolerance sieve, to remove any large particles which could damage the lens in the Malvern Mastersizer 2000, while still preserving the sediment profile. The samples were then coned and quartered to reach the desired amount of sample, which was representative of the sediment sample (**Figure 4.3**). The method of sample division was based on the initial quantity of each sample. Larger samples were quartered twice and then halved while smaller samples were only quartered once before being halved. The reduced sample was then placed in an accurate 50ml test tube and filled to 50ml with Milli-d water and sealed to prevent dust infiltration. It is important to note that, due to the small quantity of prepared sediment, it was not possible to have multiple test tubes for the Malvern as would have been ideal, however, in order to get sufficient sediment for the machine runs on all samples, only a single test tube was used for each sample.

4.2.4 Malvern Mastersizer 2000 grain size analysis

Before every session of analysis, the Malvern Mastersizer, hereafter referred to as Malvern (**Figure 4.3**), was switched on and allowed to warm up for 30 minutes before running the first sample. The operating computer and machines water supply were also turned on at the same time. Before conducting each sample run, the sample test tube was placed on a centrifuge to force the sediment into suspension. The sample was thereafter added to the dispersion unit of the Malvern, using a pipette, until an ideal laser obscuration of between 10 and 15% was achieved.

The Malvern was then allowed to run and take a measurement, a process which takes 10 minutes. Once a run was complete, the machine took approximately 5 minutes to clean itself and flush out any of the previous sample before the next sample could be tested. The pipette was cleaned at least 3 times with Milli-d water between every sample run to prevent cross-contamination. In total, each sample was run as many times as possible given the available sediment, with most being run twice, however, several of the very sandy (large grain size) samples only had enough sediment to be run once. This is due to the same total volume of more coarse sediment leading to a lower total laser obscuration than a sample composed of finer-grained material.

Once the first batch of test tubes had been completed, several of the samples needed to be run again for two separate reasons. Firstly, if the Malvern was run once, yet did not have enough

remaining sediment for a section run, a new test tube was formulated, to add validity to the result. The other reason for a retesting was due to the grain size distributions of the first two Malvern runs of a specific sample being very different from each other. A third run was needed to get a better idea of the true grain size distribution of the sediment. It must be noted that, on the second round of testing, coning and quartering was not conducted due to the extremely small amount of sediment remaining for most of the samples.

Once the runs had been completed, the results from the runs from each sample were combined to gain a distribution that most accurately represented the true grain size distribution of the sample.

4.2.5 Heavy metal quantification

Heavy metals were analysed within the laboratories of A.l. Abbott using standard SANS 11885: 2008 methodologies during March of 2019 (SABS, 2008; APHA, 1998; A.L Abbott. 2016). It should be noted that the author was not present during the following processing of the samples and therefore the following methodology represents a summary of the standard methodology stated by Al. Abbott and Associates

Acid digestion

The samples underwent acid digestion to reduce the sediment into its constituent elements. The sediment samples were burned in a muffle furnace at 600°C to remove any moisture or organic matter from the sample. One to two grams of sample were then placed into 50ml volumetric flasks, with a separate flask being assigned as a blank sample. 2ml of sulphuric acid (H_2SO_4) and 2ml of hydrogen peroxide (H_2O_2) was then added to each flask. The flasks were then heated on a hot plate and the particulate matter was digested until only a small amount of fluid remained and no particulate matter remained. The residue from this reaction was thereafter dissolved in hydrochloric acid (HCl) and the flasks were filled with water until the 50ml mark. This water had previously been treated with ion exchange resin and a water polisher.

Total heavy metal quantification via ICP-OES

The next step was to test sediment samples for total heavy metal concentrations using a Prodigy ICP-OES (Inductively Coupled Plasma Atomic Emission Spectrometry) machine. The machine was calibrated using varied standard solutions based on their typical concentrations, which were formulated into two calibration solutions known as the “low spike” and “high spike” from Merck 1000mg/l standard solutions. The low spike solution consisted of Pb: 20µg/l, Cr, Cu and As: 10µg/l, Al: 50µg/l, Cd: 3µg/l: and Zn: 0.01µg/l. The high spike consisted of Pb: 200µg/l, Cr, Cu and As: 100µg/l, Al: 500µg/l, Cd: 30µg/l and Zn: 0.05µg/l. Hg was also formulated into a standard solution with a low spike concentration of 1µg/l and high spike of 10µg/l and was used to calibrate the machine. The dilutions necessary for formulating both the samples and the standard solutions were done using acidified water (2% concentrated nitric acid, HNO_3). The ICP-OES thereafter had

several runs with a standard solution to test if it was producing results of satisfactory quality. Finally, the samples were run in the ICP-OES machine and total heavy metal concentrations were obtained.

4.4 Laboratory work for the Chongming samples

4.4.1 Initial sample preparation

Upon returning from the field, the plastic zip-seal sample bags were punctured many times with a fine needle in order to allow air flow and prevent the bags from forming a vacuum. The bags were then placed in a freezer and allowed to freeze for 24 hours at a temperature of -76°C (**Figure 4.6**). The frozen samples were thereafter placed in a vacuum freeze-dryer for 72 hours which removed the moisture through the process of sublimation (the process in which ice is converted directly into water vapour). Since the samples still had moisture after 72 hours, the samples were r transferred into 50ml plastic test tubes, covered in a permeable fabric and refrozen at -76°C for a further 24 hours, with two test tubes for every sample. The test tubes were then placed in a freeze-dryer for an additional two days to dry completely.

The dry samples were gently ground with a pestle and mortar to disaggregate the particles while retaining the grain size distribution. One sub-sample per sample was sieved with a 100μm sieve to remove any large particles (**Figure 4.7**). As a result, during grain size analysis (**see Section 6.5**) there were results for both the sieved and unsieved test tubes. This was, however, not the case for samples 1-5, in which both test tubes were sieved and therefore the only grain size results were from sieved samples. This happened due to the realization that the sieve may remove a useful portion of the grain size distribution, which only occurred after the first 5 samples had been sieved.

4.4.2 Loss on ignition

After the sieving was complete, 32 crucibles with lids were selected in order to run LOI on each sample twice, and then cleaned with water and placed in a drying oven for an hour at 90°C to dry. The dry crucibles were then placed in a muffle furnace (**Figure 4.8**) for two hours at 550°C to ensure they wouldn’t crack under the heat. Nickel boats were also placed in the furnace at the same time, which were later used for HG analysis. The crucibles were numbered from 1-32 in pencil and weighed on a high precision scale and the masses recorded in a document. Approximately 5 grams of sample was then added to the crucibles, weighed, and logged. The crucibles were then covered by their ceramic lids and place in a muffle furnace at 550°C for 3 hours. They were allowed to cool in the furnace overnight to allow for the stabilization of the mass of the sediment. Finally, the crucibles were weighed, and the final organic weight loss of the sediment was recorded.

4.4.3 Sample preparation for grain size analysis

A number of pre-treatment processes were necessary in order to make the samples suitable for grain size analysis. The first process involved removing any biological matter from the sample (**Figure 4.9**). Initially, 22 beakers were cleaned with water and ethanol to remove any residue from past analysis and dried in an oven at 90°c for an hour. 0.5 grams of dried sediment sample were then added to each beaker and the beakers were labelled, with both the un-sieved and sieved variants of the samples being included. 10ml of H_2O_2 (peroxide), was then added to each beaker and the beakers were placed on a hot plate and heated at 180°c until most of the peroxide had evaporated and only a small amount of solution remained. 10ml of dilute HCl (Hydrochloric acid), was then added to each beaker and heated at 180°c until once again only a small amount of solution remained due to the evaporation of the majority HCl.

This process resulted in the consumption of the organic matter by the two acids. The beakers were then filled with Milli-q water and allowed to cool for 12 hours. Once cooled, the excess (sediment-free) water in the top of the beaker was poured out so that only a small amount of water and the sediment at the bottom of each beaker remained. 10ml of $(NaPO_3)^6$ (Sodium Hexa-metaphosphate) was then added to each beaker as a dispersion agent to disaggregate the sediment particles. The beakers were placed into a vibrating water bath to further disperse the particles before GS analysis.

4.4.4 Grain size analysis by Malvern Mastersizer 2000

The methodology to quantify grain size was very similar to that used in the laboratory at UCT (see **Section 4.1.7**), with a few minor differences due to a slightly different machine configuration. The most important difference was that the machine was configured to use a much smaller dispersion unit and therefore allows for much smaller quantities of sediment to be accurately tested, which is why it was possible to treat only 0.5 grams of sample. This configuration also meant that each machine run was significantly quicker than the 10 minutes required to do a single run at UCT.

The next difference was that the machine did not use an automatic cleaner as the department did not want to use tap water in their machine, so, as a result, the machine must be cleaned manually between sample runs with distilled water. Once cleaned, the machine was run once to get a background result and to test whether any sediment from the previous sample run was left in the machine. Once the machine was cleaned and ready, sediment was added using a pipette until a laser obscuration value of 12-16% was achieved. The machine was then run, and a reading was recorded. The first sample: MO1-1 was tested 3 times to test whether the sediment distribution graphs were consistent and thereafter, the remainder of the samples were tested twice, which would later be combined into a single result during data analysis.

4.4.5 Heavy metal analysis

Acid digestion

The digestion process involved allowing the sediment samples to be digested by several acids until the sediment is broken down into their constituent elements. The rate of this digestion can be increased through heating (**Figure 4.11**). The methodology is as follows:

Teflon bottles were cleaned using Milli-Q water and ethanol to remove residual waste. Approximately 0.05 grams of dried, sieved sample was added to the bottles. 1.5 ml of highly concentrated (65-68%) $HN0_3$ (nitric acid) and 4 ml of Hf (hydrofluoric acid), with a concentration of 40%, was then added and the bottles were heated at 150°c for 24 hours (**Figure 4.11**). The bottles were then heated at 180°c for an additional 72 hours. Lids were removed from the Teflon bottles and 0.5ml $HClO_4$ (perchloric acid) was added. Samples were then heated at 150°c on a hot plate and evaporation took place until only the digested sample and perchloric acid remained - approximately 0.5ml total volume. The samples were then decanted into beakers with 2% $HN0_3$ to a total volume of 50ml. The samples were then filtered into 10ml vials to remove large particles, however, it is important to note that the total volume of liquid is still 50ml. Samples were then diluted 50 times with Milli-Q water by using 200µl of sample in 10ml of total solution. The samples composed of standard solution were, however, not diluted. The blank samples were kept in both diluted and undiluted forms to test whether the dilution process would have an effect when conducting ICP-OES analysis later.

Heavy metal analysis via ICP-OES

Heavy metal quantification via the ICP-OES instrument began a day prior to analysis, when the Agilient Varien 710 ES ICP- OES machine was calibrated using standard solutions with concentrations of 0, 5, 20, 50, 200 and 1000ppb for all metals in the study, to form the standard curve of the machine. On the day of analysis, an additional 100ppb standard solution was also used to calibrate the machine (**Figure 4.12**). The machine was operated using the "ICP Expert 2" software package.

The samples were then run using the machine, which quantified the heavy metals in the test tube solutions from the previous section. The heavy metals were expressed as a concentration in parts per billion (ppb), which would later be adjusted based on the dilution factors and converted into a concentration in mg/kg. This process was facilitated and aided by Dr Yonjie Wang and Mr Wong Qi.

Mercury analysis

Mercury quantification was conducted using a LECO AMA254 Mercury Analyzer (**Figure 4.13**) and the testing methodology is as follows. Approximately 20 nickel boats were selected, cleaned, and heated at 500°c for 30 minutes to remove any excess mercury that may have been present on the boats. This was, however, an insufficient number of boats for all the samples, so they were cleaned several times during the process. The machine was thereafter calibrated by running the machine with no boats four times until a Hg concentration of 0 was present. The machine was thereafter further calibrated by running the machine with an empty nickel boat. Finally, the machine was run twice with sediment composed of a standard sediment sample with Hg concentrations of 100 +/- 10ppm to finish the calibration process. Approximately 0.015 grams of actual sediment samples were thereafter placed in the nickel boats, weighed, and run twice per sample, or three times, should the first two runs show very different results. Each of these machine runs took a total of 7 minutes. The results from each sample would later be combined into a single, more accurate, result.

Appendix B: Descriptive Tables of the Knysna Results.

Table 5.1: Descriptive table of site names and sampling zones		
Site label	**Zone**	**Detailed site name**
Site 1	1: Northern Ashmead	George Rex/ N2 Culvert
Site 2		Costa Sarda #1
Site 3		Costa Sarda #2
Site 4		Costa Sarda #3
Site 5		Costa Sarda #4
Site 6		Pumphouse
Site 7		Reed Bed Drain
Site 8	2: East CBD	CBD 1
Site 9		CBD 2
Site 10		CBD 3
Site 11		CBD 4
Site 12		CBD 5
Site 13		CBD 6
Site 14		CBD 7
Site 15		CBD 8
Site 16	3: West CBD	Long Street discharge point
Site 17		Long Street Channel (upper)
Site 18		Long Street Channel (lower)
Site 19		Waterfront/ Gray street discharge
Site 20		Bricklebos Stream Discharge (below Trotter Street)
Site 21		Bricklebos Stream-Trotter Street culvert
Site 24	4: East Ashmead	NE Ashmead transect 1
Site 22		NE Ashmead transect 2
Site 23		NE Ashmead transect 3
Site 25		George Rex Park/ Bongani #1
Site 26		George Rex Park/ Bongani #2
Site 27		George Rex Park/ Bongani #3
Site 28		Lower Bongani
Site 30	2: Bongani Catchment	Industrial Area Bridge
Site 31		Vigilance drive
Site 33		Bongani Below Forest
Site 34		Upper Bongani
Site 35		Bongani Below N2
Site 29	3: Bigai Catchment	Bigai Mountain Tributary
Site 32		Upper Bigai (Sunridge Street)
Site 36		Bigai near one of the springs

Table 5.3: Descriptive statistics of the entire Knysna sample							
	N	Range	Minimum	Maximum	Mean		Std. Deviation
	Statistic	Statistic	Statistic	Statistic	Statistic	Std. Error	Statistic
Chromium (mg/kg)	36	22.3	.5	22.8	7.37	.949	5.69
Cadmium (mg/kg)	36	.0	.5	.5	.5	.0	.0
Copper (mg/kg)	36	29.9	.5	30.4	6.43	1.27	7.61
Lead (mg/kg)	36	21.8	.5	22.3	7.43	1.02	6.09
Zinc (mg/kg)	36	343	1.3	345	57.4	11.30	67.82
Mercury (mg/kg)	36	.0	.5	.5	.5	.0	.0
Arsenic (mg/kg)	36	1.4	.5	1.9	.56	.042	.25
Aluminium (mg/kg)	36	7106	494	7600	2138	265.5	1592
Avg TOC (%)	36	18.7	.5	19.2	5.23	.745	4.47
Mean (GMOM)	36	435.4	18.5	453.9	173.0	17.12	102.7
Valid N (listwise)	36						

Table 5.4 Descriptive statistics of Samples 1-7 (Northern Ashmead)							
	N	Range	Minimum	Maximum	Mean		Std. Deviation
	Statistic	Statistic	Statistic	Statistic	Statistic	Std. Error	Statistic
Chromium (mg/kg)	7	16.7	.5	17.2	4.90	2.10	5.57
Cadmium (mg/kg)	7	.0	.5	.5	.5	.0	.0
Copper (mg/kg)	7	2.1	.5	2.6	1.27	.37	.97
Lead (mg/kg)	7	2.1	.5	2.6	1.36	.406	1.07
Zinc (mg/kg)	7	10.7	11.2	21.9	16.7	1.23	3.26
Mercury (mg/kg)	7	.0	.5	.5	.5	.0	.0
Arsenic (mg/kg)	7	.0	.5	.5	.5	.0	.0
Aluminium (mg/kg)	7	2392	905	3297	1517	320.6	848.3
Avg TOC (%)	7	10.0	2.4	12.4	5.63	1.40	3.71
Mean (GMOM)	7	306.6	51.0	357.6	157.6	38.84	102.8
Valid N (listwise)	7						

Table 5.5: Descriptive statistics of Samples 8-15 (East CBD)							
	N	Range	Minimum	Maximum	Mean		Std. Deviation
	Statistic	Statistic	Statistic	Statistic	Statistic	Std. Error	Statistic
Chromium (mg/kg)	8	12.6	2.6	15.2	5.63	1.43	4.06
Cadmium (mg/kg)	8	.0	.5	.5	.5	.0	.0
Copper (mg/kg)	8	27.8	1.2	29.0	7.53	3.20	9.05
Lead (mg/kg)	8	19.4	2.9	22.3	11.6	2.31	6.53
Zinc (mg/kg)	8	324	20.7	345	75.0	38.9	110
Mercury (mg/kg)	8	.0	.5	.5	.5	.0	.0
Arsenic (mg/kg)	8	1.4	.5	1.9	.68	.18	.50
Aluminium (mg/kg)	8	3002	580	3582	1865	322.7	912.7
Avg TOC (%)	8	18.5	.5	18.9	5.78	2.13	6.04
Mean (GMOM)	8	323.3	18.50	341.8	141.9	34.17	96.65
Valid N (listwise)	8						

Table 5.6: Descriptive statistics of Samples 16-21 (West CBD)						
	N	**Minimum**	**Maximum**	**Mean**		**Std. Deviation**
	Statistic	**Statistic**	**Statistic**	**Statistic**	**Std. Error**	**Statistic**
Chromium (mg/kg)	6	1.1	14.7	7.67	1.90	4.65
Cadmium (mg/kg)	6	.5	.5	.5	.0	.0
Copper (mg/kg)	6	3.7	21.6	11.2	3.00	7.34
Lead (mg/kg)	6	3.6	20.2	12.5	2.65	6.48
Zinc (mg/kg)	6	55.9	172	103	21.0	51.3
Mercury (mg/kg)	6	.5	.5	.5	.0	.0
Arsenic (mg/kg)	6	.5	.5	.5	.0	.0
Aluminium (mg/kg)	6	494.0	2670	1686	302.2	740.2
Avg TOC (%)	6	.8	9.0	4.78	1.19	2.91
Mean (GMOM)	6	80.9	420.2	170.8	51.54	126.2
Valid N (listwise)	6					

Table 5.7: Descriptive statistics of Samples 22-28 (Eastern Ashmead)							
	N	Range	Minimum	Maximum	Mean		Std. Deviation
	Statistic	Statistic	Statistic	Statistic	Statistic	Std. Error	Statistic
Chromium (mg/kg)	7	10.1	4.1	14.2	7.11	1.24	3.28
Cadmium (mg/kg)	7	.0	.5	.5	.5	.0	.0
Copper (mg/kg)	7	11.0	.5	11.5	3.81	1.57	4.15
Lead (mg/kg)	7	7.7	3.1	10.8	5.36	1.06	2.82
Zinc (mg/kg)	7	109.6	11.4	121	34.7	14.8	39.1
Mercury (mg/kg)	7	.0	.5	.5	.5	.0	.0
Arsenic (mg/kg)	7	.6	.5	1.1	.59	.09	.23
Aluminium (mg/kg)	7	5060	975	6035	2135	6803	1800
Avg TOC (%)	7	17.8	1.4	19.2	6.28	2.38	6.31
Mean (GMOM)	7	203.1	33.30	236.4	137.4	25.05	66.27
Valid N (listwise)	7						

Table 5.8: Descriptive statistics of Samples 30-31 & 33-35 (Bongani catchment)							
	N	**Range**	**Minimum**	**Maximum**	**Mean**		**Std. deviation**
	Statistic	**Statistic**	**Statistic**	**Statistic**	**Statistic**	**Std. Error**	**Statistic**
Chromium (mg/kg)	5	17.4	5.4	22.8	14.2	3.13	7.00
Cadmium (mg/kg)	5	.0	.5	.5	.5	.0	.0
Copper (mg/kg)	5	25.9	4.5	30.4	12.6	4.64	10.4
Lead (mg/kg)	5	7.7	4.9	12.6	8.56	1.60	3.57
Zinc (mg/kg)	5	140.6	41.4	182	89.1	24.6	55.1
Mercury (mg/kg)	5	.0	.5	.5	.5	.0	.0
Arsenic (mg/kg)	5	.0	.5	.5	.5	.0	.0
Aluminium (mg/kg)	5	6065	1535	7600	3935	1064	2379
Avg TOC (%)	5	7.7	1.4	9.0	5.08	1.24	2.78
Mean (GMOM)	5	190.2	118.5	308.7	221.0	32.39	72.43
Valid N (listwise)	5						

Table 5.9: Descriptive statistics of samples 29, 32, 36 (Bigai catchment)							
	N	**Range**	**Minimum**	**Maximum**	**Mean**		**Std. deviation**
	Statistic	**Statistic**	**Statistic**	**Statistic**	**Statistic**	**Std. Error**	**Statistic**
Chromium (mg/kg)	3	16.1	.5	16.6	6.30	5.16	8.94
Cadmium (mg/kg)	3	.0	.5	.5	.5	.0	.0
Copper (mg/kg)	3	4.0	.5	4.5	1.83	1.33	2.31
Lead (mg/kg)	3	8.4	.5	8.9	3.30	2.80	4.85
Zinc (mg/kg)	3	29.0	1.3	30.3	13.5	8.68	15.0
Mercury (mg/kg)	3	.0	.5	.5	.5	.0	.0
Arsenic (mg/kg)	3	.0	.5	.5	.5	.0	.0
Aluminium (mg/kg)	3	4668	512	5180	2233	1481	2564
Avg TOC (%)	3	2.3	.6	2.8	1.82	.665	1.15
Mean (GMOM)	3	241.6	212.3	453.9	299.4	77.46	134.2
Valid N (listwise)	3						

Table 5.10: Correlation matrix of entire Knysna (2019) sample											
		Chromium (mg/kg)	Cadmium (mg/kg)	Copper (mg/kg)	Lead (mg/kg)	Zinc (mg/kg)	Mercury (mg/kg)	Arsenic (mg/kg)	Aluminium (mg/kg)	Avg TOC (%)	Mean (GMOM)
Chromium (mg/kg)	Pearson Correlation	1	.[a]	.690**	.465**	.601**	.[a]	-.141	.511**	.300	-.137
	Sig. (2-tailed)		.	.000	.004	.000	.	.411	.001	.076	.427
	N	36	36	36	36	36	36	36	36	36	36
Cadmium (mg/kg)	Pearson Correlation	.[a]	.[a]	.[a]	.[a]	.[a]	.[a]	.[a]	.[a]	.[a]	.[a]
	Sig. (2-tailed)	.		.	.	.	.	.	.	.	.
	N	36	36	36	36	36	36	36	36	36	36
Copper (mg/kg)	Pearson Correlation	.690**	.[a]	1	.767**	.937**	.[a]	-.131	.198	.386*	-.152
	Sig. (2-tailed)	.000	.		.000	.000	.	.446	.247	.020	.377
	N	36	36	36	36	36	36	36	36	36	36
	Pearson	.465**	.[a]	.767**	1	.763**	.[a]	-.104	.268	.366*	-.325

Lead (mg/kg)	Correlation										
	Sig. (2-tailed)	.004	.	.000		.000	.	.546	.114	.028	.053
	N	36	36	36	36	36	36	36	36	36	36
Zinc (mg/kg)	Pearson Correlation	.601**	.[a]	.937**	.763**	1	.[a]	-.129	.207	.525**	-.224
	Sig. (2-tailed)	.000	.	.000	.000		.	.455	.226	.001	.188
	N	36	36	36	36	36	36	36	36	36	36
Mercury (mg/kg)	Pearson Correlation	.[a]	.[a]	.[a]	.[a]	.[a]	.[a]	.[a]	.[a]	.[a]	.[a]
	Sig. (2-tailed)	.	.	.	.	.		.	.	.	.
	N	36	36	36	36	36	36	36	36	36	36
Arsenic (mg/kg)	Pearson Correlation	-.141	.[a]	-.131	-.104	-.129	.[a]	1	-.079	-.171	-.029
	Sig. (2-tailed)	.411	.	.446	.546	.455	.		.649	.318	.864
	N	36	36	36	36	36	36	36	36	36	36
Aluminium (mg/kg)	Pearson Correlation	.511**	.[a]	.198	.268	.207	.[a]	-.079	1	.427**	-.263
	Sig. (2-tailed)	.001	.	.247	.114	.226	.	.649		.009	.122
	N	36	36	36	36	36	36	36	36	36	36
Avg TOC (%)	Pearson Correlation	.300	.[a]	.386*	.366*	.525**	.[a]	-.171	.427**	1	-.690**
	Sig. (2-tailed)	.076	.	.020	.028	.001	.	.318	.009		.000
	N	36	36	36	36	36	36	36	36	36	36
Mean (GMOM)	Pearson Correlation	-.137	.[a]	-.152	-.325	-.224	.[a]	-.029	-.263	-.690**	1
	Sig. (2-tailed)	.427	.	.377	.053	.188	.	.864	.122	.000	
	N	36	36	36	36	36	36	36	36	36	36

**. Correlation is significant at the 0.01 level (2-tailed).

*. Correlation is significant at the 0.05 level (2-tailed).

a. Cannot be computed because at least one of the variables is constant.

Table 5.11: TOC and grain size results for the Knysna sediment samples					
	Variable name:				
Sample number	% Avg TOC	GMOM mean	GMOM sorting	GMOM skewness	GMOM kurtosis
1	2.4	357.6	2.457	-3.096	14.928
2	6.5	125.8	3.999	-1.125	3.910
3	12.4	51.0	3.545	-0.733	4.039
4	2.5	212.7	2.917	-1.874	7.020
5	8.4	71.0	4.064	-0.683	3.525
6	3.1	144.3	3.738	-1.279	4.604
7	4.1	140.8	3.468	-1.338	5.087
8	2.2	143.9	3.362	-1.629	5.843
9	2.2	182.9	3.158	-1.701	6.441
10	4.5	128.4	3.412	-1.379	5.164
11	2.0	155.1	3.304	-1.434	5.386
12	9.0	59.1	3.781	-0.657	3.818
13	18.9	18.5	3.251	-0.474	3.948
14	0.5	341.8	1.503	-0.083	2.389
15	7.0	105.8	3.609	-1.189	4.645
16	9.0	80.9	3.425	-1.025	4.563
17	0.8	420.2	1.431	-0.056	2.423
18	4.8	155.4	3.054	-1.767	6.855
19	6.5	140.4	3.729	-1.364	4.785
20	5.0	143.5	3.891	-1.217	4.289
21	2.5	84.2	3.646	-1.180	4.343
22	2.3	173.5	2.748	-2.008	7.908
23	1.4	236.4	2.284	-2.397	10.666
24	1.8	170.4	2.617	-2.009	8.020
25	7.4	80.0	3.777	-0.748	3.772
26	3.7	133.3	3.534	-1.256	4.645
27	8.3	134.9	3.393	-1.280	4.940
28	19.2	33.3	3.179	-1.324	4.562
29	0.6	453.9	1.503	-0.072	2.412
30	4.6	232.4	2.857	-2.078	7.957
31	1.4	308.7	1.657	-1.202	6.861
32	2.8	212.3	2.888	-2.093	8.100
33	9.0	118.5	4.086	-1.003	3.833
34	6.0	259.1	2.440	-2.100	8.820
35	4.5	186.3	2.917	-1.917	7.504
36	2.1	232.0	2.452	-2.101	9.111

Table 5.12: Final Ef ratios and classes for Armitage (2019)								
	Cr		Zn		Pb		Cu	
Site	Ef	Ef class	Ef	Ef class	EF	Ef class	EF	EF class
1	0.1	1	6.50	4	0.2	1	0.3	1
2	4.31	3	6.3	4	0.3	1	0.4	1
3	0.30	1	2.4	3	0.2	1	0.2	1
4	0.78	1	3.72	3	0.2	1	0.4	1
5	0.74	1	4.88	3	1.1	2	1.8	2
6	0.84	1	4.35	3	1.1	2	1.3	2
7	0.91	1	6.56	4	1.3	2	1.6	2
8	0.93	1	10.1	4	4.6	3	3.4	3
9	0.71	1	7.06	4	5.95	4	2.4	3
10	0.98	1	17.0	4	7.56	4	5.7	3
11	0.60	1	5.52	4	2.3	3	1.7	2
12	1.2	2	12.5	4	3.2	3	3.9	3
13	2.41	3	60.9	6	7.74	4	14.1	4
14	1.6	2	13	4	1.6	2	1.0	2
15	0.3	1	3.89	3	3.64	3	0.99	1
16	1.3	2	16.5	4	6.10	4	5.43	4
17	0.3	1	28.5	5	2.0	3	3.2	3
18	2.38	3	52.4	6	7.57	4	14.7	4
19	2.68	3	35.2	5	7.89	4	10.3	4
20	1.2	2	18.1	5	4.0	3	4.6	3
21	1.1	2	14.6	5	3.2	3	2.8	3
22	1.0	1	3.03	3	1.1	2	0.80	1
23	1.0	1	3.83	3	3.4	3	0.4	1
24	1	2	3.85	3	1.3	2	0.3	1
25	1.3	2	8.8	4	2.7	3	2.5	3
26	1.6	2	5.16	4	1.6	2	1.3	2
27	1.6	2	10.4	4	1.9	2	4.8	3
28	1.33	2	10.7	4	2.36	3	3.35	3
29	0.1	1	0.7	1	0.3	1	0.4	1
30	0.95	1	13.4	4	1.9	2	4.0	3
31	4.76	3	49.1	6	5.32	4	19.3	4
32	0.44	1	3.2	3	0.2	1	0.4	1
33	1	2	5.64	4	2.0	2	1.8	2
34	2.0	3	10.5	4	3.27	3	4.43	3
35	1.25	2	4.58	3	1.2	2	2	2
36	1.74	2	3.08	3	2.2	3	1.5	2

Table 5.13: Final Ef ratios and classes for Armitage (2018)								
	Cr		Cu		Pb		Zn	
Site	EF	EF class	EF	EF class	EF	EF class	EF	EF class
1	1.75	2	2.6	3	4.33	3	3.52	3
2	2.36	3	2.0	3	1.82	2	3.01	3
3	2.05	3	1.5	2	2.25	3	1.91	2
4	0.71	1	1.0	1	1.71	2	2.07	3
5	2.84	3	1.9	2	2.81	3	3.85	3
6	4.37	3	4.6	3	3.88	3	7.03	4
7	1.75	2	0.8	1	1.10	2	1.41	2
8	0.70	1	0.3	1	0.00	1	0.59	1
9	0.69	1	0.4	1	0.00	1	0.54	1
10	1.89	2	1.0	1	1.72	2	1.58	2

Table 5.14: Final Ef ratios and classes for Monteiro *et al.* (2000)								
	Cr		Cu		Zn		Pb	
ID	EF	EF class	EF	EF class	EF	EF class	EF	EF class
KSC1	0.988	1	0.807	1	0.744	1	1.2	2
KSC2	0.635	1	0.383	1	0.397	1	0.332	1
KSC3	0.660	1	0.765	1	0.918	1	0.47	1
KSC4	0.665	1	0.65	1	0.871	1	0.30	1
KSC5	0.758	1	0.692	1	0.798	1	0.48	1
KSC6	1.54	2	1.01	2	1.25	2	0.68	1
KSC7	0.873	1	0.6	1	0.601	1	0.53	1
KSC8	0.851	1	2	3	0.347	1	1.14	2
KSC9	0.814	1	0.63	1	0.873	1	0.50	1
KSC10	0.737	1	0.44	1	0.480	1	0.3	1
KSC11	1.16	2	1.35	2	3.92	3	0.699	1
KSC12	1.26	2	0.960	1	0.926	1	0.41	1
KSC13	0.811	1	0.580	1	0.742	1	0.68	1
KSC14	0.970	1	0.745	1	0.606	1	0.23	1
KSC15	0.876	1	0.906	1	0.606	1	0.68	1
KSC16	0.871	1	0.3	1	0.374	1	1.0	2
KSC18	1.07	2	0.671	1	0.891	1	0.71	1
KSC24	1.10	2	0.5	1	0.77	1	0.49	1

Table 5.15: Final Ef ratios and classes for Watling & Watling (1977)								
	Zn		Cu		Pb		Cr	
Site	EF	EF class	EF	EF class	EF	EF class	EF	EF class
W61	1.97	2	3	3	3.4	3	1.4	2
W60	1.26	2	2	2	2.2	3	1.2	2
W59	7.28	4	5.3	4	14	4	2.2	3
W58	1.80	2	1	1	2.4	3	1.6	2
W57	2.73	3	2.0	2	3.9	3	1.6	2
W1	1.16	2	1	2	2.2	3	1.8	2
W2	0.729	1	0.9	1	2.6	3	1.5	2
W3	0.975	1	1	2	2	2	2.3	3
W4	1.2	2	0.9	1	3	3	2.2	3
W5	0.56	1	1	2	1	2	1.3	2
W6	1.00	1	2	2	2	2	1.7	2
W56	1.27	2	2.6	3	2.4	3	1.2	2
W55	1.13	2	1	2	2.3	3	1.3	2
W54	1.4	2	0.8	1	3.0	3	1.5	2
W157	1.18	2	1	2	2	2	0.6	1
W116	0.88	1	0.6	1	2	2	1.2	2
W156	1.45	2	1	2	2.1	3	0.82	1
W130	1.38	2	1	2	2.0	2	1.2	2
W129	1.45	2	1	2	1.9	2	1.0	2
W128	1.01	2	0.6	1	1	2	0.94	1
W127	0.853	1	0.6	1	1	2	1.1	2
W126	0.957	1	0.5	1	1	2	1.4	2
W125	0.958	1	0.6	1	1	1	1.4	2
W124	0.97	1	0.6	1	2.4	3	1.2	2
W123	0.86	1	0.6	1	0.9	1	0.9	1
W158	1.12	2	0.7	1	2	2	0.8	1

Appendix C: Descriptive data tables for the Chongming Island results.

Table 6.2: Descriptive statistics for the entire Chongming data set							
	N	Range	Minimum	Maximum	Mean		Std. deviation
	Statistic	Statistic	Statistic	Statistic	Statistic	Std. error	Statistic
Al (mg/kg)	15	8000	24000	32000	27900	681	2640
Co (mg/kg)	15	37	0	37	12.5	3.09	12.0
Cr (mg/kg)	15	105	63	168	124	7.44	28.8
Cu (mg/kg)	15	61	0	61	19.7	4.89	18.9
Fe (mg/kg)	15	12100	31300	43400	36800	957	371
Mn (mg/kg)	15	1260	0	1260	340	76.9	298
Ni (mg/kg)	15	75	0	75	23.9	6.53	25.3
Pb (mg/kg)	15	160	0	160	39.6	17.6	68.1
Sr (mg/kg)	15	20	83	103	92.6	1.62	6.29
Zn (mg/kg)	15	67	96	163	133	4.83	18.7
Hg (mg/kg)	15	.0914	.086	.185	.1288	.0069	.0269
TOC (%)	15	6.4	4.5	10.9	7.27	.506	1.96
Mean grain size (µm)	15	6.45	6.51	12.96	9.517	.6083	2.356
Mud (%)	15	5.10	94.70	99.80	97.90	.4073	1.578
Valid N (listwise)	15						

Table 6.3: Descriptive statistics for Gangyang							
	N	Range	Minimum	Maximum	Mean		Std. deviation
	Statistic	Statistic	Statistic	Statistic	Statistic	Std. error	Statistic
Al (mg/kg)	9	8000	24000	32000	27900	912	2740
Co (mg/kg)	9	37	0	37	17.3	4.35	13.0
Cr (mg/kg)	9	97	72	168	129	9.00	27.0
Cu (mg/kg)	9	49	0	49	13.2	5.43	16.3
Fe (mg/kg)	9	12100	31300	43400	38100	1320	3950
Mn (mg/kg)	9	385	90	475	293	46.5	139
Ni (mg/kg)	9	67	0	67	27.1	7.71	23.1
Pb (mg/kg)	9	154	0	154	32.7	21.6	64.9
Sr (mg/kg)	9	19	83	102	92.7	2.27	6.79
Zn (mg/kg)	9	67	96	163	135	7.73	23.2
Hg (mg/kg)	9	.039	.086	.125	.113	.00489	.0147
TOC (%)	9	6.4	4.5	10.9	8.05	.714	2.14
Mean grain size (µm)	9	6.45	6.51	12.96	8.414	.7546	2.264
Mud (%)	9	5.10	94.70	99.80	98.36	.5313	1.594
Valid N (listwise)	9						

Table 6.4: Descriptive statistics for Xisha							
	N	Range	Minimum	Maximum	Mean		Std. deviation
	Statistic	Statistic	Statistic	Statistic	Statistic	Std. error	Statistic
Al (mg/kg)	6	4700	24100	28800	25900.00	881	2160
Co (mg/kg)	6	12	0	12	5.29	2.07	5.07
Cr (mg/kg)	6	96	63	159	117	13.2	32.4
Cu (mg/kg)	6	61	0	61	29.4	8.02	19.7
Fe (mg/kg)	6	6900	31400	38300	34900	1040	2540
Mn (mg/kg)	6	1260	0	1260	410	186	455
Ni (mg/kg)	6	75	0	75	19.2	12.2	29.8
Pb (mg/kg)	6	160	0	160	50.0	31.7	77.7
Sr (mg/kg)	6	16	87	103	92.4	2.48	6.08
Zn (mg/kg)	6	27	116	143	130	4.00	9.79
Hg (mg/kg)	6	.067	.118	.185	.153	.00907	.0222
TOC (%)	6	2.04	5.29	7.33	6.082	.3138	.7662

Mean grain size (µm)	6	3.68	9.04	12.72	11.17	.5580	1.367
Mud (%)	6	3.90	95.70	99.60	97.22	.5730	1.403
Valid N (listwise)	6						

Table 6.5: Grain size descriptive data for Chongming (Blott and Pyre, 2001).

	Sample type:	Textural group:	Sediment name:	Mean	Sorting	Skewness	Kurtosis	% Mud:
M01	Unimodal, Poorly Sorted	Mud	Coarse Silt	11.44	3.072	-0.573	2.823	96.8%
M02	Unimodal, Poorly Sorted	Mud	Coarse Silt	12.72	3.054	-0.579	2.816	95.7%
M03	Unimodal, Poorly Sorted	Mud	Coarse Silt	11.18	3.050	-0.578	2.875	97.0%
M05	Unimodal, Poorly Sorted	Mud	Medium Silt	9.037	2.718	-0.599	3.011	99.6%
M06	Unimodal, Poorly Sorted	Mud	Medium Silt	10.26	2.752	-0.403	2.954	98.0%
M07	Unimodal, Poorly Sorted	Mud	Coarse Silt	12.39	2.967	-0.541	2.846	96.2%
B01	Unimodal, Poorly Sorted	Mud	Medium Silt	7.894	2.592	-0.215	3.139	98.9%
B02	Unimodal, Poorly Sorted	Mud	Medium Silt	8.550	2.962	-0.493	2.593	99.5%
B03	Unimodal, Poorly Sorted	Mud	Coarse Silt	12.96	3.106	-0.483	2.604	94.7%
B04	Unimodal, Poorly Sorted	Mud	Coarse Silt	11.46	3.250	-0.674	2.684	97.5%
B05	Unimodal, Poorly Sorted	Mud	Medium Silt	6.514	2.813	-0.264	2.513	99.8%
B06	Unimodal, Poorly Sorted	Mud	Medium Silt	6.901	2.739	-0.133	3.000	98.7%
B07	Unimodal, Poorly Sorted	Mud	Fine Silt	7.001	2.723	0.183	3.450	97.6%
B08	Unimodal, Poorly Sorted	Mud	Medium Silt	7.348	2.895	-0.345	2.561	99.6%
B09	Unimodal, Poorly Sorted	Mud	Medium Silt	7.097	2.899	-0.194	2.691	98.9%

Table 6.6: Sediment compositional data for Chongming (Blott & Pyre 2001)															
	M01	**M02**	**M03**	**M05**	**M06**	**M07**	**B01**	**B02**	**B03**	**B04**	**B05**	**B06**	**B07**	**B08**	**B09**
% GRAVEL:	0.0%	0.0%	0.0%	0.0%	0.0%	0.0%	0.0%	0.0%	0.0%	0.0%	0.0%	0.0%	0.0%	0.0%	0.0%
% SAND:	3.2%	4.3%	3.0%	0.4%	2.0%	3.8%	1.1%	0.5%	5.3%	2.5%	0.2%	1.3%	2.4%	0.4%	1.1%
% MUD:	96.8%	95.7%	97.0%	99.6%	98.0%	96.2%	98.9%	99.5%	94.7%	97.5%	99.8%	98.7%	97.6%	99.6%	98.9%
% V COARSE GRAVEL:	0.0%	0.0%	0.0%	0.0%	0.0%	0.0%	0.0%	0.0%	0.0%	0.0%	0.0%	0.0%	0.0%	0.0%	0.0%
% COARSE GRAVEL:	0.0%	0.0%	0.0%	0.0%	0.0%	0.0%	0.0%	0.0%	0.0%	0.0%	0.0%	0.0%	0.0%	0.0%	0.0%
% MEDIUM GRAVEL:	0.0%	0.0%	0.0%	0.0%	0.0%	0.0%	0.0%	0.0%	0.0%	0.0%	0.0%	0.0%	0.0%	0.0%	0.0%
% FINE GRAVEL:	0.0%	0.0%	0.0%	0.0%	0.0%	0.0%	0.0%	0.0%	0.0%	0.0%	0.0%	0.0%	0.0%	0.0%	0.0%
% V FINE GRAVEL:	0.0%	0.0%	0.0%	0.0%	0.0%	0.0%	0.0%	0.0%	0.0%	0.0%	0.0%	0.0%	0.0%	0.0%	0.0%
% V COARSE SAND:	0.0%	0.0%	0.0%	0.0%	0.0%	0.0%	0.0%	0.0%	0.0%	0.0%	0.0%	0.0%	0.0%	0.0%	0.0%
% COARSE SAND:	0.0%	0.0%	0.0%	0.0%	0.0%	0.0%	0.0%	0.0%	0.0%	0.0%	0.0%	0.0%	0.0%	0.0%	0.0%
% MEDIUM SAND:	0.0%	0.0%	0.0%	0.0%	0.0%	0.0%	0.0%	0.0%	0.0%	0.0%	0.0%	0.0%	0.0%	0.0%	0.0%
% FINE SAND:	0.0%	0.0%	0.0%	0.0%	0.1%	0.0%	0.2%	0.0%	0.1%	0.0%	0.0%	0.3%	0.7%	0.0%	0.2%
% V FINE SAND:	3.2%	4.3%	2.9%	0.4%	1.9%	3.7%	0.9%	0.5%	5.2%	2.5%	0.2%	1.0%	1.7%	0.4%	0.9%
% V COARSE SILT:	16.3%	19.3%	15.5%	8.2%	11.2%	17.9%	5.0%	9.8%	20.4%	19.0%	5.1%	4.3%	4.1%	7.2%	6.2%
% COARSE SILT:	25.2%	24.8%	24.8%	23.7%	23.2%	25.1%	17.7%	23.5%	23.3%	26.8%	16.4%	14.9%	12.6%	18.8%	16.9%
% MEDIUM SILT:	22.1%	20.7%	23.2%	28.6%	26.7%	21.5%	28.6%	23.9%	18.8%	18.6%	24.1%	26.5%	25.7%	24.6%	24.4%
% FINE SILT:	15.6%	15.3%	16.2%	19.9%	20.1%	16.5%	25.7%	18.7%	16.2%	13.5%	23.7%	25.7%	28.6%	22.0%	23.2%
% V FINE SILT:	9.3%	8.6%	9.0%	10.5%	10.2%	8.9%	13.9%	12.4%	9.7%	9.6%	16.7%	15.9%	17.1%	14.5%	15.6%
% CLAY:	8.3%	6.9%	8.4%	8.7%	6.5%	6.3%	7.9%	11.2%	6.4%	10.0%	13.8%	11.4%	9.6%	12.5%	12.5%

Table 6.7: Enrichment factor results and classes for the Chongming samples								
Sample	**Cr**		**Cu**		**Pb**		**Zn**	
	EF	**EF class**	**EF**	**EF class**	**EF**	**EF class**	**EF**	**EF class**
Xisha								
M01	4.49	3	3.61	3	0.00	1	5.70	4
M02	2.22	3	4.13	3	14.6	4	4.32	3
M03	4.64	3	7.98	4	0.00	1	5.29	4
M05	6.38	4	3.79	3	0.00	1	6.11	4
M06	4.94	3	2.62	3	16.9	4	5.03	4
M07	4.93	3	0.00	1	0.00	1	6.03	4
Gangyang								
B01	4.26	3	0.120	1	0.00	1	4.72	3
B02	4.74	3	2.76	3	15.1	4	4.79	3
B03	3.97	3	0.319	1	0.00	1	3.83	3
B04	3.00	3	1.73	2	0.00	1	4.31	3
B05	4.38	3	0.492	1	0.00	1	5.43	4
B06	4.80	3	2.73	3	0.00	1	6.41	4
B07	6.25	4	0.000	1	18.3	4	6.81	4
B08	5.16	4	0.240	1	0.00	1	5.50	4
B09	5.38	4	5.06	4	0.00	1	5.26	4
Basic descriptive statistics								
Mean Xisha	4.60	3.17	3.69	2.83	5.24	2	5.41	3.83
σ Xisha	1.35	0.408	2.58	0.983	8.15	1.55	0.679	0.408
Mean GNG	4.66	3.33	1.49	1.89	3.72	1.67	5.23	3.56
σ GNG	0.921	0.500	1.73	1.17	7.42	1.32	0.953	0.527
Mean Total	4.63	3.27	2.37	2.27	4.33	1.80	5.30	3.67
σ Total	1.06	0.458	2.31	1.16	7.47	1.37	0.833	0.488
All EF values are stated to 3 significant figures								

Table 6.8: Correlation matrix for the entire Chongming sample set									
		Al (mg/kg)	Cr (mg/kg)	Cu (mg/kg)	Pb (mg/kg)	Zn (mg/kg)	Hg (mg/kg)	TOC (%)	Mean grain size (μm)
Al (mg/kg)	Pearson correlation	1	.246	.031	.104	.174	-.247	.199	-.267
	Sig. (2-tailed)		.377	.912	.713	.536	.376	.476	.336
	N	15	15	15	15	15	15	15	15
Cr (mg/kg)	Pearson correlation	.246	1	-.024	-.007	.752**	.406	.618*	-.684**
	Sig. (2-tailed)	.377		.931	.980	.001	.133	.014	.005
	N	15	15	15	15	15	15	15	15
Cu (mg/kg)	Pearson correlation	.031	-.024	1	.024	-.030	.371	-.162	.134
	Sig. (2-tailed)	.912	.931		.933	.915	.173	.565	.633
	N	15	15	15	15	15	15	15	15
Pb (mg/kg)	Pearson correlation	.104	-.007	.024	1	.030	.109	.111	.021
	Sig. (2-tailed)	.713	.980	.933		.914	.699	.693	.940
	N	15	15	15	15	15	15	15	15
Zn (mg/kg)	Pearson correlation	.174	.752**	-.030	.030	1	.342	.874**	-.767**
	Sig. (2-tailed)	.536	.001	.915	.914		.212	.000	.001
	N	15	15	15	15	15	15	15	15
Hg (mg/kg)	Pearson correlation	-.247	.406	.371	.109	.342	1	-.014	-.022
	Sig. (2-tailed)	.376	.133	.173	.699	.212		.960	.937
	N	15	15	15	15	15	15	15	15
TOC (%)	Pearson correlation	.199	.618*	-.162	.111	.874**	-.014	1	-.855**
	Sig. (2-tailed)	.476	.014	.565	.693	.000	.960		.000
	N	15	15	15	15	15	15	15	15
Mean grain size (μm)	Pearson correlation	-.267	-.684**	.134	.021	-.767**	-.022	-.855**	1
	Sig. (2-tailed)	.336	.005	.633	.940	.001	.937	.000	
	N	15	15	15	15	15	15	15	15
**. Correlation is significant at the 0.01 level (2-tailed).									
*. Correlation is significant at the 0.05 level (2-tailed).									